

NEW HOLISTIC STRUCTURAL ROBUSTNESS AND STRUCTURAL
REDUNDANCY INDICES FOR TRUSS BRIDGES: FORMULATION AND
PRACTICAL APPLICATIONS

by

Edward Steeves

Submitted in partial fulfilment of the requirements
for the degree of Master of Applied Science

at

Dalhousie University
Halifax, Nova Scotia
August 2024

Dalhousie University is located in Mi'kma'ki, the
ancestral and unceded territory of the Mi'kmaq.
We are all Treaty people.

© Copyright by Edward Steeves, 2024

TABLE OF CONTENTS

LIST OF TABLES	vi
LIST OF FIGURES	vii
ABSTRACT.....	ix
LIST OF ABBREVIATIONS AND SYMBOLS USED.....	x
ACKNOWLEDGMENTS	xv
CHAPTER 1: INTRODUCTION.....	1
1.1 Motivation and Background	1
1.2 Research Objectives.....	3
1.3 Thesis Structure	3
CHAPTER 2: NEW HOLISTIC STRUCTURAL ROBUSTNESS INDEX FOR BRIDGES.....	6
2.1 Abstract	6
2.2 Introduction.....	6
2.3 Review of Existing Structural Robustness Measures	8
2.3.1 Progression and Critical Review of Definitions	8
2.3.2 Survey of Available Measures and Research Needs.....	10
2.4 Formulation of Structural Robustness Index	14
2.4.1 Definitions	14

2.4.2 Concept	15
2.4.3 Mathematical Expressions	21
2.5 Framework of Required Structural Analysis	24
2.6 Numerical Example	26
2.6.1 Results for Truss Systems With Brittle, Ductile, and Hybrid Hinge Definitions ..	27
2.6.2 Discussion of Results.....	29
2.6.2.1 Discussion of Results From New Structural Robustness Index ($R_{k,Q}^B$).....	29
2.6.2.2 Comparison of Proposed Index ($R_{k,Q}^B$) With Existing Structural Robustness Measures.....	30
2.7 Conclusion	32
CHAPTER 3: PRACTICAL APPLICATIONS OF NEW STRUCTURAL ROBUSTNESS AND STRUCTURAL REDUNDANCY INDICES	34
3.1 Abstract	34
3.2 Introduction.....	34
3.3 Review of Existing Robustness Measures	36
3.4 New Indices and Framework of Analysis	38
3.4.1 Definitions	38
3.4.2 Mathematical Form.....	38
3.4.3 User-friendly Framework of Analysis	40

3.5 Numerical Example and Comparison with Existing Measures	41
3.6 Practical Application of Existing Truss Bridge Evaluation	44
3.7 Asset Management Framework	48
3.8 Conclusion	49
CHAPTER 4: NOVEL OPTIMIZATION FRAMEWORK TO MAXIMIZE THE STRUCTURAL ROBUSTNESS OF EXISTING TRUSS BRIDGES THROUGH STRATEGIC UPGRADES	51
4.1 Abstract	51
4.2 Introduction.....	51
4.3 Review of Existing Structural Robustness Measures and Optimization Techniques	54
4.3.1 Structural Robustness Measures	54
4.3.2 Existing Guidelines and Optimization Techniques to Improve Structural Robustness	57
4.4 Formulation of Novel Optimization Framework	59
4.5 Practical Application of Existing Steel Truss Bridge Upgrade.....	64
4.5.1 Bridge Overview.....	64
4.5.2 Upgrade Methodology and Techniques	66
4.5.3 Results Using the Built-Up Technique	68
4.5.4 Results Using the In-Plane Support, New Members, and Hybrid Techniques	72
4.6 Conclusion	76

CHAPTER 5: CONCLUSIONS AND RECOMMENDATIONS	78
5.1 Summary	78
5.2 Outcomes and Major Findings.....	79
5.3 Practical Recommendations.....	83
5.4 Future Research	84
REFERENCES	86
APPENDIX A: SUMMARY OF EXISTING STRUCTURAL ROBUSTNESS MEASURES ...	95
APPENDIX B: SAMPLE CALCULATION FOR PARTIAL DAMAGE OF SQUARE TRUSS WITH DUCTILE HINGES	105
APPENDIX C: HINGE DEFINITIONS FROM ASCE 41-17	107
APPENDIX D: SPREADSHEET INTERFACE WITH MATLAB SCRIPTS.....	108
APPENDIX E: CONNECTION CAPACITY CALCULATIONS	109

LIST OF TABLES

Table 2.1 Comparison of $R_{k,Q}^B$ and R_Q^D with existing robustness measures for square truss with brittle, ductile, and hybrid hinge definitions.....	28
Table 2.2 List of elements from most critical to least critical for all truss systems and damaged states.....	32
Table 3.1 Comparison of $R_{k,Q}^B$ and R_Q^D with existing measures for complete element failure.....	42
Table 4.1 Section properties associated with structural members and connections from steel truss bridge in Figure 4.3.	65
Table 4.2 Evaluation results for truss bridge achieved per CSA S6:19 (CSA 2019).....	66
Table 4.3 Description of different upgrade techniques used in practical application.	67
Table 4.4 Structural robustness, structural redundancy, and upgrade material volume of damaged condition and three upgrade solutions using Built-Up technique.	70
Table A.1 Deterministic measures.	96
Table A.2 Category legend.....	101
Table A.3 Probabilistic measures.....	102
Table A.4 Risk-based measures.	104

LIST OF FIGURES

Figure 2.1 Plot of external loads for structural redundancy assessment.	16
Figure 2.2 Plot of possible utilization ratios for structural redundancy assessment.	18
Figure 2.3 Possible external loads plotted for structural robustness assessment.	20
Figure 2.4 Plot of possible utilization ratios for structural robustness assessment.	21
Figure 2.5 Framework of analysis for structural robustness assessment of bridges.	25
Figure 2.6 2D truss structure used for structural robustness assessment.	26
Figure 2.7 Force-displacement curves for tension and compression hinges: (a) brittle; and (b) ductile.	27
Figure 3.1 Framework of analysis for structural robustness and structural redundancy assessments.	40
Figure 3.2 2D square truss subjected to lateral load.	41
Figure 3.3 Robustness and redundancy measures plotted versus varying damaged states for elements 5 and 6 of square truss illustrated in Figure 3.2.	43
Figure 3.4 Steel through truss modeled in SAP2000 (CSI 2016) based off existing bridge in NS, Canada.	44
Figure 3.5 Section properties of steel through truss members referenced in Figure 3.4.	46
Figure 3.6 Robustness and redundancy indices for truss bridge subjected to penetration depths of 0.3, 0.5, and 0.7 mm under concentrated and uniform loading conditions.	46
Figure 3.7 Procedure to employ structural robustness as asset management tool.	48
Figure 3.8 Refined procedure to employ structural robustness as asset management tool using global condition ratings.	49

Figure 4.1 Hypothetical output from novel optimization framework to showcase functionality and constraints.	60
Figure 4.2 Novel optimization framework to upgrade damaged truss bridges.	63
Figure 4.3 Steel truss bridge based off real-life structure in NB, Canada.	64
Figure 4.4 Robustness and redundancy versus material volume achieved from novel optimization framework and CSA S6:19 (CSA 2019) using Built-Up technique.	69
Figure 4.5 Global force-displacement curves for three upgrade solutions from Table 4.4.	71
Figure 4.6 Robustness and redundancy versus increase in collapse load achieved from novel optimization framework and CSA S6:19 (CSA 2019) using Built-Up technique.	72
Figure 4.7 Robustness and redundancy versus material volume achieved from novel optimization framework using all upgrade techniques from Table 4.3.	73
Figure 4.8 Configurations of In-Plane Support and New Members upgrade techniques.	74
Figure 4.9 Robustness and redundancy versus increase in collapse load achieved from novel optimization framework using all upgrade techniques from Table 4.3.	75
Figure B.1 External loads for structural robustness assessment associated with the square truss with ductile hinges and the $0.5C_2$ damaged state.	106
Figure C.1 Generalized force-displacement curves for tension, compression, and brittle hinge definitions from ASCE 41-17 (ASCE 2017).	107

ABSTRACT

Bridges are critical assets in transportation networks but are vulnerable to either environmental damage stemming from the confluence of aging infrastructure and climate change, or mechanical damage such as explosions or impact. Furthermore, steel truss bridges are often identified as vulnerable to collapse when subjected to local damage. In response, the objectives of this thesis are to 1) formulate a new holistic structural robustness index for truss bridges, along with a separate index for structural redundancy, 2) apply the new indices to assess a steel truss bridge against three levels of corrosion damage showcasing their value within a new asset management framework, and 3) develop a novel optimization framework to maximize structural robustness and other properties, such as redundancy, while minimizing the volume of material required for upgrade. In short, the new indices are simple, calculable, and expressive, and are therefore the recommended option for practicing structural engineers as opposed to other existing measures. Secondly, the new asset management framework allows owners to target critical bridges for repair or replacement given budgetary constraints. Thirdly, the novel optimization framework strategically upgrades the bridge at every iteration by targeting the first element failure in the collapse simulation and can be adapted to any robustness measure(s). Its utility is tested on another steel truss bridge subjected to corrosion damage offering an upgrade scheme that is more robust and redundant than a code-compliant repair achieved per CSA S6:19. After concluding that code-based repairs can yield non-redundant systems, some practical solutions are also provided for engineers beyond simply implementing the novel optimization framework. The results from this thesis facilitate direct technology transfer to consulting engineering to help engineers improve the structural safety of existing truss bridges.

LIST OF ABBREVIATIONS AND SYMBOLS USED

AASHTO	American Association of State Highway and Transportation Officials
ASCE	American Society of Civil Engineers
CHBDC	Canadian Highway Bridge Design Code
CSA	Canadian Standards Association
CSCE	Canadian Society for Civil Engineering
CSI	Computers & Structures, Inc.
D	Damaged
DAF	Dynamic Amplification Factor
DCR	Demand to Capacity Ratio
FE	Finite Element
HSS	Hollow Structural Section
I	Intact
ISO	International Organization for Standardization
LRFD	Load and Resistance Factor Design
MATLAB	Matrix Laboratory
MITACS	Mathematics of Information Technology and Complex Systems
NB	New Brunswick
NS	Nova Scotia
NSERC	Natural Sciences and Engineering Research Council of Canada
NSGS	Nova Scotia Graduate Scholarship
ROI	Return on Investment

SAR	Structural Assessment and Retrofit
SMAR	Smart Monitoring, Assessment and Rehabilitation
1D	One-dimensional
2D	Two-dimensional
3D	Three-dimensional
C	Member strength
D^S	System ductility
D_D^S	System ductility of damaged state
D_I^S	System ductility of intact state
d	Hinge displacement
$d_{ultimate}$	Ultimate hinge displacement
d_{yield}	Hinge displacement at yielding
dV	Material volume within range of <i>tolerance</i>
E	Elastic modulus
EL	External load
EL_{max}	Maximum external load
$EL_i^{Deviatoric}$	i^{th} deviatoric external load
$EL_i^{Deviatoric,D}$	i^{th} deviatoric external load in Damaged distribution
EL_i^{Ideal}	i^{th} external load in Ideal distribution
$EL_i^{Ideal,D}$	i^{th} external load in Ideal, D distribution
$EL_i^{max(Target,D I, Ideal,D)}$	i^{th} external load in maximum of Target, D I and Ideal, D distributions

$EL_i^{max (Target,Ideal)}$	i^{th} external load in maximum of Target and Ideal distributions
$EL_i^{Target,D I}$	i^{th} external load in Target, D I distribution
$EL_i^{1^{st} EL}$	i^{th} external load in 1 st <i>EL</i> distribution
F	Hinge force
F_{max}	Maximum hinge force
I_{Rob}	Robustness index
L	Length
$L_{damaged}$	Load carrying capacity of the damaged structure
L_{intact}	Load carrying capacity of the intact structure
LF_d	HS-20 load multiplier for damaged condition limit state
LF_f	HS-20 load multiplier for functionality limit state
LF_u	HS-20 load multiplier for ultimate limit state
LF_1	HS-20 load multiplier for first member failure limit state
Q	Applied load
$Q_{damaged}$	Load that causes the collapse of the damaged system
Q_{intact}	Load that causes the collapse of the originally intact system
R	Response modification factor
R_{Dir}	Direct risk associated with a given damage scenario
R_d	System reserve ratio for damaged condition limit state
R_f	System reserve ratio for functionality limit state
R_{Ind}	Indirect risk associated with a given damage scenario
R_i	Structural bearing capacity after the failure of component i

R_u	System reserve ratio for ultimate limit state
R_0	Initial structural bearing capacity
R_1	Residual redundant factor
R_2	Redundant factor
R_k^B	Structural robustness index
$R_{k,Q}^B$	Structural robustness index, given failure or damage of element k , for a specified loading condition Q
R_Q^D	Structural redundancy index for specified loading condition Q
R^j	j^{th} robustness measure
$R_{+ve}^{Max,Local}$	Local maximum that results in an increase in arbitrary robustness measure, R
$R_{+ve,k,Q}^{Max,Local,B}$	Local maximum that results in an increase in structural robustness index, $R_{k,Q}^B$
$R_{+ve,Q}^{Max,Local,D}$	Local maximum that results in an increase in structural redundancy index, R_Q^D
$R_{+ve}^{Max,Local,j}$	Local maximum that results in an increase in j^{th} robustness measure, R^j
<i>tolerance</i>	Tolerance for optimum material volume
UR	Utilization ratio
UR_f	Factored utilization ratio
$UR_i^{Deviatoric}$	i^{th} deviatoric utilization ratio
$UR_i^{Deviatoric,D}$	i^{th} deviatoric utilization ratio in Damaged distribution

UR_i^{Ideal}	i^{th} utilization ratio in Ideal distribution
$UR_i^{Ideal,D}$	i^{th} utilization ratio in Ideal, D distribution
UR_i^{Target}	i^{th} utilization ratio in Target distribution
$UR_i^{Target,D I}$	i^{th} utilization ratio in Target, D I distribution
V	Material volume
V_i	i^{th} material volume
V^{Opt}	Optimum material volume
ΔQ	Robustness measure
$\Delta R_{+ve}^{Max,Local}$	Change in increasing local maximums for arbitrary robustness measure, R
$\Delta R_{+ve}^{Max,Local,j}$	Change in increasing local maximums for arbitrary robustness measure, R^j
ΔV	Change in material volume
ΔV_i	i^{th} change in material volume
β	Reliability index of the intact system
β'_k	Reliability index conditioned on the loss of element k
γ_i	Component importance coefficient
δ	Global displacement
$\delta_{collapse}$	Collapse displacement of the system
$\delta_{ultimate}$	Ultimate displacement of the system

ACKNOWLEDGEMENTS

Firstly, I would like to express my sincere gratitude and appreciation for my academic supervisor, Dr. Fadi Oudah, who has supported and mentored me through my undergraduate and graduate studies at Dalhousie University. He is a daily inspiration, and I am honoured that he has provided me the opportunity to work alongside him and the Structural Assessment and Retrofit (SAR) research group to champion the cause of designing and building more resilient structures in the face of aging infrastructure and climate change. Our shared beliefs in education and working hard for something far beyond yourself will stay with me for the remainder of my life, and I am confident our work will bear fruit for the lives of future generations.

I am also deeply grateful for my partnership with CBCL Limited (CBCL) through the efforts of Colin Jim and the entire Bridge Department. I am honoured to have CBCL as a vessel for industry experience and mentorship, as well as future technology transfer to implement the research in real-life practice. I would like to further acknowledge the financial support provided by CBCL through the Mathematics of Information Technology and Complex Systems (MITACS) Accelerate Program, along with the financial support from the Natural Sciences and Engineering Research Council of Canada (NSERC) Scholarship, the Nova Scotia Graduate Scholarship (NSGS), and the Dr. Robert Gillespie Graduate Scholarship.

Finally, I would be remiss if I did not mention my friends and family, namely my parents, Margaret and Toben Steeves, who raised me, supported me, and instilled in me the importance and practice of integrity. I owe it all to them for the person I am today.

CHAPTER 1: INTRODUCTION

1.1 Motivation and Background

As a technical term, progressive collapse has been attributed to the propagation of local damage which results in collapse of a significant portion of the structure (Bhattacharya 2021); progressive collapse has been distinguished from disproportionate collapse simply meaning a distinct disproportion between the initial damage and resulting magnitude of collapse (Adam et al. 2018). This research focuses on the collapse of bridges triggered by a local damage irrespective of its progressive or disproportionate nature. Even though there is no universal definition, structural robustness has been defined as the ability of a structure to absorb a local damage and not collapse, albeit robustness has various meanings in different fields of engineering (Bhattacharya 2021); in this thesis, “local” damage is extended to environmental deterioration that locally impacts all structural components. Although often used interchangeably with robustness, structural redundancy is the ability of the originally intact system to continue to carry load after first element failure (Miao and Ghosn 2016) and has been advocated as beneficial for robustness (Izzuddin et al. 2008). While frequently used in a similar context, resilience refers to a bridge’s ability to maintain a level of robustness in a damaged condition and return to a desired level of performance in a timely manner (Minaie and Moon 2017). The focus of this thesis is structural robustness, and by extension redundancy, as opposed to resilience which encompasses other non-structural concepts such as how quickly the system recovers after an event given available resources (Argyroudis 2022). All these definitions relate to the system performance of the bridge, where quantifying the safety of a bridge demands an understanding of system behaviour and system failure (Bhattacharya 2021).

CHAPTER 1: INTRODUCTION

The consequences of structural collapse, and by extension its mitigation through structural robustness and structural redundancy, have been acknowledged by the structural engineering community for decades. Following the partial collapse of the Ronan Point apartment building in London in 1968, the risks associated with progressive collapse became a consideration for building codes and design guidelines (Adam et al. 2018). Moreover, research related to progressive collapse and structural robustness dramatically increased following the collapse of the two World Trade Center towers in New York City in 2001 (Adam et al. 2018). Despite a strong emphasis on building engineering in research, there have also been many tragic bridge collapses throughout history. Noteworthy examples of collapse include the famous Quebec Bridge in 1907, the I-35W truss bridge in Minneapolis in 2007, and more recently the Francis Scott Key Bridge in Baltimore in 2024 (López et al. 2023). Beyond the external stressors of aging infrastructure and climate change, the objective of a bridge is to cross obstacles such as roads or water bodies making them particularly vulnerable to hazards (Capacci et al. 2022). Of all the different bridge types (e.g., girder, truss, arch, cable-stayed, suspension), truss bridges have been identified as particularly vulnerable to failure or collapse given their lack of redundancy (Li et al. 2022; López et al. 2023).

Certainly, for a bridge to be safe it must first be able to withstand the loads expected to occur during its lifetime. For bridges in Canada, the Canadian Highway Bridge Design Code (CHBDC), or CSA S6:19 (CSA 2019), prescribes such loads. However, bridges should also be designed or rehabilitated to carry additional load after member failure (i.e., redundancy) and should be able to absorb some level of local damage and not collapse (i.e., robustness). Stemming from their past performance and interest from the research community, this thesis will predominately focus on the assessment and rehabilitation of existing truss bridges as opposed to new bridge design. Despite concerns given the history of bridge failures in the past, CSA S6:19 (CSA 2019) does not provide

CHAPTER 1: INTRODUCTION

quantitative measures for the structural redundancy or structural robustness of bridges under any damaged state, although the Manual for Bridge Evaluation in the United States has integrated some redundancy measures into their evaluation process (AASHTO 2018). Albeit terms like single-load-path structure and redundancy from CSA S6:19 (CSA 2019) are sometimes used in consulting engineering, there is no consensus among practicing engineers regarding the quantification of properties such as robustness or redundancy, or how to ensure that rehabilitations improve these necessary structural attributes if they are found to be lacking. Considering the confluence of aging infrastructure and budgetary constraints faced by bridge owners (ASCE 2024), optimization is needed when upgrading existing truss bridges to maximize structural safety while minimizing cost.

1.2 Research Objectives

Stemming from this motivation and background, there are three objectives for this research:

Objective 1: Formulation of new holistic structural robustness and structural redundancy indices for truss bridges along with a user-friendly framework of analysis to apply these indices in practice.

Objective 2: Practical application of new indices showcasing their utility within a new asset management framework.

Objective 3: Development of novel optimization framework to maximize the structural robustness and structural redundancy of existing truss bridges through strategic upgrades while minimizing material volume.

1.3 Thesis Structure

This thesis is a publication format thesis, or paper based. Chapters 2, 3, and 4 are comprised of three research papers designed to address the three objectives outlined in Section 1.2. The research

CHAPTER 1: INTRODUCTION

and writing for all three papers were completed by the thesis author, and some content was added from a conference paper by Steeves and Oudah (2024b) accepted for the Smart Monitoring, Assessment and Rehabilitation (SMAR) of Civil Structures 2024 conference proceedings. Chapter 2 is currently under review by the Journal of Bridge Engineering, Chapter 3 has been accepted as part of the Canadian Society for Civil Engineering (CSCE) 2024 conference proceedings, and Chapter 4 is currently under review by Engineering Structures. Following these papers, Chapter 5 provides conclusions and recommendations. The title and a description of each chapter is summarized below:

Chapter 2: *New Holistic Structural Robustness Index for Bridges.* This chapter introduces the formulation for a new holistic structural robustness index for bridges, along with a separate index for structural redundancy, complemented by a user-friendly framework of analysis. The index is conveniently formulated for truss bridges, but applicable to all bridge types in general. A numerical example of a simple two-dimensional (2D) truss is explored comparing the proposed indices with five existing measures published elsewhere.

Chapter 3: *Practical Applications of New Structural Robustness and Structural Redundancy Indices.* This chapter firstly summarizes the results from Chapter 2, then showcases the utility of the new indices through a practical application of a steel truss bridge evaluation, where the bridge is based off a real-life structure in Nova Scotia (NS), Canada, subjected to three levels of corrosion damage. An asset management framework is then proposed which utilizes the new structural robustness index to help owners strategically prioritize bridges for rehabilitation or replacement given budgetary constraints.

CHAPTER 1: INTRODUCTION

Chapter 4: *Novel Optimization Framework to Maximize the Structural Robustness of Existing*

Truss Bridges Through Strategic Upgrades. This chapter proposes a novel optimization framework to increase the structural robustness and other related structural properties of existing truss bridges while minimizing the volume of material required for upgrade. The new framework is used to rehabilitate a steel truss bridge based off a real-life structure in New Brunswick (NB), Canada, subjected to corrosion damage, and the results are compared with a repair achieved per CSA S6:19 (CSA 2019).

Chapter 5: *Conclusions and Recommendations.* This chapter provides a summary of the research included in the thesis, highlights outcomes and major findings from Chapters 2, 3, and 4, then provides practical recommendations and future research to be completed.

CHAPTER 2: NEW HOLISTIC STRUCTURAL ROBUSTNESS INDEX FOR BRIDGES

2.1 Abstract

This paper proposes a new structural robustness index for bridges along with a user-friendly framework of analysis. Bounded between zero and one, the index accounts for the structural response holistically by incorporating the system response up to and including first element failure, the redundancy of the damaged state with respect to the intact version, and system ductility. For the first time, the concepts of redundancy and robustness are distinguished in the formulation, where redundancy is the ability of a system to carry additional load after member failure, while robustness is the structure's ability to absorb a local damage and not collapse. The framework of analysis using the developed robustness index is demonstrated on a simple two-dimensional (2D) truss structure subjected to lateral load with both brittle and ductile hinges, where brittle, ductile, and hybrid systems are considered. The proposed index is used to identify critical elements for two different damaged states and the results are compared with those from five robustness measures published elsewhere. Ultimately, the new structural robustness index can provide valuable insight when evaluating existing bridges and rehabilitating those deemed deficient, presenting a step forward in the safety assessment of bridge structures.

2.2 Introduction

Progressive collapse refers to the propagation of failure throughout a structure, stemming from a local damage, that results in disproportionate collapse (Bhattacharya 2021); although literature often uses the terminology “progressive” or “disproportionate” collapse (Adam et al. 2018), the focus of this research is simply a local damage that results in collapse. Damage can be manifested through environmental-related events (deterioration) or mechanical-related events (impact,

CHAPTER 2: NEW HOLISTIC STRUCTURAL ROBUSTNESS INDEX FOR BRIDGES

explosion) (Brett and Lu 2013). The structure's response to this local damage is a dynamic behaviour that is often complex and ergo difficult to quantify. Following the Ronan Point residential building failure in 1968, progressive collapse gained more attention in the engineering community (Adam et al. 2018). Further catalysts for research included the bombing of the Alfred P. Murrah Federal Building in Oklahoma in 1995, and most notably the collapse of the twin towers in New York City in 2001 (Starossek 2006). There were also many tragic bridge collapses throughout the past century. Common examples include the Quebec Bridge disaster in 1907 and the I-35W truss bridge collapse in Minneapolis in 2007 (Starossek 2006). In fact, truss structures have often been studied as a baseline for understanding redundancy and alternate load paths (Frangopol and Curley 1987).

Various design strategies have been suggested to mitigate progressive collapse, such as providing high safety against local failure, or isolation by compartmentalization, the latter referring to isolating the local failure to prevent a subsequent chain reaction of failures that could impact the global bridge structure (Starossek 2006). Others have proposed the strategy of increasing the continuity of the system as opposed to segmenting or compartmentalizing the structure (Bontempi 2019). Collapse-resistant mechanisms of planar truss structures have been studied, concluding that upon a sudden member loss to the system, the truss can exhibit arching or catenary action to resist the applied loading, depending on the location of the member failure (Yan et al. 2017). Needless to say, it has been argued that progressive collapse is the least predictable and the most difficult to analyse aspect of structural performance (Bhattacharya 2021).

Current bridge design codes such as the Canadian Highway Bridge Design Code (CHBDC), CSA S6:19 (CSA 2019), and AASHTO LRFD Bridge Design Specifications (AASHTO 2020), do not specify quantitative measures for the susceptibility of bridges to progressive collapse in the

case of member damage. A survey of literature related to structural collapse research by Gerasimidis and Ellingwood (2023) identified only two papers focused on the progressive collapse of bridges (Fiorillo and Ghosn 2022; Wang et al. 2022). Evidently there is a lack of research related to structural robustness quantification for bridge structures (Caredda et al. 2022), where robustness has been defined as the ability of a bridge to absorb a local damage and not collapse (Bhattacharya 2021), accompanied by a missing link between academia and industry where these measures can be efficiently implemented in practice.

The objective of this paper is to develop a new structural robustness index for bridges and an associated framework of analysis to obtain index parameters. The index is bounded between zero and one, possesses a simple yet rational formulation, and considers the structural response holistically by incorporating the performance of all elements in a quantifiable manner. The simplicity of the index formulation lends itself to future application in engineering practice, where there is a growing interest in asset management of aging infrastructure across North America (Minaie and Moon 2017). A review of existing robustness measures, the formulation for the new index, and a framework of analysis will be presented next. Lastly, given the collapse of several truss bridges in recent history (Caredda et al. 2022), coupled with the level of research effort in the robustness of truss structures specifically, a numerical example of a simple truss will be explored comparing the proposed formulation with five existing measures.

2.3 Review of Existing Structural Robustness Measures

2.3.1 Progression and Critical Review of Definitions

Although often used synonymously with robustness, redundancy has been defined as the ability of the intact system to continue to carry load beyond the level causing first member failure (Miao and

CHAPTER 2: NEW HOLISTIC STRUCTURAL ROBUSTNESS INDEX FOR BRIDGES

Ghosn 2016), a characteristic often advocated as beneficial for robustness (Izzuddin et al. 2008). The same definition was offered earlier in 1998 as the capability of a bridge superstructure to continue to carry load after the damage of one of its elements (Ghosn and Moses 1998) but was reworded in 2022 as the availability of alternate load paths allowing a load to transfer from the point of application to the point(s) of resistance if the primary load path is compromised (Fiorillo and Ghosn 2022). Another definition suggests redundancy is generally attributed to force redistribution so that more load can be carried than that indicated by structural analysis (Galambos 1990), or the ability of a system to redistribute loads and continue to carry additional load after one or more members reach their full capacity (Ghosn et al. 2016). Lastly, system redundancy has been summarized as the availability of warning before collapse occurs (Hendawi and Frangopol 1994). Based on these definitions, redundancy in this research is a property that does not distinguish between damaged and intact versions of a given structure. Redundancy must account for the system's ability to carry additional load after member failure, redistribute forces to engage as many members as possible, and should be higher for systems that have element-level ductility along with those that can carry more additional load than others irrespective of the condition of the structure (damage versus intact).

The concept of structural robustness emerged in progressive collapse literature following the partial collapse of the Ronan Point apartment building (Brett and Lu 2013). Although there is no universal definition in the engineering community, structural robustness is often attributed to a system's ability to absorb an initial damage and not collapse (Bhattacharya 2021), or the insensitivity to local failure (Brett and Lu 2013; Starossek 2006; Starossek and Haberland 2011). It has also been defined as the ability of the structural system to withstand local damage (Miao and Ghosn 2016), a measure of the capacity of a building system to withstand loss of local load carrying

capacity (Khandelwal and El-Tawil 2011), and a measure of the ability to remain functional in the event of a local failure (Buitrago et al. 2021). Structural robustness depends on the presence of multiple load paths, ductility, and strength (Ghosn et al. 2016). As in other works, robustness is recognized as an intrinsic property of a structural system (Bhattacharya 2021; Brett and Lu 2013). Albeit a purely structural property and independent of the hazard (Anitori et al. 2013), robustness is a function of the externally applied loading condition, its position, direction, and distribution. Stemming from these definitions in literature, structural robustness accounts for redundancy, capacity, and ductility of the damaged system with respect to the intact version.

Lastly, robustness and redundancy should be distinguished from resilience, which has been defined as the ability of a community built around a structure to recover from economic losses resulting from damage (Bhattacharya 2021). Resiliency has been presented as a function of redundancy and robustness (Argyroudis 2022) and has also been described as the structure's ability to maintain a level of robustness in a damaged state and return to a desired level of performance in an expeditious timeframe (Minaie and Moon 2017). This paper is focused on advancing the current measures of structural robustness and structural redundancy as opposed to resilience, since the former are structural engineering concepts and research related to the latter must account for socio-economic aspects of structural collapse.

2.3.2 Survey of Available Measures and Research Needs

There have been numerous measures of structural robustness published since the 1980's. The tables provided in Appendix A summarize existing structural robustness measures that have been published in peer-reviewed journals and technical documents since 1987. Many of the 55 measures were published with terminology other than "structural robustness measure" for the reason that definitions have been evolving since their conception (Bhattacharya 2021). Nevertheless, the

CHAPTER 2: NEW HOLISTIC STRUCTURAL ROBUSTNESS INDEX FOR BRIDGES

measures that are presented in Appendix A were selected based on their adherence to one or more definitions of robustness presented previously.

Appendix A provides measures in three tables: Deterministic (33 measures) in Table A.1, Probabilistic (16) in Table A.3, and Risk-based (6) in Table A.4. Most of the measures fall into the category of deterministic, which can be further classified into the following subcategories: load capacity-based (14), stiffness-based (10), topology-based (5), energy-based (3), damage-based (5), and displacement-based (2). The proposed structural robustness index is classified as a load capacity-based measure, thus the following measures from Appendix A were selected for comparison with the robustness index developed in this research:

Residual redundant factor (Frangopol and Curley 1987):

$$R_1 = \frac{L_{damaged}}{L_{intact}} \quad (2.1)$$

Redundant factor (Frangopol and Curley 1987):

$$R_2 = \frac{L_{intact}}{(L_{intact} - L_{damaged})} \quad (2.2)$$

System reserve ratios (Ghosn and Moses 1998):

$$R_u = \frac{LF_u}{LF_1} \geq 1.30 \quad (2.3a)$$

$$R_f = \frac{LF_f}{LF_1} \geq 1.10 \quad (2.3b)$$

$$R_d = \frac{LF_d}{LF_1} \geq 0.50 \quad (2.3c)$$

CHAPTER 2: NEW HOLISTIC STRUCTURAL ROBUSTNESS INDEX FOR BRIDGES

Component importance coefficient (Chen et al. 2016):

$$\gamma_i = 1 - \frac{R_i}{R_0} \quad (2.4)$$

Robustness measure (Ghosn et al. 2016):

$$\Delta Q = Q_{intact} - Q_{damaged} \quad (2.5)$$

According to Starossek and Haberland (2011), a robustness measure should, among other requirements, express all aspects of robustness (expressive), be as simple as possible (simple), and be quantifiable without excessive effort (calculable). The majority of the deterministic measures in Table A.1 are simple ratios between a damaged and intact structural property (i.e., load capacity, stiffness, energy, or displacement). For the load capacity-based ratios, these are typically simple and calculable, but are often unbounded, and are thus difficult to compare for different damage scenarios (Bhattacharya 2021). The stiffness, topology, and energy-based measures on the other hand require significant effort to calculate and involve concepts not typically encountered in structural engineering practice. Simple ratios as measures generally lack expressiveness as well because they neglect the system performance leading up to collapse, as well as the system failure mode (e.g., brittle, ductile). Regarding the damage-based robustness measures, the analysis required can be too complex for practical use (Starossek and Haberland 2011).

The existing deterministic measures are in certain cases too simple to provide a meaningful, holistic measure of robustness, and in other cases use concepts not practical for real-life applications (Starossek and Haberland 2011). Wang et al. (2022) and Chen et al. (2023) assessed the structural robustness of long span suspension and cable-stayed bridges without any published metrics. Rather, the demand to capacity ratio (DCR) for each suspender and cable for the suspension and cable-stayed bridges, respectively, as well as the dynamic amplification factor

(DAF) for the cable-stayed bridge, were monitored until collapse to determine the structural robustness against specific damages.

As for the probabilistic and risk-based measures, the main benefit is that the aleatoric uncertainties associated with load and resistance are taken into account when computing the probability of failure or reliability index (Bhattacharya 2021). Many of the probabilistic measures take the same form as the deterministic ones, being presented as a ratio between damaged and intact performance. Bhattacharya (2021) presented a new structural robustness index based on first principles from reliability theory. However, the system response is considered to be binary, and the enumerative scheme adopted for the example problem is computationally prohibitive for large structures. In general, the calculability of probabilistic measures is challenging due to complexity in modeling uncertainty (Chen et al. 2016) and probabilistic analysis (Cavaco et al. 2013). Risk-based procedures also suffer from being computationally onerous (Baker et al. 2008).

Among the measures discussed, there is a clear lack of distinction between the concepts of robustness and redundancy, an issue addressed quantitatively in this work. A summary of existing literature reveals the following research gaps to be addressed:

- **Holistic index:** Lack of holistic structural robustness index that is bounded between zero and one, accounts for the performance of all elements, and incorporates 1) the system response up to and including first element failure, 2) the redundancy of the damaged state with respect to the intact system performance, and 3) system ductility.
- **User-friendly framework of analysis:** lack of user-friendly framework of analysis that is 1) based on concepts familiar with practicing engineers, and 2) programmable, allowing for the incorporation of different material behaviours (i.e., brittle, ductile, hardening),

connection capacities, flexible choice of damaged states (i.e., partially utilized or failed), and a variable scale of assessed structure (i.e., number of members constituting the system).

2.4 Formulation of Structural Robustness Index

The formulation of the structural robustness index is presented in three sequential sections. Key terms are defined first for consistency, followed by a presentation of the index formulation with a focus on describing the fundamental differences and commonalities between redundancy and robustness. Finally, the mathematical expression of the proposed robustness index is presented along with a suggested formulation for redundancy.

2.4.1 Definitions

Element: a limit state for a particular structural member or connection (e.g., flexure, shear, axial).

A singular hinge is assigned for each element, while multiple hinges can be assigned to a member (e.g., beam, column, truss, etc.).

Hinge: the material response of an element post-yielding, typically in the form of a force-displacement or moment-rotation curve.

Damage: a reduction in capacity of a given hinge or group of hinges, and/or a reduction in stiffness of a member or group of members. Damages may vary in nature, but are determined on a case-by-case basis for each bridge project.

Utilization Ratio: the ratio of unfactored load to nominal resistance for a given hinge, the resistance being the load that causes hinge formation.

Failure of an Element: a hinge that has reached its yielding point (hinge formation).

System: the global (full) structure inclusive of all members.

Collapse: It is important when performing collapse simulations to clearly define the point of collapse. For example, specifically related to a truss bridge that has lost the load carrying capacity of a given member, collapse has been defined as the point where any of its remaining, main members or connections fail (Miao and Ghosn 2016). More generally, if a structure is n -degree statically indeterminate, then $n + 1$ member failures are required for collapse (Bhattacharya 2021). Others have suggested that collapse is defined as the formation of a collapse mechanism or the point at which the structure is subjected to severe damage (Ghosn and Moses 1998). As a unifying interpretation, collapse is defined as the point in the global force-displacement curve where the stiffness of the system reduces to less than or equal to zero. This definition does not distinguish between partial or total collapse because the collapse volume is a function of the location, nature, and direction of the applied loading.

2.4.2 Concept

A unified concept of structural redundancy is first proposed, then built upon to formulate the concept of structural robustness. The concept of redundancy is established by assessing a structure with six elements, one element per member. Figure 2.1 presents a sample diagram where the external load values have been plotted in a bar chart format, and element one has failed. The external load that caused the second element to fail is labeled as “1st *EL*” (external load that causes first element failure), and the collapse load is labeled as “Collapse *EL*”. Figure 2.1 displays three different distributions for the external load diagram. The 1st *EL* distribution, and the area beneath this curve (i.e., the sum of external load values beneath the curve) is neglected for the structural redundancy assessment since redundancy is defined as the structural performance after the first element has failed (this is not true for robustness as will be discussed below). After plotting the external load diagram and observing the distribution of the data, the next step is to determine what

an ideal distribution looks like, which is a function of how the structural system performs post-first element failure.

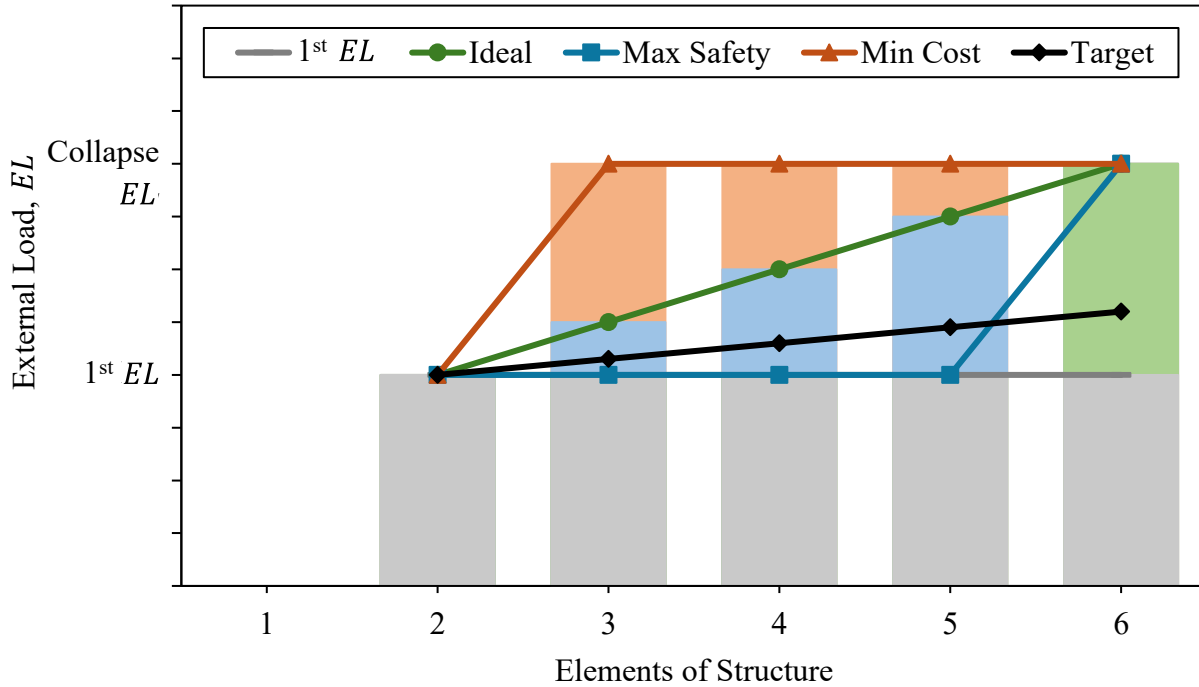


Figure 2.1 Plot of external loads for structural redundancy assessment.

The Ideal external load distribution is the curve with circle markers (green) shown in Figure 2.1, where the Target distribution (diamond markers, black) exhibits the same linear progression. The other distributions in Figure 2.1 are labeled “Min Cost” (triangle markers, orange) and “Max Safety” (square markers, blue). The Min Cost presents a cost-effective solution from a repair/maintenance perspective because a minimum number of elements would need to be repaired/replaced should the external load causing first element failure be exceeded (assuming the external load has not reached the collapse load). However, this distribution is not ideal from a safety perspective because there is minimal warning of collapse if the system fails only after the second element fails.

CHAPTER 2: NEW HOLISTIC STRUCTURAL ROBUSTNESS INDEX FOR BRIDGES

The Max Safety distribution in Figure 2.1 provides the most warning to the public that the structure is potentially nearing collapse since only one element remains in a safe state after the external load that causes first element failure is reached. However, this does not present a cost-effective option because the maximum number of members would need to be repaired after the external load causing first element failure is achieved.

Based on the arguments presented for the Min Cost and Max Safety distributions, it is suggested that the Ideal distribution provides a balance between economy and safety. Other benefits emerge from this distribution, including its natural predictability: the same increase in external load is required to achieve the next element failure. Furthermore, it is desirable to avoid flat regions in the curves because these imply that elements fail simultaneously or progressively, two behaviours antithetical to a structurally redundant system.

The Target distribution has the same distribution as the Ideal, and exhibits the target increase in external load following the level at first element failure. For the sake of illustration, the Ideal distribution is shown to extend above the Target, but in reality this may not be the case. The target increase selected for this work was taken as the value calibrated by Ghosn and Moses (1998) of 1.3 shown in Eq. (2.3a). This implies that if the external load at collapse increases to 30% larger than the load that causes the first element to fail in a linear fashion, the Target distribution is achieved. As discussed, this Target distribution is applicable for damaged and intact systems.

Although the external load diagram theoretically includes the external loads at each element failure, not all the elements may fail at collapse. Nevertheless, to assess redundancy the diagram must include an external load associated with every hinge. If a hinge has not formed, the external load is the collapse load, and this data point is added to the end of the diagram, consequently appending a flat region to the plot. Evidently, the external load diagram on its own is insufficient

information for a redundancy assessment because a flat region at the end of the distribution does not indicate whether the associated hinges have formed or not. Therefore, the utilization ratios for each hinge need to be investigated along with the external loads.

Figure 2.2 presents a diagram where the utilization ratios have been plotted in a bar chart format. It is assumed that this distribution corresponds to the Min Cost curve from Figure 2.1. To reward systems with force redistribution, stemming from the fundamental concepts in system reliability of series versus parallel, the Ideal and Target utilization ratio distributions follow the flat curve in Figure 2.2 signifying that all the hinges have formed at collapse, i.e., a parallel system (Nowak and Collins 2013). However, in this case, the Min Cost distribution deviates from the Ideal and Target, implying that this structure is not parallel. In essence, the utilization ratio diagram maps out the space between the binary concepts of series and parallel.

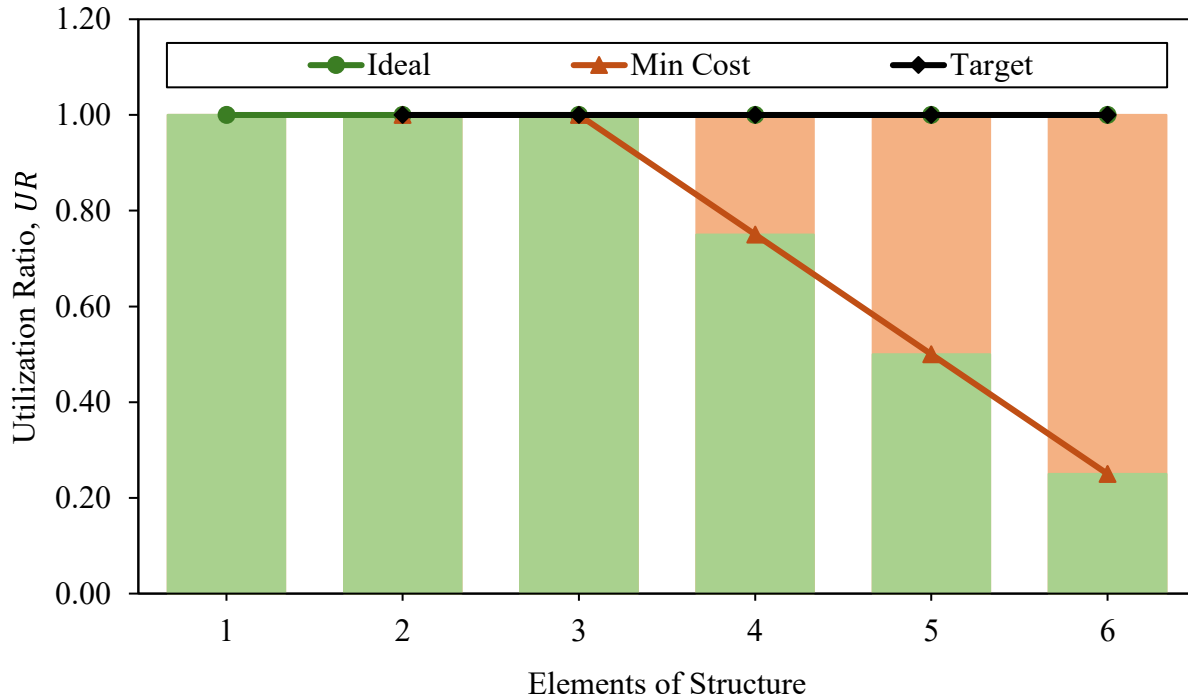


Figure 2.2 Plot of possible utilization ratios for structural redundancy assessment.

CHAPTER 2: NEW HOLISTIC STRUCTURAL ROBUSTNESS INDEX FOR BRIDGES

It is important to note that these distributions are theoretical. Actual structural performance may lie somewhere in between these extremes. Although the Ideal distribution has been selected as the one that balances safety and economy, it may be project specific and require input from the bridge owner. In summary, the redundancy of a given structure can be assessed based on how well the plot of the external loads and utilization ratios match the Target distributions.

Building off the concept of redundancy, the assessment of structural robustness begins again with the external load diagram. Figure 2.3 presents the external loads associated with the Min Cost distribution from Figure 2.1, assuming it is the damaged state, displayed in the legend as Min Cost, D (this distribution is maintained from Figure 2.1 for consistency with the understanding that a true Min Cost distribution for robustness would extend to the collapse load at element two). Comparing Figure 2.3 with Figure 2.1, we see the 1st *EL* distribution has been removed, and the Ideal distribution extends from the first to last element of the structure; the Ideal plot is also associated with the damaged state, so it is presented as Ideal, D. This distinction arises because redundancy is concerned with the behaviour of the structure after the first element has failed, while robustness is concerned with the damaged system's performance compared with the intact version, so all the elements need to be accounted for in the analysis.

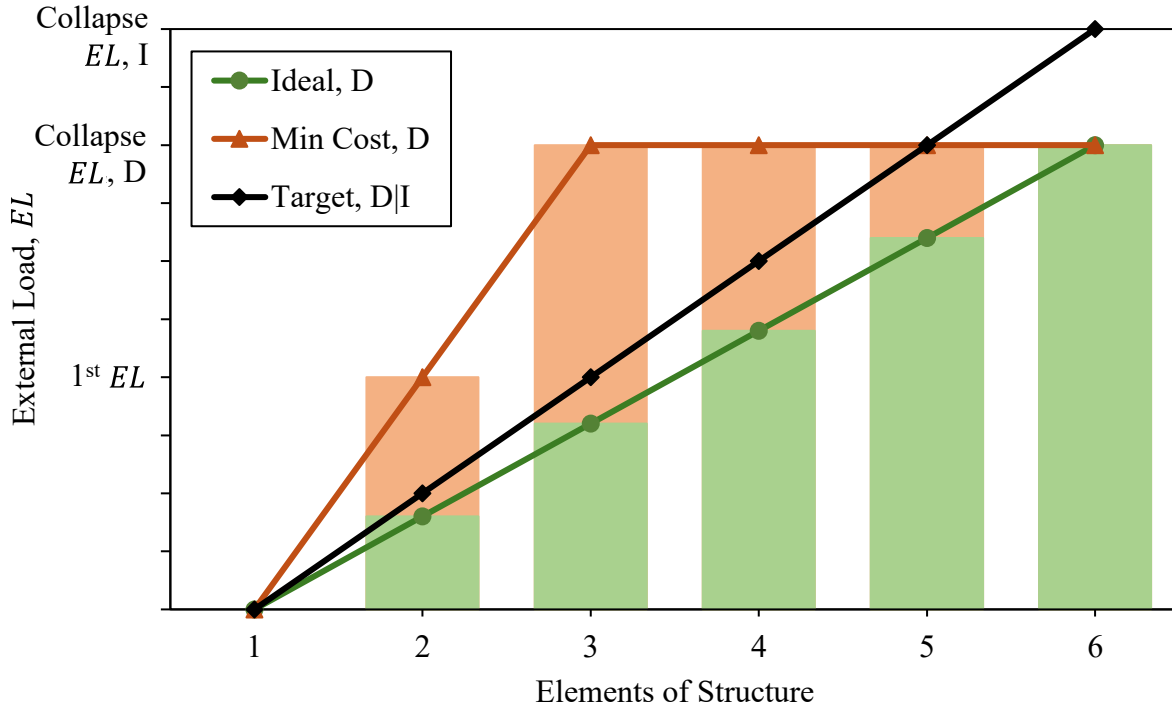


Figure 2.3 Possible external loads plotted for structural robustness assessment.

The other difference is the Target, D|I (Target, Damaged distribution given the Intact performance) curve that exists in Figure 2.3, which starts at the same point as the damaged distributions but extends to the intact collapse load (Collapse EL, I), assuming the intact system can withstand more load than the damaged version (Collapse EL, D). This curve follows a linear distribution for the same reasons as discussed earlier. In words, this means for a system to be fully robust to a given damage, the damaged state must follow a linear distribution, all the members must be fully utilized, and the damaged state must achieve the same collapse load as the intact version. Figure 2.4 showcases a sample utilization ratio diagram, where the only difference between Figures 2.2 and 2.4 is that Figure 2.4 incorporates all elements in the Target distribution, concealing the Ideal curve.

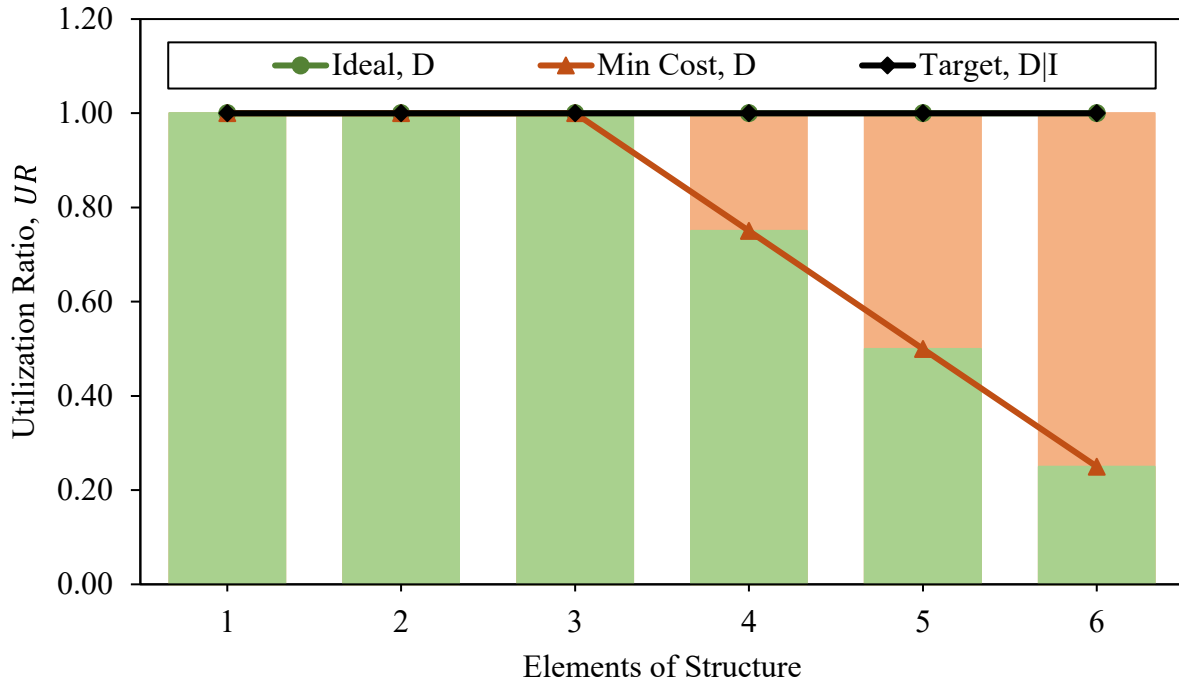


Figure 2.4 Plot of possible utilization ratios for structural robustness assessment.

As with redundancy, the robustness of a given structure can be assessed based on how well the external loads and utilization ratios match the Target distributions. The only remaining attribute to be incorporated into the formulation is system ductility, the ability of the system to sustain the collapse load after the global stiffness reduces to zero. It was decided that a system is fully robust if the system ductility of the damaged state is at least equal to that of the intact state.

2.4.3 Mathematical Expressions

Following from these considerations, the structural robustness index ($R_{k,Q}^B$), given the failure or damage of element k , for a specified loading condition Q , is expressed in Eq. (2.6):

$$R_{k,Q}^B = \left[\frac{\sum_{i=1}^{i=n} EL_i^{Ideal,D} - \sum_{i=1}^{i=n} EL_i^{Deviatoric,D}}{\sum_{i=1}^{i=n} EL_i^{Target,D|I}} \right] \cdot \left[\frac{\sum_{i=1}^{i=n} UR_i^{Ideal,D} - \sum_{i=1}^{i=n} UR_i^{Deviatoric,D}}{\sum_{i=1}^{i=n} UR_i^{Target,D|I}} \right] \cdot \left[\min \left(\left(\frac{D_D^S}{D_I^S} \right), 1 \right) \right] \quad (2.6)$$

This equation is composed of three terms. The first term calculates the difference between the Ideal, D and the deviatoric external loads, where deviatoric generally implies the difference between the actual and the Ideal, in this case the actual damaged (e.g., Min Cost, D) and Ideal, D external loads as illustrated in Figure 2.3. The second term calculates the difference between the Ideal, D and deviatoric utilization ratios as seen in Figure 2.4. Both terms are evaluated with respect to the area beneath their respective Target, D|I distributions as seen in the denominators. Following from the definition of redundancy, these two terms quantify the system's ability to carry additional loads after element failure and redistribute loads to engage multiple members. Element-level ductility is captured, and the difference between the collapse load of the damaged and intact state is accounted for through the Target, D|I distribution. In short, in order for a system to be fully robust, it simply needs *enough* redundancy to allow the damage system to achieve the same collapse load as the intact version following the Target, D|I distribution.

While the first two terms encapsulate the redundancy and capacity of the damaged system with respect to the intact, the third term was added to account for system ductility. Eq. (2.7) quantifies the system ductility of a structure at collapse:

$$D^S = \frac{\delta_{ultimate}}{\delta_{collapse}} \quad (2.7)$$

$\delta_{ultimate}$ is the ultimate displacement of the system, and $\delta_{collapse}$ is the displacement of the system at the point when the collapse load is reached.

As mentioned in the objective of this work, the structural robustness index defined in Eq. (2.6) is bounded between zero and one allowing for simple comparisons to be made with other systems. This was achieved by mathematically bounding each of the three terms between zero and one; the first two terms are essentially a relative difference, while the third term is bounded through a minimization function. In general, the structural robustness index is only bounded between zero and one if the system is coherent, implying the damaged system is not more reliable than the intact version, a property common to civil engineering structures (Bhattacharya 2021).

Evaluating against the research gaps outlined previously, this new structural robustness index captures the structure's response holistically by incorporating the system response up to and including first element failure, the redundancy of damaged system with respect to the intact, and the ductility after the collapse load is reached. Additionally, the index uses values familiar with all practicing structural engineers, namely external loads, utilization ratios, and displacements.

As a consequence of formulating the structural robustness index as a function of redundancy, Eq. (2.8) presents a suggested structural redundancy index (R_Q^D) for specified loading condition Q :

$$R_Q^D = \left[\frac{\sum_{i=1^{st} EL}^{i=n} EL_i^{Ideal} - \sum_{i=1^{st} EL}^{i=n} EL_i^{1^{st} EL} - \sum_{i=1^{st} EL}^{i=n} EL_i^{Deviatoric}}{\sum_{i=1^{st} EL}^{i=n} EL_i^{max(Target, Ideal)} - \sum_{i=1^{st} EL}^{i=n} EL_i^{1^{st} EL}} \right] \cdot \left[\frac{\sum_{i=1^{st} EL}^{i=n} UR_i^{Ideal} - \sum_{i=1^{st} EL}^{i=n} UR_i^{Deviatoric}}{\sum_{i=1^{st} EL}^{i=n} UR_i^{Target}} \right] \quad (2.8)$$

As opposed to the robustness index, Eq. (2.8) is composed of two terms. The first term calculates the difference between the Ideal external loads after first element failure and the deviatoric external loads (Figure 2.1), while the second term calculates the difference between the Ideal and deviatoric utilization ratios (Figure 2.2). Both terms are evaluated with respect to the area beneath their respective Target distributions. These two terms serve to quantify the system's ability to carry

additional load after element failure and redistribute loads to engage as many members as possible. They also account for element-level ductility since systems with ductile elements typically exhibit more load redistribution. As with the structural robustness index, R_Q^D is bounded between zero and one. Starting with the redundancy index, the structural robustness index is obtained by adding back in the 1st EL distribution, changing the bounds for the summations to include all elements, changing the target distribution definitions, then adding on the third term to account for system ductility.

The structural robustness index is conveniently formulated for truss bridges, systems which can easily be discretized into elements. The framework of analysis presented next illustrates a truss bridge as a sample structure, and a simple truss is studied in the numerical example, but the proposed index has the potential to be applied to other bridge types and structures in general.

2.5 Framework of Required Structural Analysis

A framework for the structural analysis required to compute $R_{k,Q}^B$ is shown in Figure 2.5. A finite element (FE) model of the examined bridge must be developed and an incremental nonlinear static pushover or pushdown analysis, depending on the nature of loading, must be performed. The FE model can be two or three-dimensional (3D) where nonlinearities can be captured using zero-length hinges with elastic one-dimensional (1D) elements or by defining nonlinear material properties using beam, shell, or solid elements. Refinement of the FE model, generally, implies improved prediction of $R_{k,Q}^B$.

The framework of the structural analysis is broken down into three steps. Step 1 pertains to the intact state, involving building an FE model, assigning hinges, performing an incremental pushover or pushdown analysis, and extracting results. Step 2 follows the same procedure as Step

CHAPTER 2: NEW HOLISTIC STRUCTURAL ROBUSTNESS INDEX FOR BRIDGES

1 only for the damaged state, and Step 3 involves the structural robustness assessment using the results extracted from Steps 1 and 2.

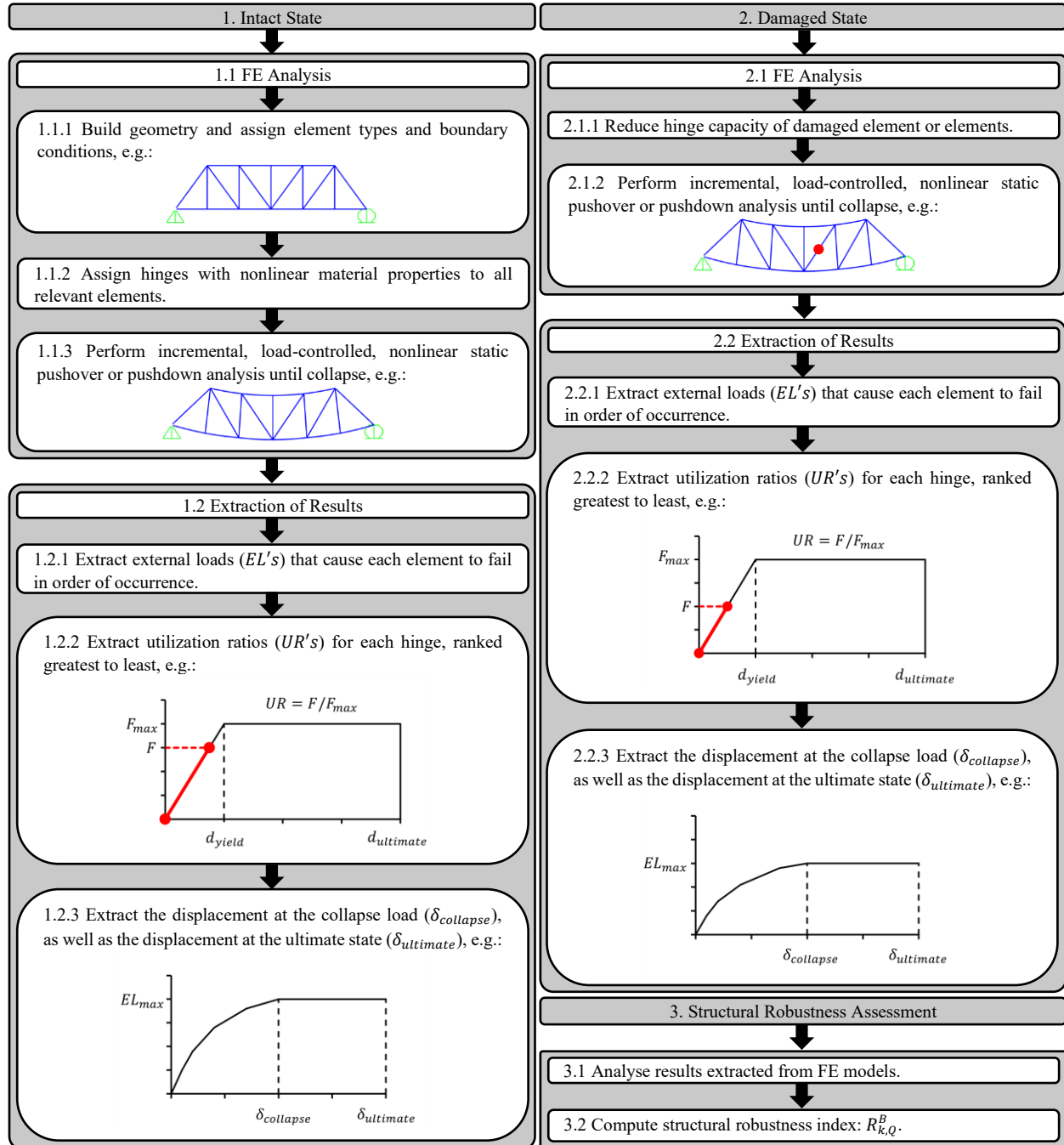


Figure 2.5 Framework of analysis for structural robustness assessment of bridges.

2.6 Numerical Example

The framework of analysis is demonstrated on a simple square truss with two diagonal braces shown in Figure 2.6. This example is based off the numerical example completed by Bhattacharya (2021), while similar examples have been used in various papers (Frangopol and Curley 1987; Fu and Frangopol 1990; Nafday 2008; Giuliani 2012) and larger versions studied in others (Paliou et al. 1990; Brett and Lu 2013; Chen et al. 2016). Only axial hinges are assigned, and the strength magnitudes are the same in tension and compression. The six strength magnitudes, $[C_1, C_2, C_3, C_4, C_5, C_6]$, were selected as $[200, 200, 250, 250, 250, 200]$ kN, which are the mean values from the resistance distributions employed by Bhattacharya (2021). The applied load Q in Figure 2.6 presents the location and direction of the pushover load.

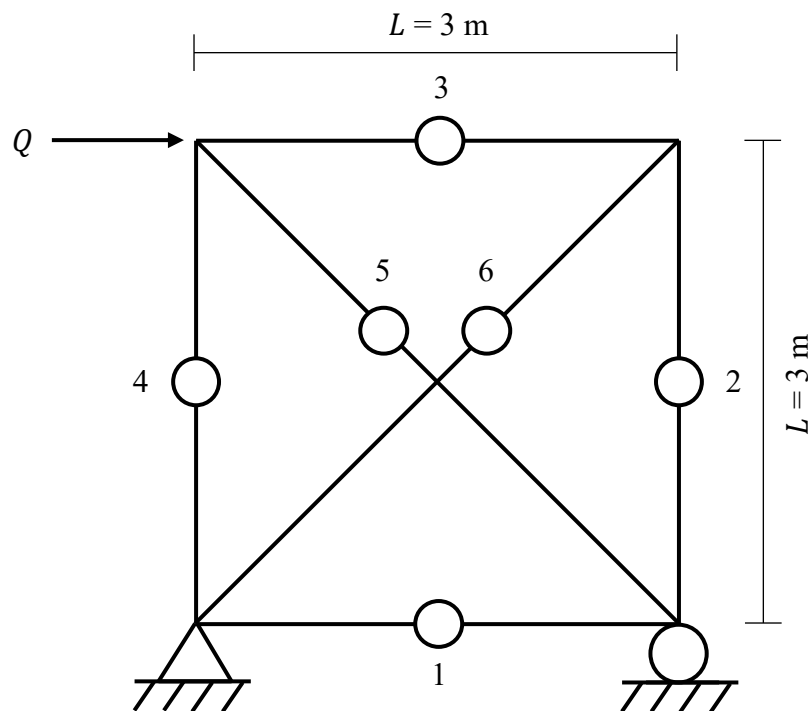


Figure 2.6 2D truss structure used for structural robustness assessment.

Following the framework of analysis described in Figure 2.5, the FE software SAP2000 (CSI 2016) was used to perform the structural analysis. The dimensions of the truss are given in Figure 2.6, HSS 102x102x9.5's were assigned to all members, and steel was selected as the material (Elastic Modulus, $E = 200$ GPa). The analysis was performed separately for trusses with all brittle and ductile hinge definitions, as well as a hybrid where compression members were assigned brittle hinges and tension members were assigned ductile hinges. Force-displacement curves for brittle and ductile hinges are illustrated in Figure 2.7. For the ductile hinges, a response modification factor (R in Figure 2.7 (b)) of 4 was selected from Table 4.17 in CSA S6:19 (CSA 2019).

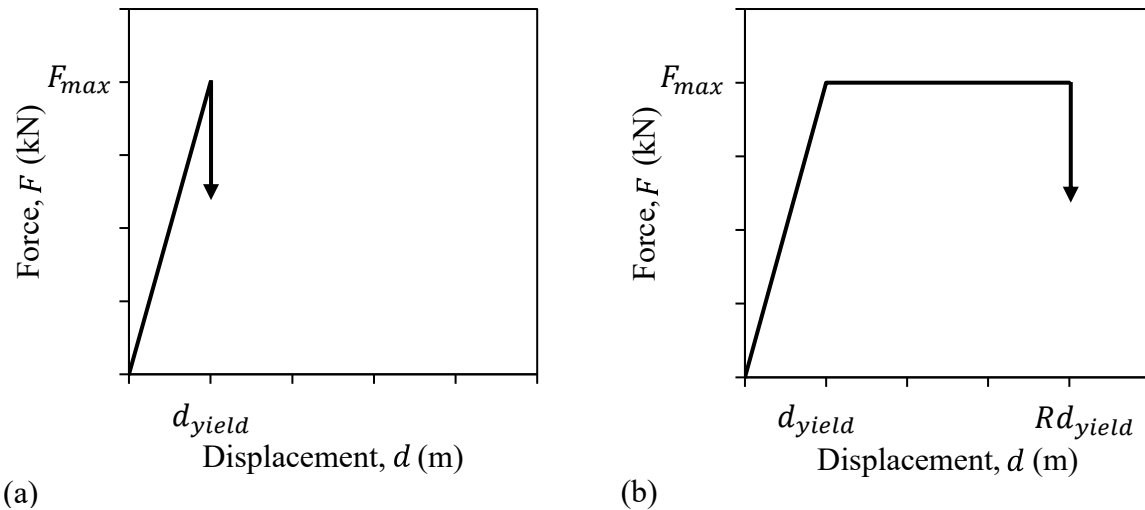


Figure 2.7 Force-displacement curves for tension and compression hinges: (a) brittle; and (b) ductile.

2.6.1 Results for Truss Systems With Brittle, Ductile, and Hybrid Hinge Definitions

From Figure 2.7 (a), all the hinge properties were first defined as linear elastic to failure, where failure is brittle. The hinge properties were then defined as elastic-perfectly-plastic as seen in Figure 2.7 (b). Lastly, the hybrid case was investigated. Two different damaged states were considered: 1) complete element failure, and 2) element capacity and stiffness reduced by 50% (partially damaged). These damages were applied to each element individually to identify the

critical elements for each damaged state. Both robustness and redundancy indices were computed, where Table 2.1 compares $R_{k,Q}^B$ and R_Q^D with the existing measures expressed in Eqs. (2.1) to (2.5).

Table 2.1 Comparison of $R_{k,Q}^B$ and R_Q^D with existing robustness measures for square truss with brittle, ductile, and hybrid hinge definitions.

Hinge Type	Element Damaged State	$R_{k,Q}^B$ (2.6)	R_Q^D (2.8)	R_1 (2.1)	R_2 (2.2)	R_u (2.3a)	R_d (2.3c)	γ_i (2.4)	ΔQ (2.5)
Brittle	C_1	0.09	0.00	0.50	2.00		0.50	0.50	141.42
	C_2	0.12	0.00	0.62	2.67		0.62	0.38	106.07
	C_3	0.12	0.00	0.62	2.67		0.62	0.38	106.07
	C_4	0.09	0.00	0.50	2.00		0.50	0.50	141.42
	C_5	0.09	0.00	0.50	2.00		0.50	0.50	141.42
	C_6	0.12	0.00	0.62	2.67		0.62	0.38	106.07
	$0.5C_1$	0.57	0.00	0.78	4.55		0.78	0.22	62.13
	$0.5C_2$	0.57	0.00	0.78	4.55		0.78	0.22	62.13
	$0.5C_3$	0.78	0.00	0.98	40.67		0.98	0.02	6.95
	$0.5C_4$	0.71	0.00	0.91	11.66		0.91	0.09	24.27
	$0.5C_5$	0.60	0.00	0.81	5.21		0.81	0.19	54.29
	$0.5C_6$	0.43	0.00	0.65	2.83		0.65	0.35	100.00
		Intact		0.00			1.00		
Ductile	C_1	0.08	0.00	0.44	1.80		0.50	0.56	176.71
	C_2	0.11	0.00	0.56	2.25		0.63	0.44	141.35
	C_3	0.11	0.00	0.56	2.25		0.63	0.44	141.35
	C_4	0.08	0.00	0.44	1.80		0.50	0.56	176.71
	C_5	0.08	0.00	0.44	1.80		0.50	0.56	176.71
	C_6	0.11	0.00	0.56	2.25		0.63	0.44	141.35
	$0.5C_1$	0.46	0.07	0.76	4.14		0.85	0.24	76.76
	$0.5C_2$	0.42	0.22	0.87	7.68		0.98	0.13	41.44
	$0.5C_3$	0.63	0.09	0.95	19.29		1.07	0.05	16.50
	$0.5C_4$	0.64	0.03	0.84	6.15		0.94	0.16	51.75
	$0.5C_5$	0.57	0.00	0.72	3.60		0.81	0.28	88.43
	$0.5C_6$	0.50	0.23	0.78	4.50		0.88	0.22	70.67
		Intact		0.11			1.13		

Hinge Type	Element Damaged State	$R_{k,Q}^B$ (2.6)	R_Q^D (2.8)	R_1 (2.1)	R_2 (2.2)	R_u (2.3a)	R_d (2.3c)	γ_i (2.4)	ΔQ (2.5)
Hybrid	C_1	0.08	0.00	0.44	1.80		0.50	0.56	176.78
	C_2	0.11	0.00	0.56	2.25		0.62	0.44	141.43
	C_3	0.11	0.00	0.56	2.25		0.62	0.44	141.43
	C_4	0.08	0.00	0.44	1.80		0.50	0.56	176.78
	C_5	0.08	0.00	0.44	1.80		0.50	0.56	176.78
	C_6	0.11	0.00	0.56	2.25		0.62	0.44	141.43
	$0.5C_1$	0.59	0.07	0.76	4.14		0.85	0.24	76.80
	$0.5C_2$	0.53	0.00	0.69	3.26		0.78	0.31	97.49
	$0.5C_3$	0.73	0.00	0.87	7.52		0.98	0.13	42.32
	$0.5C_4$	0.69	0.03	0.84	6.14		0.94	0.16	51.85
	$0.5C_5$	0.56	0.00	0.72	3.55		0.81	0.28	89.65
	$0.5C_6$	0.54	0.23	0.78	4.50		0.88	0.22	70.71
	Intact			0.11			1.13		

Note: Number in parentheses refers to equation, i.e., (2.1) refers to Eq. (2.1).

2.6.2 Discussion of Results

2.6.2.1 Discussion of Results From New Structural Robustness Index ($R_{k,Q}^B$)

Focusing on the indices related to complete element failure in Table 2.1, $R_{k,Q}^B$ gives a value slightly larger than zero, while R_Q^D is zero for all cases. A redundancy index of zero stems from the structure's inability to carry more load than that which causes first element failure; the structural robustness index can have a non-zero value even when the structural redundancy index is zero. For the ductile case, $R_{k,Q}^B$ for complete element failure decreases relative to the brittle case. This is because given one element failure, only one remaining element can fail before the structure collapses since the system is statically indeterminate to the first degree. Therefore, the system cannot take advantage of any ductility. R_Q^D remaining at zero further reflects this concept. However, the intact system is able to take advantage of the ductile hinges. Thus, the damaged state is worse relative to the intact version when ductile hinges are assigned as opposed to when brittle hinges

are used. Similar logic can be used to explain the hybrid case where the robustness values mimic those of the ductile case.

When the capacity of the hinges is reduced by 50%, the structural robustness indices increase as expected for all truss systems; logically the system should perform better when the capacity of an element is reduced as opposed to failed. For the partial damage of elements one and six, the hybrid system produces the highest robustness index, while for the remaining elements the brittle system produces the highest. Although seemingly counterintuitive, this stems from the fact that the intact brittle system has no system ductility and achieves a lesser collapse load than the intact ductile and hybrid systems. Therefore, it is generally easier for the damaged brittle systems to achieve a performance similar to that of the intact version. However, R_Q^D for the partially damaged states remain at zero for all brittle systems, while all the ductile systems have some level of redundancy, and the hybrid case produces a redundancy value when a ductile element is damaged.

2.6.2.2 Comparison of Proposed Index ($R_{k,Q}^B$) With Existing Structural Robustness Measures

As concluded by Bhattacharya (2021), the brittle system is not very robust when considering complete member failure. Although the formulation and analysis procedure for Bhattacharya's (2021) index are fundamentally different, the results share the same trend as the data presented in Table 2.1 (i.e., $R_{1,Q}^B$, $R_{4,Q}^B$, and $R_{5,Q}^B$ have the same value, and $R_{2,Q}^B$, $R_{3,Q}^B$, and $R_{6,Q}^B$ have the same value).

Investigating the other measures in Table 2.1, Eq. (2.1) from Frangopol and Curley (1987) provides values bounded between zero and one, and is certainly user-friendly for practicing engineers, but is not a holistic measure since it oversimplifies the damaged versus intact system performance by only including the collapse load. It furthermore does not distinguish redundancy

from robustness. Also, from Frangopol and Curley (1987), Eq. (2.2) warrants similar commentary as Eq. (2.1) but is unbounded and therefore presents a challenge when comparing different damage scenarios. Eq. (2.3a) from Ghosn and Moses (1998) does not meet the required load factor ratio of 1.3 for the ultimate limit state but does satisfy the required load factor of 0.5 for the damaged condition limit state for brittle, ductile, and hybrid cases. By not satisfying all the load factor ratios from Eq. (2.3), all three truss systems are deemed to be non-redundant according to Ghosn and Moses (1998). Although R_d from Eq. (2.3c) is arguably user-friendly, it is unbounded, making it difficult to use for comparative purposes. Eq. (2.4) from Chen et al. (2016) is not an apt measure of robustness for the reasons related to Eq. (2.1), as well as the fact that it is unbounded (assuming the bearing capacity of the truss can be increased by removing a member). Eq. (2.5) from Ghosn et al. (2016) is again similar to Eq. (2.1) but is unbounded. Moreover, none of the existing measures account for the system ductility after the collapse load is reached.

Table 2.2 compares the proposed index with the five existing measures by listing the elements identified as most critical to least critical for all truss systems and damaged states; the most critical element given a specified damage is the one with the lowest robustness index. Despite the discrepancies in formulation between the various measures, they all identify elements one, four, and five as the most critical given complete element failure for brittle, ductile, and hybrid cases. Even for partial damage of the brittle system, the ranking of elements is the same for all measures. However, for the partial damage of the ductile and hybrid systems, the ranking is different, with the most notable difference being the partially damaged ductile case where $R_{k,Q}^B$ identifies element two as the most critical, while the existing measures identify element five. A sample calculation for the partial damage of element two for the ductile system is provided in Appendix B. This

example illustrates the differences between $R_{k,Q}^B$ and the existing measures, but also the improved expressiveness associated with the new index, all the while remaining simple and calculable.

Table 2.2 List of elements from most critical to least critical for all truss systems and damaged states.

Hinge Type	Element Damaged State	$R_{k,Q}^B$ (2.6)	R_1 (2.1), R_2 (2.2), R_d (2.3c), γ_i (2.4), ΔQ (2.5)
Brittle	100%	[1, 4, 5], [2, 3, 6]	[1, 4, 5], [2, 3, 6]
	50%	6, [1, 2], 5, 4, 3	6, [1, 2], 5, 4, 3
Ductile	100%	[1, 4, 5], [2, 3, 6]	[1, 4, 5], [2, 3, 6]
	50%	2, 1, 6, 5, 3, 4	5, 1, 6, 4, 2, 3
Hybrid	100%	[1, 4, 5], [2, 3, 6]	[1, 4, 5], [2, 3, 6]
	50%	2, 6, 5, 1, 4, 3	2, 5, 1, 6, 4, 3

Note: 100% refers to complete element failure, and 50% refers to partial element failure; elements listed in square brackets have the same robustness index.

2.7 Conclusion

Research in the field of progressive collapse emerged following the partial collapse of the Ronan Point apartment building in 1968 (Brett and Lu 2013). Although much of the work has revolved around buildings, there have also been many tragic bridge collapses in the past century (Starossek 2006). Furthermore, truss structures have become a baseline for studying redundancy and alternate load paths for bridges. Although current bridge design codes do not specify metrics to measure the susceptibility of bridges to progressive collapse under any damaged state, multiple robustness measures have been published, ranging in complexity and practicality (Brett and Lu 2013).

Two primary concepts in progressive collapse analysis are structural redundancy and structural robustness. This paper distinguishes the two definitions and argues robustness is a function of redundancy (Izzuddin et al. 2008). As per the objective, this paper developed a new structural robustness index for bridges along with a user-friendly framework of structural analysis. A structural redundancy index is also suggested stemming from the robustness index formulation.

CHAPTER 2: NEW HOLISTIC STRUCTURAL ROBUSTNESS INDEX FOR BRIDGES

The structural robustness index considers the structural response holistically by quantitatively accounting for the performance of all elements in the system. The index is rooted in fundamental concepts of system reliability and is bounded between zero and one allowing for simple comparisons to be made. This generates a level of simplicity that is appealing both for practicing engineers as well as owners.

The framework of analysis was demonstrated on a 2D truss structure subjected to lateral load. Both brittle and ductile hinges were considered, leading to the analysis of brittle, ductile, and hybrid systems. As anticipated, structural robustness indices generally decreased when the capacity of a given element reduced, and element level ductility generally improved structural redundancy. This example showcased the index's utility in identifying critical elements given a specified damage. Having been validated, the new structural robustness index can provide valuable insight when evaluating existing bridge structures and rehabilitating those deemed deficient. The proposed index presents a step forward in the safety assessment of bridge infrastructure from a system level perspective. Future research will involve developing an asset management framework with the new index and optimizing rehabilitation schemes to maximize the structural robustness of existing truss bridges while minimizing cost.

CHAPTER 3: PRACTICAL APPLICATIONS OF NEW STRUCTURAL ROBUSTNESS AND STRUCTURAL REDUNDANCY INDICES

3.1 Abstract

Evaluations and rehabilitations of existing bridges are becoming more frequent given the increase in aging infrastructure across North America. Although numerous design strategies have been proposed to reduce the probability of progressive or disproportionate collapse of in-service bridges, the Canadian Highway Bridge Design Code (CHBDC), CSA S6:19, does not prescribe quantitative procedures or measures to assess the structural robustness of bridges. Robustness-based evaluations are therefore needed to help optimize resources for assessing and repairing the significant number of existing bridges across Canada. To address this research gap, new structural robustness and structural redundancy indices, along with a user-friendly framework of analysis, are presented and applied to a series of practical applications to showcase their value to engineering practice. The framework of analysis is first demonstrated on a simple two-dimensional (2D) truss structure subjected to lateral load, and the results are compared with five existing robustness measures published elsewhere. The utility of the indices is then shown through a practical application where the framework of analysis is used on an existing truss bridge in Nova Scotia (NS), Canada, subjected to various levels of corrosion. Lastly, a new asset management framework is presented that utilizes the new indices to improve the safety of existing bridges given the budgetary constraints of bridge owners.

3.2 Introduction

As a consequence of aging infrastructure across North America and the increasing frequency of extreme storms and floods exacerbated by climate change (Xiong et al. 2023), evaluations and rehabilitations of existing bridges are becoming more frequent. Bridges are critical assets in

CHAPTER 3: PRACTICAL APPLICATIONS OF NEW INDICES

transportation networks, requiring proper maintenance and rehabilitation to minimize disruption to the transportation system after extreme events (Argyroudis 2022). Despite efforts to design and construct reliable infrastructure, there have been many tragic bridge collapses throughout history in North America; in general, progressive collapse is defined as the propagation of failure from local damage which results in disproportionate collapse (Bhattacharya 2021). A notable example of disproportionate collapse specific to Canada is the Quebec Bridge, a steel truss which collapsed in 1907 from the buckling of a compression member, ultimately leading to 75 fatalities (Caredda et al. 2022; López et al. 2023). Furthermore, steel truss bridges are typically identified as very vulnerable to collapse (López et al. 2023): a study of bridge failures in the United States from 1980 to 2012 identified 203 steel truss bridge failures while only 444 existing truss bridges remained in service (Lee et al. 2013). A study of collapse-resistant mechanisms concluded that trusses can exhibit arching and catenary action to resist load after member failure (Yan et al. 2017), but as with the Quebec Bridge, many truss bridges have collapsed stemming from the loss of a critical member (Li et al. 2022).

The antonym of progressive collapse is structural robustness, defined as the ability of a structure to absorb a local damage and not collapse (Bhattacharya 2021), or the structure's insensitivity to local failure (Starossek 2006). Although often used interchangeably with robustness, structural redundancy is the ability of a structure to carry additional load after the failure of one of its members (Ghosn et al. 2016), a property that has been advocated as beneficial for robust systems (Izzuddin et al. 2008). Despite the necessity for robust infrastructure, current bridge design codes like the CHBDC do not specify quantitative measures for the structural robustness of bridges (CSA 2019), contributing to the missing link between academia and industry where measures can be efficiently used in practice. In short, there is a need to improve structural

CHAPTER 3: PRACTICAL APPLICATIONS OF NEW INDICES

assessment methods to optimize resources for assessing and repairing the significant number of existing bridges across Canada.

To address this research gap, the objective of this paper is to apply the new structural robustness and structural redundancy indices formulated by Steeves and Oudah (2024a) to a series of practical applications to showcase their value and utility in engineering practice. A brief review of existing measures, a description of the new indices, and a user-friendly framework of analysis will be presented first. A numerical example will then be explored where the new indices are compared with five existing measures, followed by an evaluation of an existing truss based off a real-life bridge in NS subjected to three levels of corrosion damage. Lastly, a new asset management framework will be proposed that utilizes the new structural robustness index to improve the safety of existing structures in a given bridge inventory.

3.3 Review of Existing Robustness Measures

Numerous measures of structural robustness have been published since the 1980's, often with different nomenclature than "robustness measure" given that definitions have been evolving since their introduction in literature (Bhattacharya 2021). Existing measures can be broken down into three categories: deterministic, probabilistic, and risk-based, where the new structural robustness and structural redundancy indices from Steeves and Oudah (2024a) can be classified as deterministic, load capacity-based measures. To facilitate a comparison, the new indices will be computed along with the following five deterministic, load capacity-based measures selected from literature:

$$R_1 = \frac{L_{damaged}}{L_{intact}} \quad (3.1)$$

R_1 is the residual redundant factor, where $L_{damaged}$ and L_{intact} are the load carrying capacity of the damaged and intact structures, respectively (Frangopol and Curley 1987).

$$R_2 = \frac{L_{intact}}{(L_{intact} - L_{damaged})} \quad (3.2)$$

R_2 is the redundant factor, where the other variables are defined above (Frangopol and Curley 1987).

$$R_u = \frac{LF_u}{LF_1} \geq 1.30 \quad (3.3a)$$

$$R_f = \frac{LF_f}{LF_1} \geq 1.10 \quad (3.3b)$$

$$R_d = \frac{LF_d}{LF_1} \geq 0.50 \quad (3.3c)$$

R_u , R_f , and R_d are system reserve ratios for ultimate, functionality, and damaged condition limit states, respectively, where LF is a load multiplier with subscripts u , f , and d for the aforementioned limit states, and subscript 1 for first member failure (Ghosn and Moses 1998).

$$\gamma_i = 1 - \frac{R_i}{R_0} \quad (3.4)$$

γ_i is the component importance coefficient, where R_i is the structural bearing capacity after the failure of component i , and R_0 is the initial structural bearing capacity (Chen et al. 2016).

$$\Delta Q = Q_{intact} - Q_{damaged} \quad (3.5)$$

ΔQ is the robustness measure, where Q_{intact} is the load that causes the collapse of the originally intact system, and $Q_{damaged}$ is the load that causes the collapse of the damaged system (Ghosn et al. 2016).

3.4 New Indices and Framework of Analysis

3.4.1 Definitions

The following definitions are relevant to the application of the new indices:

- **Element:** a limit state of a structural member or connection.
- **Hinge:** the material behavior of an element post-yielding. A single hinge is assigned to each element.
- **Damage:** a reduction in capacity of a hinge or group of hinges.
- **Utilization Ratio:** the ratio of unfactored load to nominal resistance of a hinge.
- **Failure of an Element:** the point when the load causing hinge formation is reached.
- **Collapse:** the point when the stiffness of the system is less than or equal to zero.

3.4.2 Mathematical Form

The indices are first introduced, followed by a high-level description regarding their formulation. Detailed derivation of the new indices can be found in Chapter 2 (Steeves and Oudah 2024a). Firstly, the holistic structural robustness index ($R_{k,Q}^B$), given the damage of element k , for a specified loading condition Q , is expressed as:

$$R_{k,Q}^B = \left[\frac{\sum_{i=1}^{i=n} EL_i^{Ideal,D} - \sum_{i=1}^{i=n} EL_i^{Deviatoric,D}}{\sum_{i=1}^{i=n} EL_i^{Target,D|I}} \right] \cdot \left[\frac{\sum_{i=1}^{i=n} UR_i^{Ideal,D} - \sum_{i=1}^{i=n} UR_i^{Deviatoric,D}}{\sum_{i=1}^{i=n} UR_i^{Target,D|I}} \right] \cdot \left[\min \left(\left(\frac{D_D^S}{D_I^S} \right), 1 \right) \right] \quad (3.6)$$

Eq. (3.6) is composed of three terms, all of which are bounded between zero and one. The first term calculates the difference between the external loads, EL , of the damaged versus intact state, while the second term relates to the difference between the utilization ratios, UR , for damaged versus intact systems. Both terms are evaluated with respect to the area beneath their respective target distributions (Steeves and Oudah 2024a). The third term is added to account for system ductility, where Eq. (3.7) expresses the system ductility at collapse:

$$D^S = \frac{\delta_{ultimate}}{\delta_{collapse}} \quad (3.7)$$

$\delta_{ultimate}$ is the ultimate displacement of the system, and $\delta_{collapse}$ is the displacement of the structure when the collapse load is reached (Steeves and Oudah 2024a).

Given that the structural robustness index is a function of redundancy, Eq. (3.8) presents a mathematical formulation for the structural redundancy index (R_Q^D) for specified loading condition Q :

$$R_Q^D = \left[\frac{\sum_{i=1^{st} EL}^{i=n} EL_i^{Ideal} - \sum_{i=1^{st} EL}^{i=n} EL_i^{1^{st} EL} - \sum_{i=1^{st} EL}^{i=n} EL_i^{Deviatoric}}{\sum_{i=1^{st} EL}^{i=n} EL_i^{max(Target, Ideal)} - \sum_{i=1^{st} EL}^{i=n} EL_i^{1^{st} EL}} \right] \cdot \left[\frac{\sum_{i=1^{st} EL}^{i=n} UR_i^{Ideal} - \sum_{i=1^{st} EL}^{i=n} UR_i^{Deviatoric}}{\sum_{i=1^{st} EL}^{i=n} UR_i^{Target}} \right] \quad (3.8)$$

Unlike the robustness index, Eq. (3.8) is composed of just two terms, both similar in form and function to the first two terms in the robustness index. A redundancy assessment can be applied to both intact and damaged systems (Steeves and Oudah 2024a).

3.4.3 User-friendly Framework of Analysis

The proposed framework of analysis to apply the new indices is illustrated in Figure 3.1. Three steps are involved: 1) building a finite element (FE) model of the bridge, 2) performing an incremental pushover or pushdown analysis, and 3) extracting results to compute the indices (Steeves and Oudah 2024a).

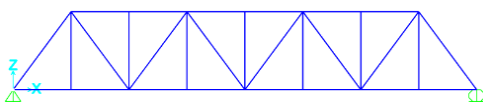
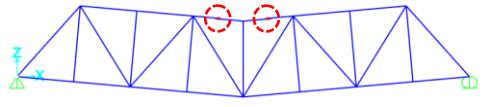
Step 1: Build FE Model	
<p><i>Steel through truss:</i></p> 	<p>1.1 Build geometry, then assign element types, boundary conditions, and hinges with nonlinear material properties (Intact).</p> <p>1.2 Reduce hinge capacity of damaged element(s) (Damaged).</p>
Step 2: Pushover or Pushdown Analysis	
<p><i>Two hinges formed at collapse:</i></p> 	<p>2.1 Perform incremental, load-controlled, nonlinear static pushover or pushdown analysis for both Intact and Damaged systems until collapse.</p>
Step 3: Extract Results	
<p>For Intact and Damaged states, extract:</p> <p style="text-align: center;">$EL's, UR's, \delta_{collapse}, \delta_{ultimate}$</p>	<p>3.1 Compute R_Q^D for Intact and Damaged states.</p> <p>3.2 Compute $R_{k,Q}^B$.</p>

Figure 3.1 Framework of analysis for structural robustness and structural redundancy assessments.

3.5 Numerical Example and Comparison with Existing Measures

The framework of analysis is first demonstrated on a simple truss shown in Figure 3.2, based off an example used by Bhattacharya (2021). HSS 102x102x9.5's were assigned to all members, and structural steel was selected as the material (Elastic Modulus, $E = 200000$ MPa). Hinges were used to capture the axial force-displacement response of the members. Similar to the example in (Bhattacharya 2021), the strength magnitudes, $[C_1, C_2, C_3, C_4, C_5, C_6]$, were selected as $[200, 200, 250, 250, 250, 200]$ kN, with the same capacities in tension and compression. Compression members were assigned brittle hinges, and tension members were assigned ductile hinges with a response modification factor, R , of 4 as per Table 4.17 in CSA S6:19 (CSA 2019). SAP2000 Version 21.0.2 (CSI 2016) was used to perform the analysis.

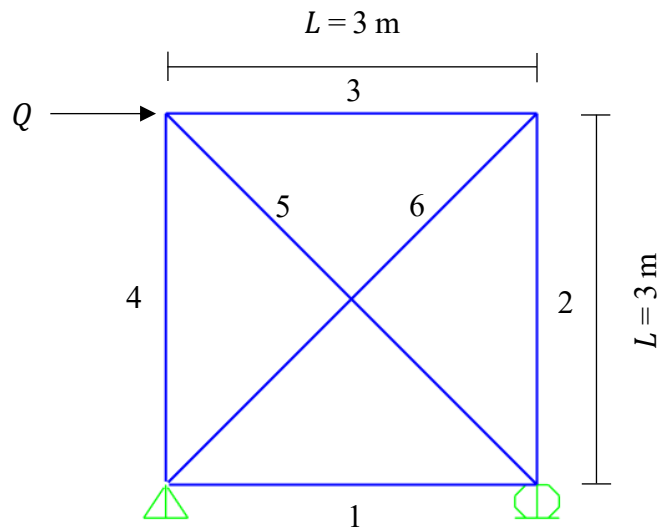


Figure 3.2 2D square truss subjected to lateral load.

The first damaged state considered in the assessment was complete element failure, and the damage was applied to each element individually. Table 3.1 compares the structural robustness index ($R_{k,Q}^B$) and the structural redundancy index (R_Q^D) with the existing measures defined by Eqs. (3.1) to (3.5) (Steeves and Oudah 2024a).

Table 3.1 Comparison of $R_{k,Q}^B$ and R_Q^D with existing measures for complete element failure.

Damaged Element	$R_{k,Q}^B$ (3.6)	R_Q^D (3.8)	R_1 (3.1)	R_2 (3.2)	R_u (3.3a)	R_d (3.3c)	γ_i (3.4)	ΔQ (3.5)
1	0.08	0.00	0.44	1.80		0.50	0.56	176.78
2	0.11	0.00	0.56	2.25		0.62	0.44	141.43
3	0.11	0.00	0.56	2.25		0.62	0.44	141.43
4	0.08	0.00	0.44	1.80		0.50	0.56	176.78
5	0.08	0.00	0.44	1.80		0.50	0.56	176.78
6	0.11	0.00	0.56	2.25		0.62	0.44	141.43
Intact		0.11			1.13			

Despite differences in formulation, all the robustness indices in Table 3.1 identify elements one, four, and five as the most critical given complete element failure. Albeit consistent in this regard, the measures produce a broad spectrum of results, varying from 0 to 176.78. Firstly, $R_{k,Q}^B$ gives values slightly larger than zero, but R_Q^D is zero for all cases stemming from the structure’s inability to carry more load after first element failure. Eqs. (3.1) and (3.4) provide values bounded between zero and one but are not comprehensive since they only consider the collapse load in their formulation. The other measures are unbounded making them difficult to use for comparative purposes; although Eq. (3.3c) satisfies the required load factor of 0.5 for the damaged condition limit states, Eq. (3.3a) does not meet the required load factor ratio of 1.3 for the ultimate limit state, so the truss is simply deemed to be non-redundant according to Ghosn and Moses (1998). Lastly, none of the existing measures distinguish robustness from redundancy, nor account for system ductility, further compromising their value and utility.

For the case of partial element failure, Figure 3.3 shows $R_{k,Q}^B$ and R_Q^D plotted versus the partial damage of elements 5 (compression) and 6 (tension); partial damage refers to a reduction in capacity of the hinge and stiffness of the member. These elements were selected because they provide the lateral load resisting system of the frame shown in Figure 3.2. By way of comparison,

R_1 from Eq. (3.1) was plotted as well since it is also bounded between zero and one and shares a similar trend as $R_{k,Q}^B$.

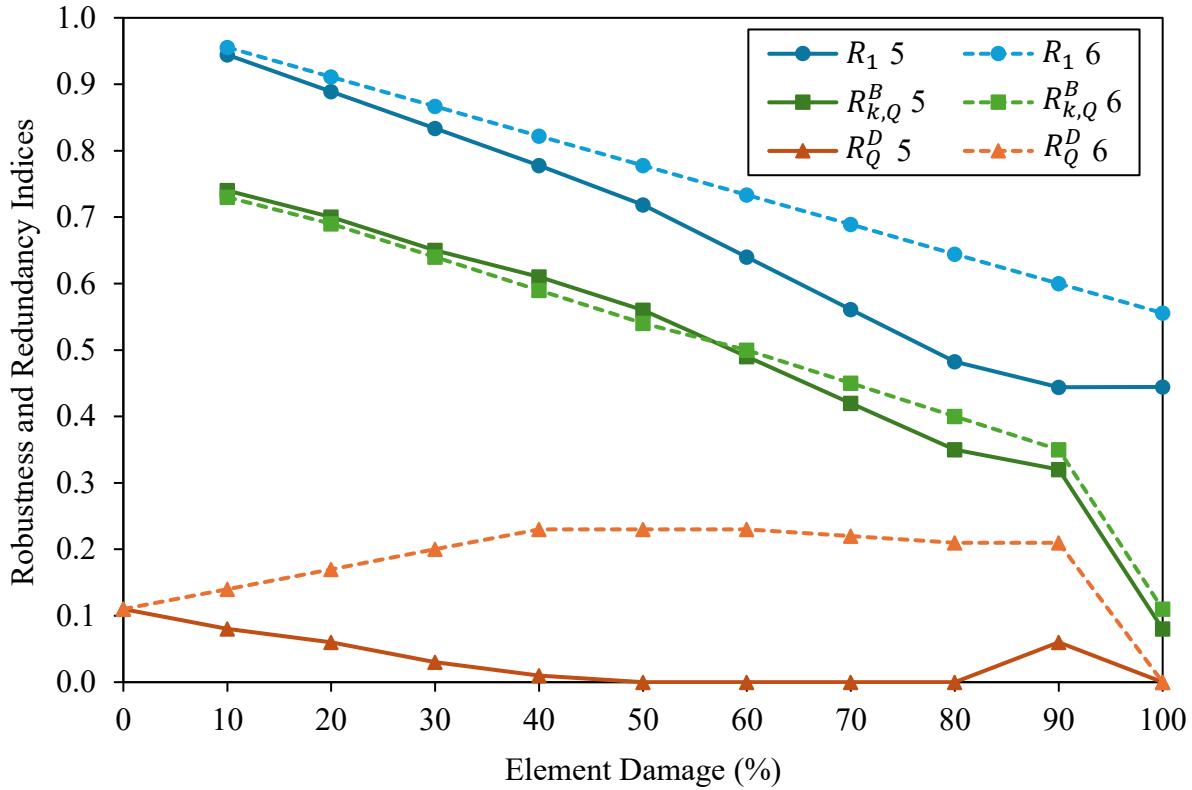


Figure 3.3 Robustness and redundancy measures plotted versus varying damaged states for elements 5 and 6 of square truss illustrated in Figure 3.2.

As expected, Figure 3.3 depicts a decrease in $R_{k,Q}^B$ as the damage level increases. Looking at R_Q^D , the redundancy for partial failure of element 6 is typically higher than that of element 5 because element 6 has a ductile failure mode, and element-level ductility improves redundancy. $R_{k,Q}^B$ is approximately the same for the damage of both elements. It is logical to anticipate that the robustness given the damage of element 6 would be higher because it has a ductile failure mode, an assumption validated by the graphs of R_1 . However, for low damages, $R_{k,Q}^B$ given the partial damage of element 5 performs slightly better because a small amount of redundancy exists (seen

in R_Q^D for damages below 50%), and the load causing first element failure is typically higher for the damage of element 5. The measures produced for R_1 are all higher than those from $R_{k,Q}^B$ because it does not properly account for all aspects of robustness in its formulation as mentioned previously.

In summary, this example illustrates the similarities and differences between $R_{k,Q}^B$ (along with R_Q^D) and the existing measures, but most notably the improved value and utility of the new indices from Steeves and Oudah (2024a) for a practicing engineer.

3.6 Practical Application of Existing Truss Bridge Evaluation

As a practical application of an in-service bridge evaluation, the framework of analysis presented in Figure 3.1 is applied to a steel through truss based off an existing bridge in rural NS, Canada, built in 1951 and shown in Figure 3.4; the owner has requested the exact location remain confidential for this research. The truss has a height of 7.62 m and eight bays spaced at 5.718 m each.

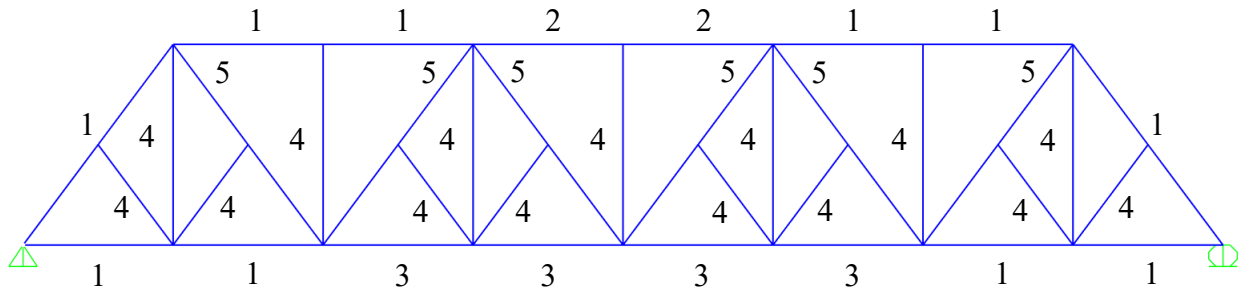


Figure 3.4 Steel through truss modeled in SAP2000 (CSI 2016) based off existing bridge in NS, Canada.

Figure 3.5 provides the section properties for each of the members labeled in Figure 3.4. The material properties for structural steel and the member capacities were achieved following CSA S6:19 (CSA 2019). For the robustness and redundancy assessment, the short brace members in each bay supporting the diagonal members of the truss were removed since they can be idealized

CHAPTER 3: PRACTICAL APPLICATIONS OF NEW INDICES

as zero-force members, although the unsupported length of the diagonal members in the plane of the truss were taken as half the length. Hinge definitions from ASCE 41-17 (ASCE 2017) were used as shown in Appendix C, with one axial hinge applied in the middle of each truss element in the FE model. Similar to the previous example of multiple damaged states, the truss bridge was evaluated against three levels of corrosion: estimated penetration depths of 0.3, 0.5, and 0.7 mm, for exposure times of 25, 50 and 75 years, respectively, were simply obtained following ISO 9223 (2012a) and 9224 (2012b). A uniform penetration depth was applied around the cross-section of all members; the limitation of applying the corrosion depth uniformly over the entire truss is that it does not account for the common variation in penetration depth and location of corrosion exhibited on real-life truss bridges. To simulate different loading conditions, the truss was pushed to collapse with both a concentrated load at midspan and a uniformly distributed load idealized as equivalent point loads along the bottom chord. A spreadsheet interface operated by MATLAB (The MathWorks, Inc. 2022) scripts was developed to automate the robustness assessments as seen in Appendix D. Figure 3.6 displays $R_{k,Q}^B$ and R_Q^D for the truss bridge subjected to the three levels of corrosion damage.

Section 1:		Section 2:	
	2 — C310x37's; 276 mm spacing between channels		2 — C310x37's; 2 — 12x230 mm plates; 276 mm spacing between channels
Section 3:		Section 4:	
	2 — C310x37's; 2 — 10x305 mm plates; 276 mm spacing between channels		W250x49
Section 5:			
	W250x67; 2 — 12x200 mm plates		

Figure 3.5 Section properties of steel through truss members referenced in Figure 3.4.

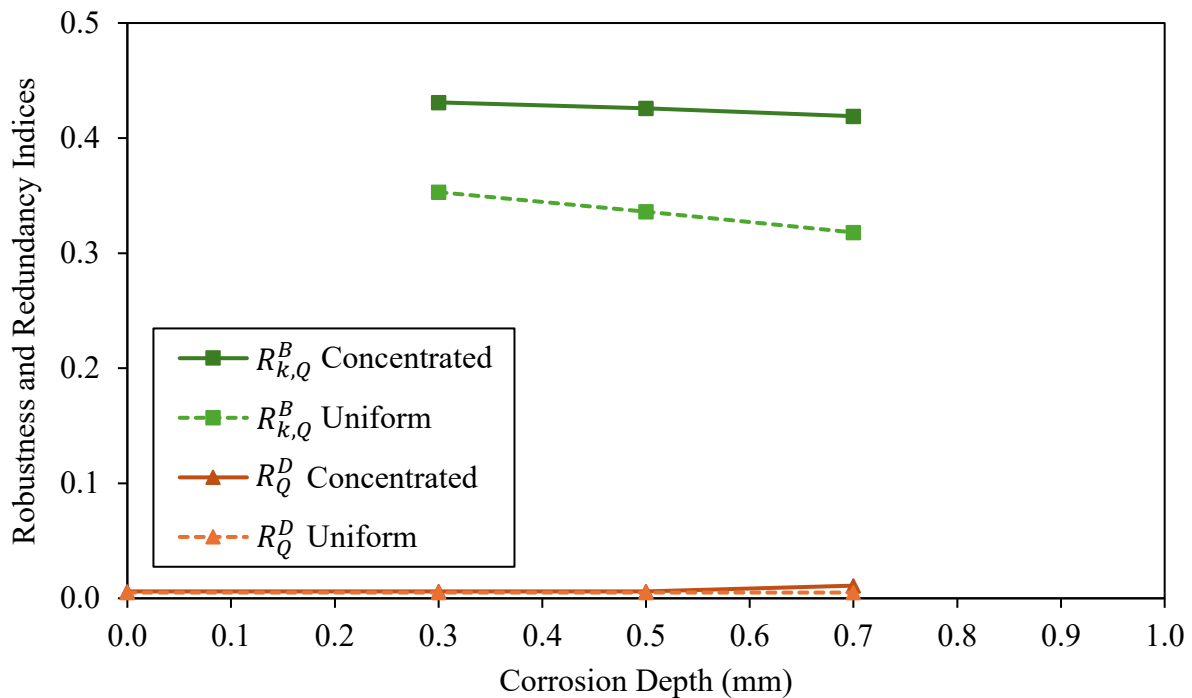


Figure 3.6 Robustness and redundancy indices for truss bridge subjected to penetration depths of 0.3, 0.5, and 0.7 mm under concentrated and uniform loading conditions.

CHAPTER 3: PRACTICAL APPLICATIONS OF NEW INDICES

As expected, the robustness indices decrease as the corrosion level increases, and the redundancy indices are near zero because the system is statically determinate. Albeit negative, the slope is shallow in part because the penetration depths under consideration cause a marginal reduction in capacity of the governing elements, and the utilization ratios for each member stay relatively constant for different damaged states: although the collapse load reduces with an increase in damage, the capacity of each member also reduces from the corrosion. Furthermore, the indices for uniform loading are typically less than those for concentrated loading: the collapse load under the former is typically higher than that under the latter, but the uniform loading case is governed by the end diagonals in compression, while the concentrated loading case is governed by the middle top chords in compression which are shorter and stockier than the former. In short, the same level of damage causes greater impact to the capacity of the end diagonals, thus reducing the robustness of the truss under uniform as opposed to concentrated loading. The truss under uniform loading is typically less utilized as well. Assuming a real-life pushdown analysis is caused by dead and live loading, the loading distribution most likely falls somewhere in between the concentrated and uniform loading case. Therefore, this study indicates that it may be more conservative to assume uniform loading for future case studies and practical applications.

The relatively flat distributions indicate that any amount of damage results in a moderate amount of robustness and near zero redundancy for either case, and the system is relatively insensitive to increases in damage over the lifespan of the bridge. From an asset management perspective, this information is helpful in projecting how damage propagation impacts the robustness and redundancy over the life-cycle of the bridge. Simply put, if the bridge happened to meet prescribed robustness and redundancy limits at an early stage of corrosion (e.g., 25-year exposure time), and if the bridge is able to maintain the required level over its lifetime similar to

the results from Figure 3.6, then the owner may decide to not repair the given structure but instead allocate resources to other bridges that are less robust to their respective damages. In the following section, a basic asset management framework is proposed to help bridge owners optimize resources to manage the safety of all structures in their bridge inventory.

3.7 Asset Management Framework

From an asset management perspective, quantifying the robustness of all structures in a given bridge inventory can help determine which bridges are the most critical for repair given budgetary constraints (this discussion will focus on robustness with the understanding that redundancy can be included as well). Figure 3.7 illustrates a simple procedure to implement the new structural robustness index and framework of analysis as an asset management tool to help owners strategically prioritize bridges for repair.

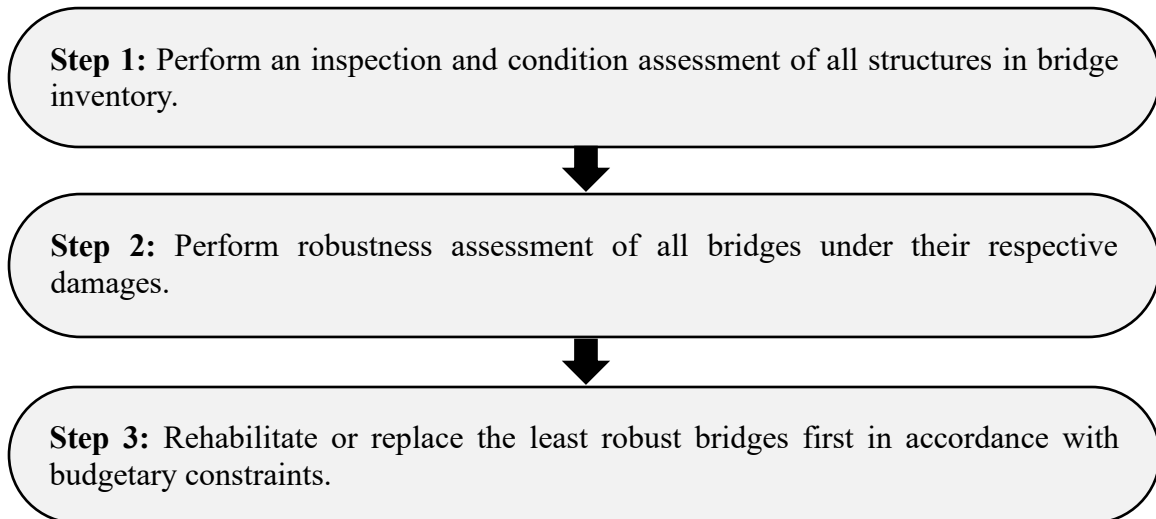


Figure 3.7 Procedure to employ structural robustness as asset management tool.

CHAPTER 3: PRACTICAL APPLICATIONS OF NEW INDICES

Provided that the engineering level of effort and associated costs are too high to assess the robustness of all bridges in the inventory, a refined procedure is presented below where global condition ratings for each bridge are obtained, through measures like the Bridge Health Index (AASHTO 2018), and then a robustness assessment is performed only on the poorly rated bridges.

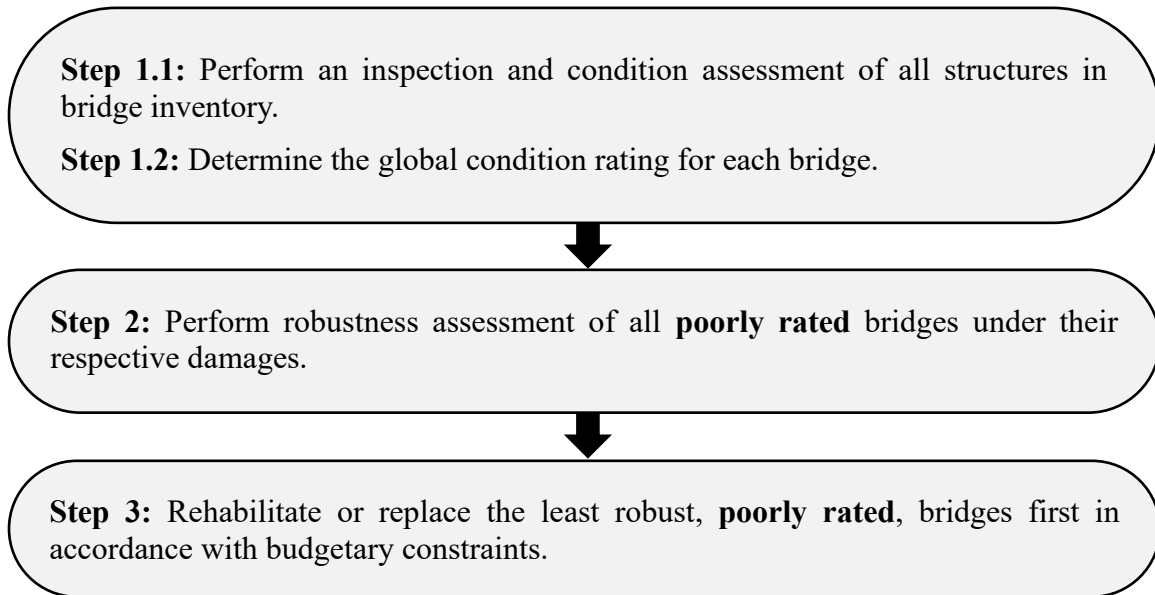


Figure 3.8 Refined procedure to employ structural robustness as asset management tool using global condition ratings.

If either of these frameworks are implemented, then the rehabilitation or replacement should improve the structural robustness under the current damage or under similar damages, respectively. To address this research gap, Chapter 4 introduces a novel optimization framework to increase the structural robustness of existing bridges while minimizing the volume of material needed for repair.

3.8 Conclusion

Many bridge collapses have occurred throughout history, with truss bridges often identified as very susceptible to failure or collapse (López et al. 2023). Although bridges play a critical role in

CHAPTER 3: PRACTICAL APPLICATIONS OF NEW INDICES

transportation networks, there is a need to improve structural assessment methods to optimize resources for evaluating and rehabilitating existing bridges across Canada. Robustness-based evaluations are needed to help make informed decisions regarding repair versus replacement of bridges and optimize upgrade schemes if the structure fails to meet prescribed robustness limits. In response, this paper applied a new holistic structural robustness index, a separate structural redundancy index, and a user-friendly framework of analysis to showcase their value and utility when evaluating truss systems.

The framework of analysis was first used on a simple square truss subjected to lateral load, and the results of which were compared with five existing robustness measures published elsewhere; the new indices were shown to be more valuable and utilitarian for practicing structural engineers. The analysis framework was then used to evaluate a bridge based off an existing truss bridge in NS, Canada, against three levels of corrosivity. As expected, the new redundancy index produced very low values for the statically determinate structure, and structural robustness decreased with increasing levels of damage; in general, the new indices present a step forward in the safety assessment of bridge infrastructure from a system level perspective. Lastly, the new indices were incorporated in an asset management framework to help owners across Canada optimize resources for the assessment and repair of bridges in their existing bridge inventory.

CHAPTER 4: NOVEL OPTIMIZATION FRAMEWORK TO MAXIMIZE THE STRUCTURAL ROBUSTNESS OF EXISTING TRUSS BRIDGES THROUGH STRATEGIC UPGRADES

4.1 Abstract

This paper presents a novel optimization framework to maximize the structural robustness and other related properties of existing truss bridges while minimizing the material volume required for upgrade. This framework is unique because it is tailored to the rehabilitation of existing truss bridges, functionally transparent and intuitive for practicing structural engineers, and applicable for any structural robustness measure(s). The utility of the novel optimization approach is showcased through a practical application on an existing steel truss bridge where the results are compared with those from a code-compliant repair achieved per CSA S6:19. Holistic structural robustness and structural redundancy indices were selected as measures to maximize. The optimum solution using the standard upgrade technique of building up members and connections provided more robustness and redundancy than the repair solution achieved per CSA S6:19 for a negligible increase in material volume. Another solution that constrained the optimum upgrade to be code-compliant provided similar results. Other upgrade techniques were investigated proving to not be as effective; nevertheless, the novel optimization algorithm was able to increase the robustness and redundancy of the damaged truss bridge for less material volume than the code-compliant solution using any of the upgrade techniques individually.

4.2 Introduction

Bridges are critical assets in transportation networks but are vulnerable to environmental and mechanical hazards (López et al. 2023); environmental damage stems from the confluence of aging infrastructure and climate change, while mechanical damage stems from man-made hazards such

CHAPTER 4: NOVEL OPTIMIZATION FRAMEWORK

as explosions or impact (Capacci et al. 2022). This is evident from the condition of existing bridges in the United States: of the 691 060 bridges recorded in the National Bridge Inventory in 2000, the Federal Highway Administration rated approximately 30% as substandard (Wardhana and Hadipriono 2003). Moreover, the 2021 ASCE Infrastructure Report Card (ASCE 2024) for bridges indicated that 7.5% of the 617 084 highway bridges in the United States were deemed structurally deficient. The Conditions and Performance Report from the Federal Highway Administration further estimated the bridge repair backlog to be \$125 billion, necessitating an increase in spending of 58%, from \$14.4 billion to \$22.7 billion annually, to improve their condition (ASCE 2024).

Compounding the issue and urgency of aging infrastructure is the occurrence of many tragic bridge failures throughout history (Wardhana and Hadipriono 2003; Lee et al. 2013; Zhang et al. 2022), in particular steel truss bridge failures where notable examples include the Quebec Bridge in 1907, the I-35W bridge in Minneapolis in 2007, and the Francis Scott Key Bridge in Baltimore in 2024 (Caredda et al. 2022). In fact, steel truss bridges are often identified as particularly vulnerable to collapse (Li et al. 2022; López et al. 2023); a study of bridge failures in the United States from 1980 to 2012 found 203 steel truss bridge failures with only 444 existing truss bridges remaining in service, where failure included total collapse, partial collapse, and distress (Lee et al. 2013). Therefore, given excessive rehabilitation costs and the history of poor bridge condition and performance, there is a need to optimize resources to provide upgrades for existing truss bridges that maximize safety and minimize cost.

The collapse of many truss bridges occurred following the loss of a critical member (Li et al. 2022), where disproportionate collapse is defined as a distinct disproportion between the initial damage and resulting magnitude of collapse (Adam et al. 2018). Often used in a similar context, progressive collapse is defined as the propagation of local failure which results in the collapse of

CHAPTER 4: NOVEL OPTIMIZATION FRAMEWORK

a significant portion of the bridge (Bhattacharya 2021). To reduce the likelihood of collapse upon local failure, a bridge requires structural robustness, defined as the intrinsic ability to absorb an initial damage and not collapse (Bhattacharya 2021). A property advocated as beneficial for robustness is redundancy (Izzuddin et al. 2008), attributed to the structural system's ability to redistribute and continue carrying load after one or more members fail (Ghosn et al. 2016). Evidenced by the extensive history of steel truss bridge collapses, properties like redundancy were generally not understood or considered in the design of steel truss bridges in the past (Li et al. 2022). These definitions relate to the global, system performance of the bridge, where quantifying the safety of a bridge requires an understanding of system behaviour and system failure (Bhattacharya 2021). As such, bridge condition ratings must first properly account for structural robustness and structural redundancy, where a more robust and redundant system should achieve a higher rating. After identifying the least robust and redundant bridges, upgrades are needed to improve their safety by increasing these critical properties.

The quantification of structural robustness through measures can aid engineers in selecting optimum upgrade solutions for existing bridges (Martinelli et al. 2024); hereafter, this paper will focus specifically on robustness with the understanding that the discussions can reasonably extend to redundancy. Although numerous structural robustness measures have been published since the 1980's, as discussed in Section 4.3.1, bridge codes such as the Canadian Highway Bridge Design Code (CHBDC), or CSA S6:19 (CSA 2019), do not provide robustness measures for bridges under any damaged state, and by extension lack tools and quantitative procedures to improve the robustness of an existing bridge under a specified damage if it is found to be unacceptably low. In general, bridge codes such as CSA S6:19 (CSA 2019) consider the probability of local failure,

while robustness considers the consequences of local failure, the latter typically more relevant to bridge condition ratings.

Several optimization frameworks have been proposed to increase the structural robustness of new building designs while minimizing cost as shown in Section 4.3.2. However, most optimization frameworks have been applied to buildings, not bridges, with none of the frameworks that were found verified for the unique application of existing truss bridges. Therefore, the objectives of this paper are to 1) develop a novel optimization framework to maximize the structural robustness along with other related properties (e.g. redundancy) of existing truss bridges while minimizing the volume of material required for upgrade, and 2) apply the framework to improve the structural robustness of a steel truss bridge based off a real-life structure located in New Brunswick (NB), Canada, and compare findings with a code-compliant rehabilitation achieved per CSA S6:19 (CSA 2019). The optimization framework employs strategic upgrades at each iteration to maximize efficiency and is adaptable for any robustness measure(s). A review of existing robustness measures along with improvement techniques will be discussed, the novel optimization framework will be introduced, and then the practical application will be completed.

4.3 Review of Existing Structural Robustness Measures and Optimization Techniques

4.3.1 Structural Robustness Measures

Over 55 structural robustness measures exist, often with terminology other than “structural robustness measure” given that definitions of robustness have evolved over time (Frangopol and Curley 1987; Ghosn and Moses 1998; Ghosn et al. 2016; Bhattacharya 2021; Steeves and Oudah 2024a). Robustness measures can be classified as either deterministic, probabilistic, or risk-based. Representative robustness measures from each of these categories are presented below, followed

by a discussion on the advantages and disadvantages of each. Refer to Chapter 2 (Steeves and Oudah 2024a) for a comprehensive review of existing structural robustness measures.

Deterministic: holistic structural robustness index (Steeves and Oudah 2024a):

$$R_{k,Q}^B = \left[\frac{\sum_{i=1}^{i=n} EL_i^{Ideal,D} - \sum_{i=1}^{i=n} EL_i^{Deviatoric,D}}{\sum_{i=1}^{i=n} EL_i^{\max(Target,D|I, Ideal,D)}} \right] \cdot \left[\frac{\sum_{i=1}^{i=n} UR_i^{Ideal,D} - \sum_{i=1}^{i=n} UR_i^{Deviatoric,D}}{\sum_{i=1}^{i=n} UR_i^{Target,D|I}} \right] \cdot \left[\min \left(\left(\frac{D_D^S}{D_I^S} \right), 1 \right) \right] \quad (4.1)$$

The first term relates to the external loads, EL , of the damaged bridge with respect to the intact version, the second term accounts for utilization ratios, UR , for each element of the structure in a similar manner, and the third term accounts for system ductility, D^S (Steeves and Oudah 2024a); Eq. (4.1) has a slight modification to the formulation presented by Steeves and Oudah (2024a) in Chapter 2, where the denominator of the first term equals the area beneath the maximum of the Target (Target, D|I) and Damaged Ideal (Ideal, D) distributions. This modification is invoked in the event that the index is utilized to upgrade existing bridges, potentially causing the collapse load of the upgraded bridge to surpass the collapse load of the intact system (Steeves and Oudah 2024a).

After distinguishing the concepts of robustness and redundancy, Steeves and Oudah (2024a) also formulated a holistic structural redundancy index, presented in Eq. (4.2).

$$R_Q^D = \left[\frac{\sum_{i=1^{st} EL}^{i=n} EL_i^{Ideal} - \sum_{i=1^{st} EL}^{i=n} EL_i^{1^{st} EL} - \sum_{i=1^{st} EL}^{i=n} EL_i^{Deviatoric}}{\sum_{i=1^{st} EL}^{i=n} EL_i^{\max(Target,Ideal)} - \sum_{i=1^{st} EL}^{i=n} EL_i^{1^{st} EL}} \right] \cdot \left[\frac{\sum_{i=1^{st} EL}^{i=n} UR_i^{Ideal} - \sum_{i=1^{st} EL}^{i=n} UR_i^{Deviatoric}}{\sum_{i=1^{st} EL}^{i=n} UR_i^{Target}} \right] \quad (4.2)$$

Similar to Eq. (4.1), the first term relates to the external loads, EL , and the second term contains utilization ratios, UR ; however, this index does not distinguish between damaged and intact

CHAPTER 4: NOVEL OPTIMIZATION FRAMEWORK

systems and as such is applied separately to both (Steeves and Oudah 2024a). Specific details regarding the formulation are included in Chapter 2.

Probabilistic: structural robustness index (Bhattacharya 2021):

$$R_k^B = \exp\left(-\frac{\beta - \beta'_k}{\beta}\right) \quad (4.3)$$

β is the reliability index of the intact system, and β'_k is the reliability index conditioned on the loss of element k (Bhattacharya 2021).

Risk-based: robustness index (Baker et al. 2008):

$$I_{Rob} = \frac{R_{Dir}}{R_{Dir} + R_{Ind}} \quad (4.4)$$

R_{Dir} is the direct risk associated with a given damage scenario, and R_{Ind} is the indirect risk associated with said damage (Baker et al. 2008).

The three measures defined above are bounded between zero and one allowing simple comparisons to be made with different damages and other bridges. The deterministic indices from Steeves and Oudah (2024a) were formulated to provide a balance between simplicity, calculability, and expressiveness as per the recommendation of Starossek and Haberland (2011) for the formulation of robustness measures. They are simple because they use concepts familiar to structural engineers, and expressive because they account for the performance of all elements of the bridge in a quantifiable manner. Furthermore, the aforementioned indices are quantified following a user-friendly framework of analysis to maintain calculability (Steeves and Oudah 2024a). Unlike these deterministic measures, probabilistic and risk-based robustness measures, as in Eqs. (4.3) and (4.4), account for the aleatoric uncertainties associated with loads and resistances; although more expressive in this sense, these measures can be computationally onerous, limiting

their calculability. Lastly, Steeves and Oudah (2024a) are the only researchers to distinguish between robustness and redundancy within their index formulations. Based on the comparison between deterministic, probabilistic, and risk-based measures, the deterministic indices introduced by Steeves and Oudah (2024a) are used in this paper through the novel optimization framework for the practical application presented in Section 4.5.

4.3.2 Existing Guidelines and Optimization Techniques to Improve Structural Robustness

Strategies to improve the collapse resistance of bridges have been explored, such as improving the local resistance of critical elements, ensuring multiple load paths after some damage has occurred, and isolation by compartmentalization to prevent a chain reaction of failures impacting the entire system (Starossek 2006; Wang and Zhou 2012). Furthermore, Ghosn and Moses (1998) introduced an approach to measure bridge redundancy through system reserve ratios following an incremental structural analysis, then completed a system reliability calibration to determine the required ratios based on the performance of bridges known to be redundant. This led to the development of system factors to be applied to the factored member resistance in the Load and Resistance Factor Design (LRFD) equation which captures the level of safety and redundancy of the bridge: a system factor greater than one implies a sufficient level of redundancy, whereas a system factor less than one indicates insufficient redundancy. To improve bridge redundancy, Ghosn and Moses (1998) proposed changing the geometric configuration of the bridge by adding members or strengthening the members of the bridge through the application of the system factors. For the evaluation of existing bridges, the system factors can also be used to calculate rating factors if the members cannot be strengthened (Ghosn and Moses 1998). Consequently, system factors have been integrated into the Manual for Bridge Evaluation in the United States (AASHTO 2018).

CHAPTER 4: NOVEL OPTIMIZATION FRAMEWORK

Furthermore, several optimization frameworks have been introduced in literature to maximize robustness while minimizing cost. Mondoro et al. (2018) proposed three different bi-objective optimization formulations to determine the optimal strategy for bridge adaptation under climate change, where the optimal strategy includes adaptation action and time of application. A robustness index related to the payoff for each adaptation strategy was invoked in one of the optimization approaches, and the three formulations were applied in the adaptation of a riverine bridge under the climate hazard of flooding (Mondoro et al. 2018). Related to buildings, El Hajj Diab et al. (2022) proposed a strategy to assess robustness through bi-objective optimization problems using two new structural robustness measures (i.e., failure propagation index and energy index) in order to identify critical failure scenarios. The structural robustness of a steel-framed building was investigated under 190 local failure scenarios consisting of column removals, followed by an assessment of four upgrade schemes to improve the robustness of the design configuration (El Hajj Diab et al. 2022). Also, Praxedes and Yuan (2022) presented a new robustness-oriented design method involving a bi-objective optimization that maximizes a risk-based robustness index while minimizing additional longitudinal reinforcement for reinforced concrete frame structures under a column removal scenario. Lastly, Charmpis and Kontogiannis (2016) explored the increase in cost associated with satisfying requirements for progressive collapse resistance in structural design through an optimization approach that enforces robustness and standard code design constraints while aiming to minimize structural cost. The structural optimization approach was tested on two elastoplastic steel frames under column loss scenarios by optimizing the dimensions of structural members in the frames (Charmpis and Kontogiannis 2016).

Evidently there have been optimization approaches proposed to increase the robustness of structures under local damage, but many frameworks focus on new design instead of structural

rehabilitation, and the majority of research revolves around buildings, not bridges. Stemming from this literature review, a research gap related to the lack of user-friendly optimization frameworks for truss bridges is identified. The research gap is addressed by proposing a user-friendly optimization framework that is 1) designed to maximize the structural robustness of existing truss bridges by optimizing upgrade schemes, 2) functionally transparent and intuitive by strategically targeting failed elements to upgrade, and 3) adaptable for any structural robustness measure.

4.4 Formulation of Novel Optimization Framework

From a consulting engineering perspective, to increase the structural robustness of an existing bridge under a specific damage, the proposed upgrade must be cost-effective and practical. Stemming from this logic, it is important to optimize upgrade schemes to maximize structural robustness while minimizing the cost of repair and consider upgrades that are simple, practical, and constructable. Typically, optimization problems require one or more objective functions subject to a number of constraints to generate optimum solutions (Briggs et al. 2015). The novel framework proposed in this paper aims to maximize any number of structural robustness measures while minimizing the material volume, V , required for upgrade; material volume is considered a quasi-representative measure of cost in this research, where the cost of structural repairs typically includes other factors such as mobilization of contractor, ease of installation, etc. Figure 4.1 displays the functionality and constraints of the novel optimization framework.

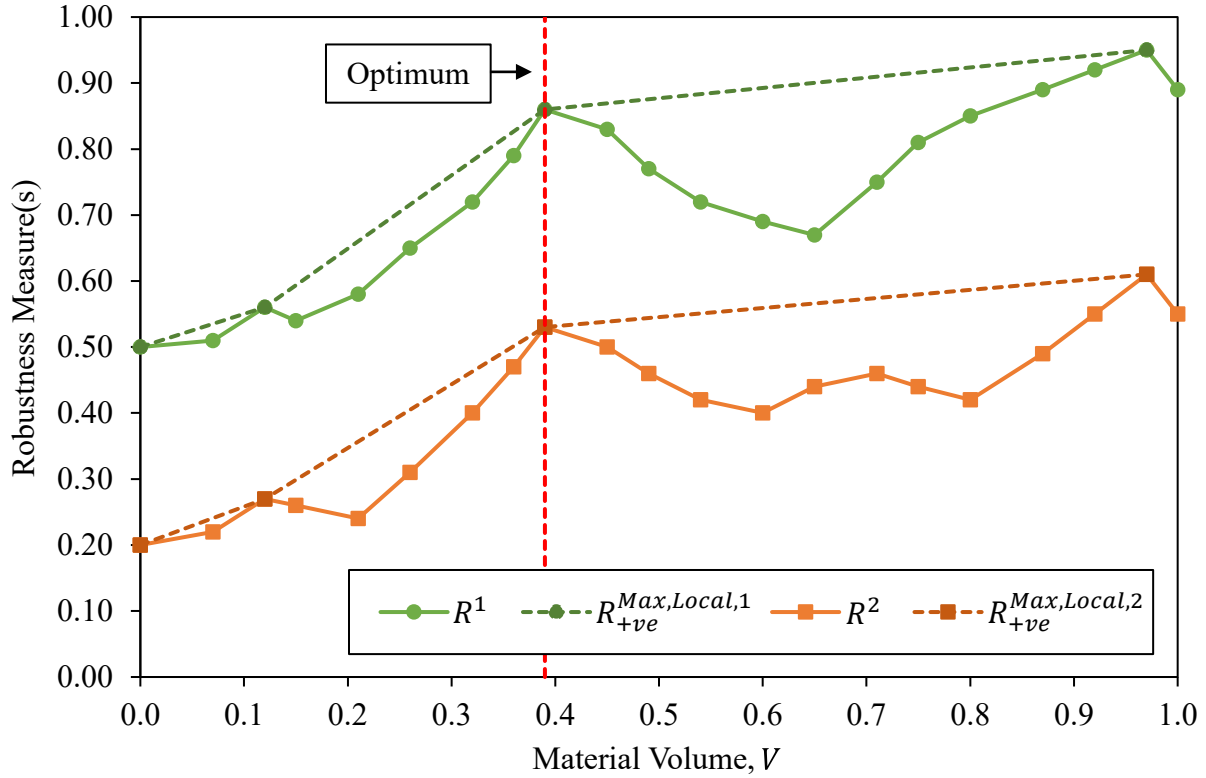


Figure 4.1 Hypothetical output from novel optimization framework to showcase functionality and constraints.

Figure 4.1 presents a plot of robustness versus material volume for an arbitrary truss bridge, where in this case two different robustness measures are being investigated with the understanding that the framework can accommodate any number of robustness or other related measures at the same time (e.g., robustness and redundancy indices from Steeves and Oudah (2024a)). Every data point for the two robustness measures (i.e., R^1 and R^2), except for the initial values intercepting the y-axis associated with the damaged system, represent upgrades applied to the bridge. The distribution of $R_{+ve}^{Max,Local}$ for each measure starts at the y-intercept value and follows the local maximums that result in an increase in robustness, thereby skipping the local maximums that do not provide an increase. The slope of this distribution between increasing local maximums provides the constraint for the novel framework: the slope of each segment must be greater than or equal to the slope in

the previous segment. In short, the optimum value (indicated by the dashed, vertical red line in Figure 4.1), labeled “Optimum”, is achieved when the slope of the $R_{+ve}^{Max,Local}$ distribution beyond the material volume under consideration is less than the slope of the preceding segment. Optimum essentially maximizes the return on investment (ROI), $\frac{\Delta R_{+ve}^{Max,Local}}{\Delta V}$, so that when the ROI does not improve, the algorithm terminates. Moreover, the ROI must improve for all measures for the optimization to continue. If more than one measure is being optimized, the increasing local maximum values must correspond to the same material volume; provided this is not a realistic constraint, a *tolerance* can be applied to the material volume on a case-by-case basis as seen in the mathematical formulation presented below.

Stemming from this discussion, the formulation for the new multi-objective optimization framework is presented in Eq. (4.5).

$$Find V^{Opt} \tag{4.5}$$

that maximizes $R^j(V)$, for $j = 1, \dots, n$

that minimizes V

$$subject\ to\ \frac{\Delta R_{+ve}^{Max,Local,j}}{\Delta V_i} [dV - \Delta V_i, dV] \leq \frac{\Delta R_{+ve}^{Max,Local,j}}{\Delta V_{i+1}} [dV, dV + \Delta V_{i+1}],$$

$$for\ j = 1, \dots, n$$

$$where\ \frac{\Delta R_{+ve}^{Max,Local}}{\Delta V} [V, V + \Delta V] = \frac{R_{+ve}^{Max,Local}(V + \Delta V) - R_{+ve}^{Max,Local}(V)}{\Delta V},$$

$$and\ dV = V_i \pm \left(\frac{tolerance}{100} \right) * V_i$$

The proposed algorithm searches for V^{Opt} , which is the optimum material volume to maximize structural robustness. The *tolerance* is input as a percentage in this formulation, the value of

CHAPTER 4: NOVEL OPTIMIZATION FRAMEWORK

which depends on the studied bridge. Generally, the objective functions are to maximize $R^j(V)$, for $j = 1, \dots, n$, where n is the number of robustness or other related measures being optimized, and to minimize volume, V . The minimization happens 1) by always selecting the next available (and therefore cheapest) upgrade to apply to the damaged structure, and 2) by constraining the optimization to maximize ROI.

Figure 4.2 illustrates the novel optimization framework developed in this research, broken down into five steps. Step 1 involves a structural robustness assessment of the damaged bridge, where a recommended framework of analysis was introduced by Steeves and Oudah (2024a) in Chapter 2: the analysis framework simply includes incremental static pushdown analyses of finite element (FE) models with nonlinear hinge definitions. In Step 2, the damaged bridge is rehabilitated by strategically upgrading the element that failed first in the collapse simulation to maximize efficiency; for this paper element failure refers to the first hinge that loses its ultimate capacity following the framework provided by Steeves and Oudah (2024a). For Step 3, Steps 1 and 2 are repeated until two increasing local maximums are obtained. The constraint is then checked in Step 4, and Step 5 evaluates whether the optimum material volume has been achieved, or if more iterations are required. Evidently, results from this novel optimization framework depend on the definition of element failure used to identify elements to upgrade in Step 2. Lastly, although this framework has been tailored to truss bridges, it can be reformulated to optimize upgrades for other bridge and structure types as well.

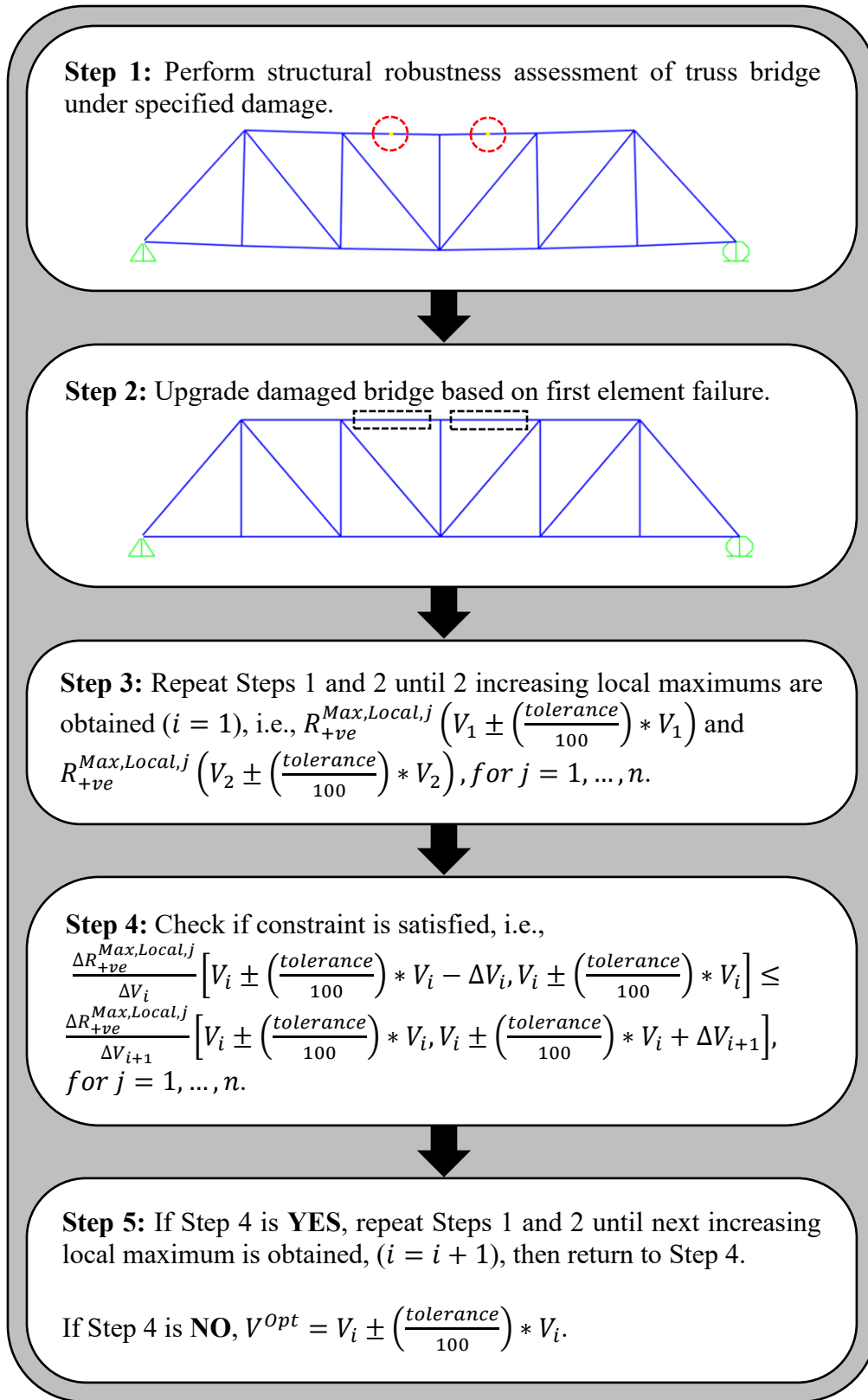


Figure 4.2 Novel optimization framework to upgrade damaged truss bridges.

4.5 Practical Application of Existing Steel Truss Bridge Upgrade

4.5.1 Bridge Overview

The novel optimization framework and CSA S6:19 (CSA 2019) are employed separately to evaluate and upgrade/repair a steel truss bridge subjected to a 75-year corrosion level: corrosion has been identified as the major cause of deterioration in steel bridges (AASHTO 2018), and 75 years corresponds to the design service life of a new bridge following CSA S6:19 (CSA 2019). A corrosion penetration depth of 0.4 mm obtained following ISO 9223 (2012a) and ISO 9224 (2012b) was applied uniformly to all members and on one side of each gusset plate. The bridge is based off an existing truss built in 1930 located in rural NB, Canada. Figure 4.3 displays an FE model of the bridge in SAP2000 (CSI 2016) where each of the members and connections have been labeled; section properties for the members and connections are provided in Table 4.1. The height of the truss is 6.096 m, with each bay measuring 5.22 m horizontally.

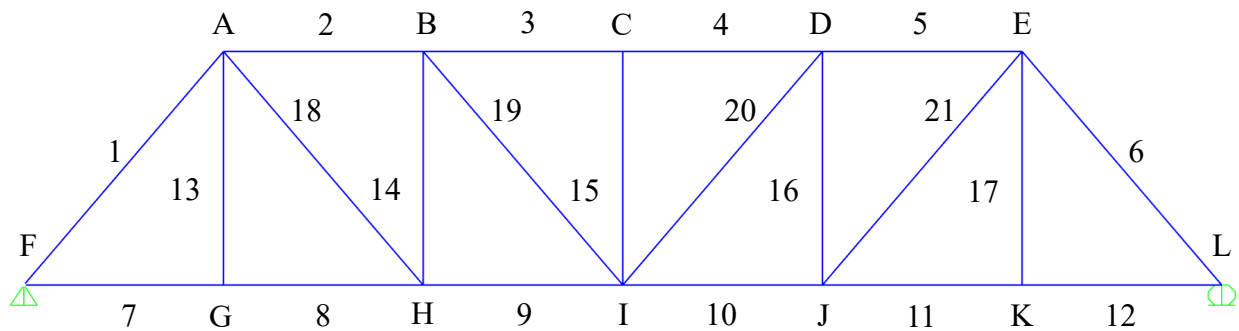


Figure 4.3 Steel truss bridge based off real-life structure in NB, Canada.

Table 4.1 Section properties associated with structural members and connections from steel truss bridge in Figure 4.3.

Member and Connection Type	Section Properties (inches, unless otherwise noted)
Top Chord — 2, 3, 4, 5	2 — 8 x 2 3/8 x 5/16 C @ 13.75 lb/ft spaced at 8 7/8
End Diagonal — 1, 6	2 — 8 x 2 3/8 x 3/8 C @ 16.25 lb/ft spaced at 8 7/8
Diagonal — 18, 19, 20, 21	8 x 6 1/2 M @ 30.5 lb/ft
Vertical — 13, 14, 15, 16, 17	8 x 6 1/2 M @ 30.5 lb/ft
Bottom Chord — 7, 8, 9, 10, 11, 12	8 x 6 1/2 M @ 30.5 lb/ft
Top Connection — A, E	Thickness of 3/8, total area of 477379 mm ²
Top Connection — B, D	Thickness of 3/8, total area of 191653 mm ²
Top Connection — C	Thickness of 3/8, total area of 192213 mm ²
Bottom Connection — F, L	Thickness of 3/8, total area of 682505 mm ²
Bottom Connection — G, K	Thickness of 3/8, total area of 296116 mm ²
Bottom Connection — H, J	Thickness of 3/8, total area of 445724 mm ²
Bottom Connection — I	Thickness of 3/8, total area of 395723 mm ²

Member and local connection capacities were obtained following guidance from CSA S6:19 (CSA 2019) and the Manual for Bridge Evaluation (AASHTO 2018). Connection and member geometry were obtained from existing drawings, while material properties were taken from CSA S6:19 (CSA 2019); the owner has requested the detailed drawing package remain confidential for this research. From CSA S6:19 (CSA 2019), the bridge was evaluated following Section 14 against dead loads and evaluation level 3 live loads with a uniformly distributed load attributed to a Class C highway. The results of the truss bridge evaluation achieved per Section 14 of CSA S6:19 (CSA 2019) are displayed in Table 4.2 where the critical members and connections are presented along with their governing failure mode and factored utilization ratios, UR_f .

Table 4.2 Evaluation results for truss bridge achieved per CSA S6:19 (CSA 2019).

Element	Failure Mode	Utilization Ratio, UR_f
Top Chord — 2, 5	Buckling — Compression	1.92
Top Chord — 3, 4	Buckling — Compression	2.15
End Diagonal — 1, 6	Buckling — Compression	1.91
Connection — C	Shearing of rivets — Compression	1.02
Connection — F, L	Yielding of partial shear plane — Compression	1.05

4.5.2 Upgrade Methodology and Techniques

The novel optimization framework was applied on the damaged truss bridge to maximize its structural robustness and redundancy, where for this example, the structural robustness index ($R_{k,Q}^B$) and structural redundancy index (R_Q^D) from Eqs. (4.1) and (4.2) were selected as measures to maximize, and *tolerance* was set to zero. All evaluations and robustness assessments were completed using a spreadsheet interface in Excel operated by MATLAB (The MathWorks, Inc. 2022) scripts to help automate and expedite computations. Two sample calculations are provided as seen in Appendix D, one for the CSA S6:19 (CSA 2019) evaluation and robustness assessment of the damaged truss, and the other for the first upgrade achieved using the novel optimization framework discussed in Section 4.5.3. Connection capacity calculations for the steel truss bridge can be reviewed in Appendix E.

For the nonlinear FE analyses required for the novel framework, hinge definitions from ASCE 41-17 (ASCE 2017) were used for member capacities, while simple brittle hinge definitions were used for connection capacities, where generalized hinge definitions from ASCE 41-17 are provided in Appendix C. Member hinges were assigned at the middle of the element, and connection hinges were assigned at the ends. SAP2000 Version 21.0.2 (CSI 2016) was used to perform the collapse

CHAPTER 4: NOVEL OPTIMIZATION FRAMEWORK

simulations, and the bridge was pushed to collapse using a uniformly distributed load represented as point loads applied to the bottom chord of the truss.

Four rehabilitation techniques were investigated to upgrade the steel truss bridge through the novel optimization framework as summarized in Table 4.3: Built-Up, In-Plane Support, New Members, and Hybrid. These techniques represent practical options typically investigated by bridge engineers to upgrade existing bridges. The upgrade configurations and analysis results are presented in the following sections: given that code-compliant solutions often invoke Built-Up as an upgrade technique, Section 4.5.3 provides a comparison between the rehabilitations from CSA S6:19 (CSA 2019) and the novel optimization framework using the Built-Up technique, while Section 4.5.4 explores the results from Built-Up compared with the alternative techniques from Table 4.3.

Table 4.3 Description of different upgrade techniques used in practical application.

#	Upgrade Technique Label	Description
1	Built-Up	Standard technique of building up members and connections
2	In-Plane Support	Adding members to the truss to reduce the effective length of compression members
3	New Members	Adding new structural members to the system intended to support load
4	Hybrid	Any combination of techniques 1, 2, or 3

All upgrades were assumed to be fully active for simplicity, implying the entire rehabilitated member carries the load effect (e.g., effect from dead and live load from CSA S6:19 (CSA 2019)) uniformly. Practical discretization in the various upgrade schemes was accounted for using the next available, preferred plate thicknesses provided in the Handbook of Steel Construction (CISC 2021). To save computational cost for every iteration within the novel optimization framework, the volume of material needed to upgrade the connections was estimated instead of obtained from

engineering detailing. The approach developed for this paper was to increase the thickness of the gusset plate under consideration in proportion to the strength increase required to move the failure mode to the member, stemming from the logic that many of the local connection capacity checks are proportional or approximately proportional to the thickness of the connection plate (AASHTO 2018; CSA 2019). From there, the increase in volume can be calculated using the connection areas in Table 4.1.

4.5.3 Results Using the Built-Up Technique

Figure 4.4 displays the results of the novel optimization framework using the Built-Up upgrade technique. $R_{k,Q}^B$ and R_Q^D for the code-compliant CSA S6:19 (CSA 2019) repair are also plotted as single data points to facilitate a comparison; to repair the bridge per the code, the relevant connection capacities were increased, and the top chords and end diagonals were built up with 7 x 350 mm continuous cover plates to satisfy UR_f and new design requirements.

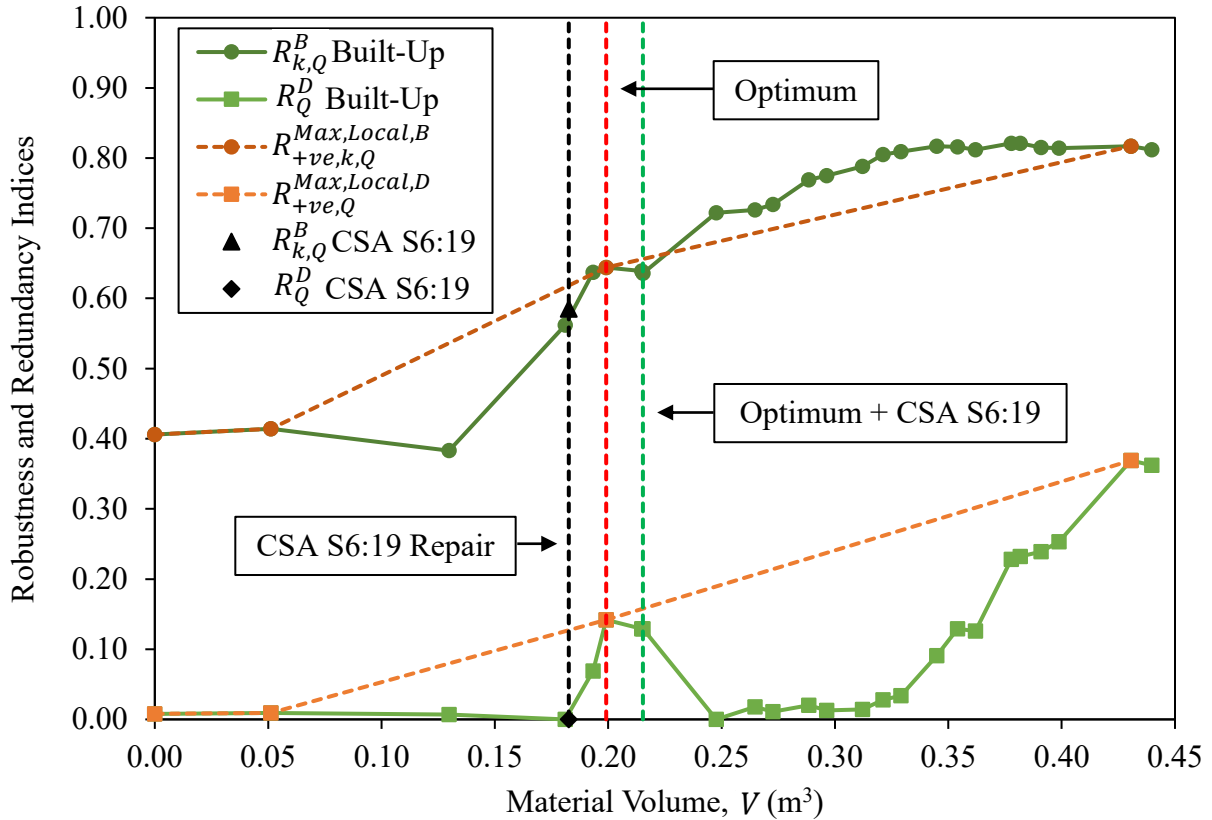


Figure 4.4 Robustness and redundancy versus material volume achieved from novel optimization framework and CSA S6:19 (CSA 2019) using Built-Up technique.

The results from Steps 1 and 2 from the framework presented in Figure 4.2 are shown by the $R_{k,Q}^B$ Built-Up and R_Q^D Built-Up distributions, while the constraint outlined in Step 4 of the framework is shown as the $R_{+ve,k,Q}^{Max,Local,B}$ and $R_{+ve,Q}^{Max,Local,D}$ distributions for robustness and redundancy, respectively. There are three dashed, vertical lines in the figure. The first dashed, vertical line (black) aligns with the CSA S6:19 (CSA 2019) repair solution, labeled “CSA S6:19 Repair”, the second (red) aligns with the optimum solution following the novel framework, labeled “Optimum”, and the third (green) aligns with the first code-compliant solution per CSA S6:19 (CSA 2019) achieved following the novel optimization approach, implying that the UR_f 's are less than or equal to one for all members and connections under the loads imposed for the CSA S6:19

(CSA 2019) evaluation, labeled “Optimum + CSA S6:19”. Noteworthy in Figure 4.4 is how Optimum maximizes the ROI for robustness thus terminating the algorithm, but the ROI for redundancy is still improving. Table 4.4 summarizes $R_{k,Q}^B$, R_Q^D , and the material volume, V , associated with the three aforementioned options along with the damaged state.

Table 4.4 Structural robustness, structural redundancy, and upgrade material volume of damaged condition and three upgrade solutions using Built-Up technique.

Solution	$R_{k,Q}^B$	R_Q^D	V (m ³)
Optimum + CSA S6:19	0.636	0.129	0.2153
Optimum	0.644	0.142	0.1991
CSA S6:19 Repair	0.585	0.000	0.1826
Damaged	0.406	0.008	0.0000

Table 4.4 illustrates that all three upgrade options increase $R_{k,Q}^B$ and R_Q^D with respect to the damaged system, except for CSA S6:19 Repair which has zero redundancy. Compared with CSA S6:19 Repair, Optimum gains 10% more robustness and achieves a redundancy value of 0.142 instead of 0 for 9% more material volume. For 18% more material volume, Optimum + CSA S6:19 provides 9% more robustness and increases the redundancy from 0 to 0.129 as compared with CSA S6:19 Repair. The performance of CSA S6:19 Repair is governed by the simultaneous brittle failures of bottom connection — F and L from the load effect in the end diagonals, while the first hinge formation in the two optimum solutions occurs simultaneously in bottom chord 9 and 10 which are in tension, allowing the system to experience strain hardening. This concept is reinforced through Figure 4.5 which shows the global force-displacement curves for each of the three rehabilitation options presented in Table 4.4.

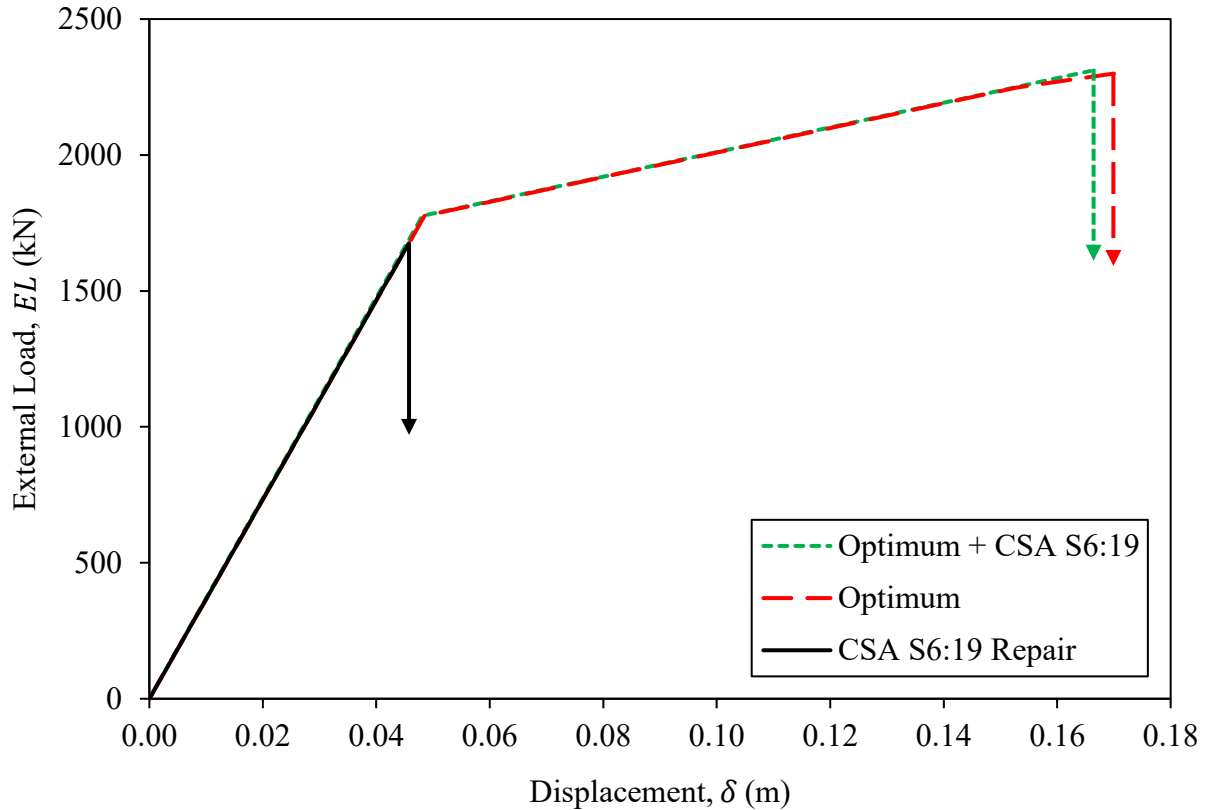


Figure 4.5 Global force-displacement curves for three upgrade solutions from Table 4.4.

Figure 4.5 clearly depicts the brittle failure mode of CSA S6:19 Repair, while the other two exhibit strain hardening at the system level after a reduction in stiffness. The increase in displacement between Optimum + CSA S6:19 and Optimum compared with CSA S6:19 Repair is approximately 262% and 273%, respectively. Also noteworthy is the increase in collapse load for Optimum + CSA S6:19 and Optimum compared with CSA S6:19 Repair, specifically 38% and 37%, respectively. Stemming from this observation, the following figure provides the increase in collapse load for each of the optimization trials along with the code-compliant solution, again using the same dashed, vertical lines to identify the three upgrade options:

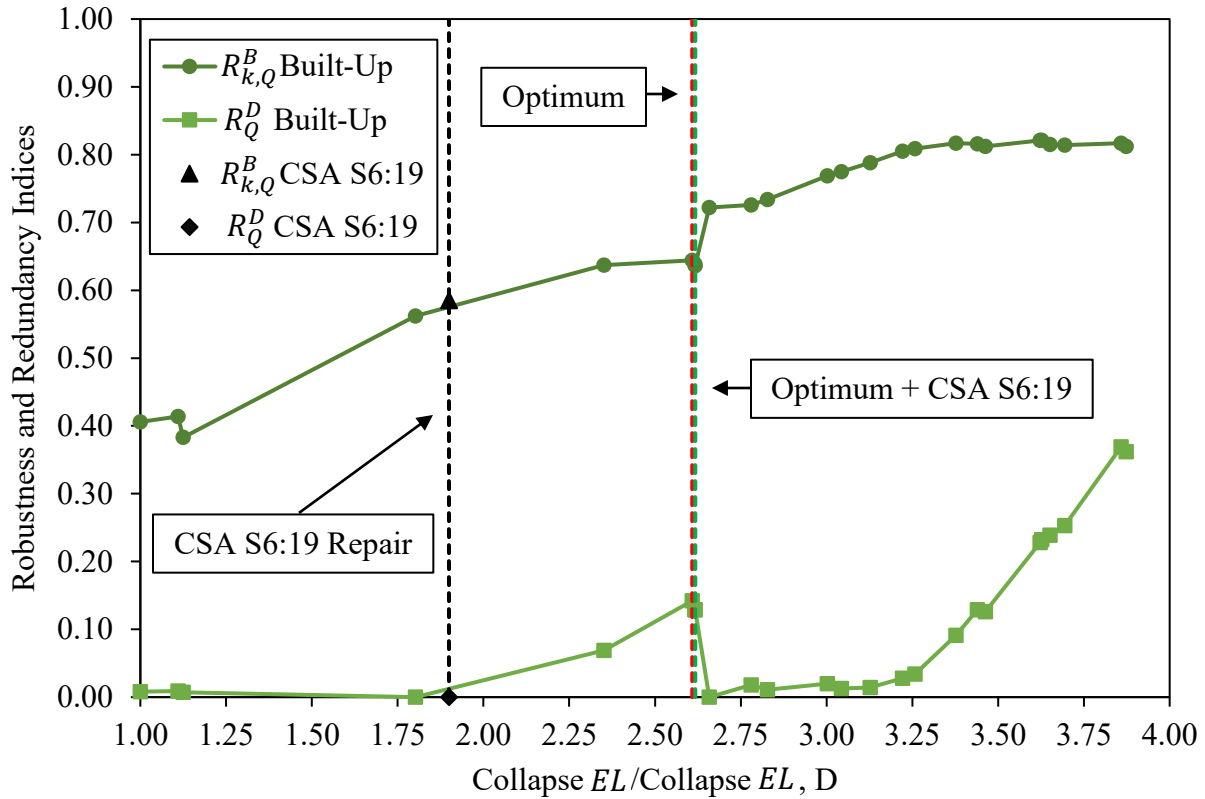


Figure 4.6 Robustness and redundancy versus increase in collapse load achieved from novel optimization framework and CSA S6:19 (CSA 2019) using Built-Up technique.

Comparing the novel optimization versus code procedures with the Built-Up technique, the recommended option is certainly Optimum from a robustness and redundancy perspective; however, given an interest from an owner to keep the rehabilitation compliant per CSA S6:19 (CSA 2019), the novel optimization framework provides another solution that satisfies this requirement and still yields improved robustness and redundancy, namely Optimum + CSA S6:19.

4.5.4 Results Using the In-Plane Support, New Members, and Hybrid Techniques

Figure 4.7 displays the results of the In-Plane Support, New Members, and Hybrid upgrade techniques included in Table 4.3 along with the first portion of the Built-Up technique from Figure 4.4 for the sake of comparison (V ranging from zero to 0.27 m^3). The upgrade configurations

associated with In-Plane Support and New Members labeled in Figure 4.7 are schematically illustrated in Figure 4.8. The members added to the truss system were HSS 203x203x6.4's with a material grade of 350W. In-Plane Support and New Members were investigated through the novel optimization framework in Figure 4.2 by adding supports or members nearest to first element failure in order to satisfy Step 2. This results in three iterations for In-Plane Support, and two for New Members. From there, the Hybrid technique was used by invoking Built-Up for the next iteration. The optimization was terminated after one iteration using the Hybrid technique for both cases (i.e., In-Plane Support + Hybrid and New Members + Hybrid) because they both passed Optimum (dashed, vertical red line in Figure 4.7) without providing an improvement in robustness or redundancy.

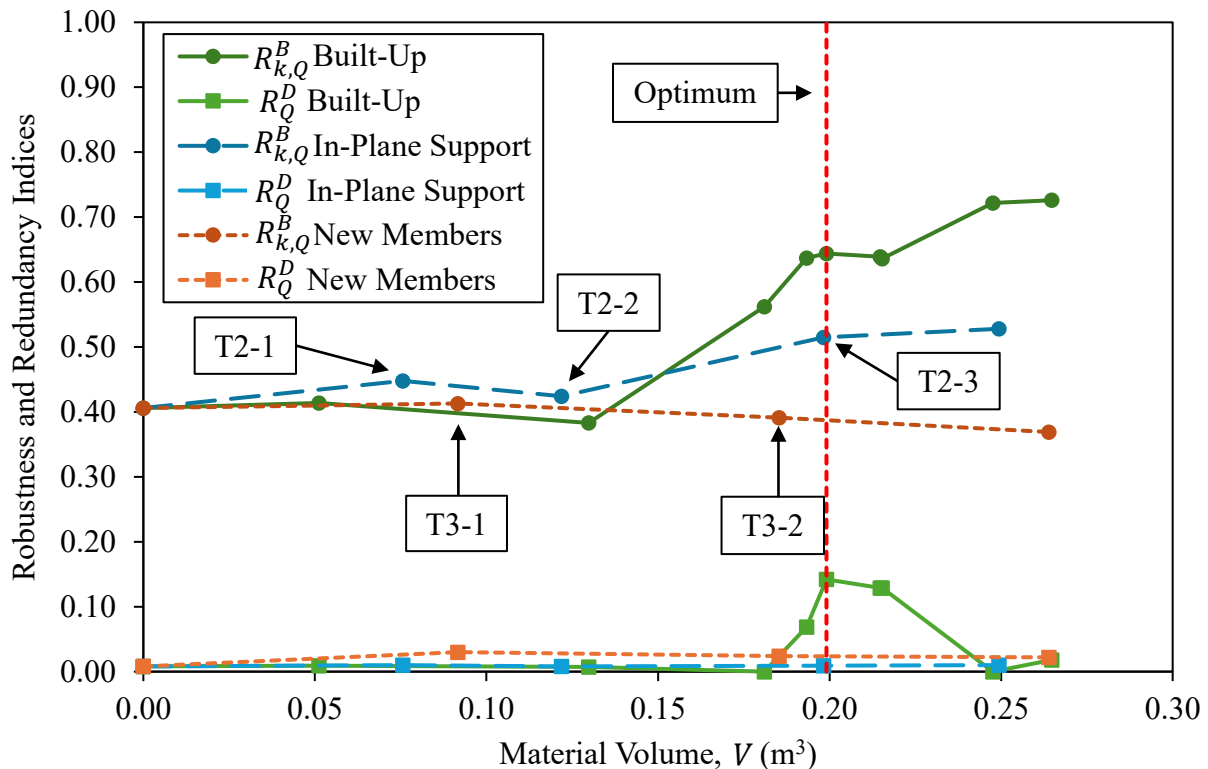


Figure 4.7 Robustness and redundancy versus material volume achieved from novel optimization framework using all upgrade techniques from Table 4.3.

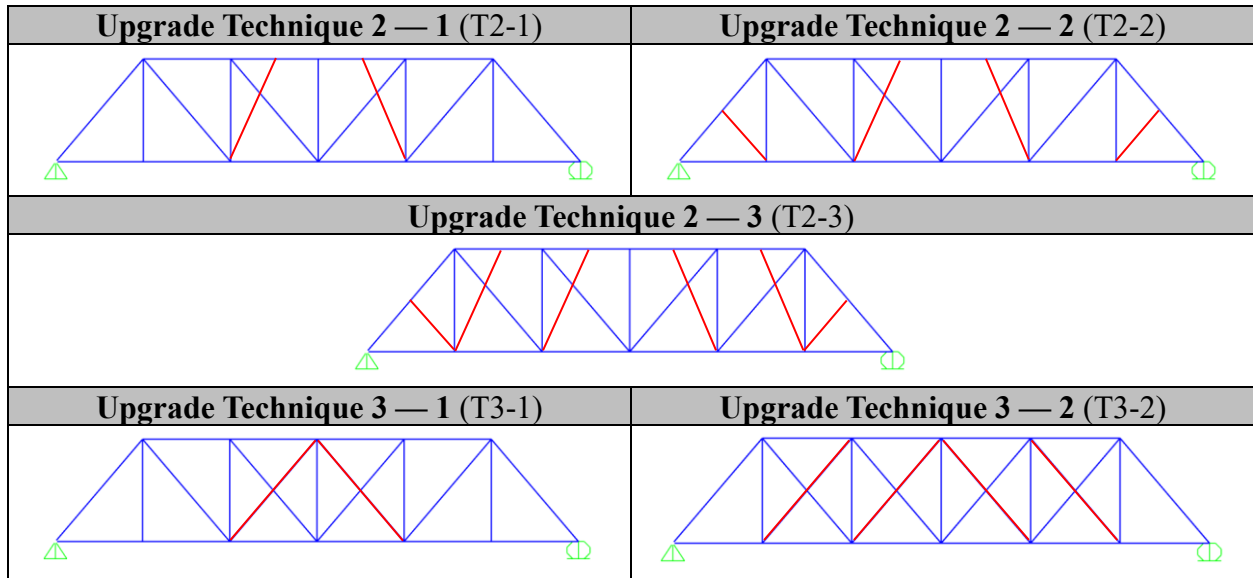


Figure 4.8 Configurations of In-Plane Support and New Members upgrade techniques.

Figure 4.9 provides the robustness and redundancy versus an increase in collapse load for all the upgrade techniques from Table 4.3, showing Optimum as a dashed, vertical red line. Evidently, Built-Up is much more effective in increasing the global capacity of the system than In-Plane Support, New Members, or Hybrid: with a V of 0.27 m^3 , Built-Up provides a 74% greater capacity than In-Plane Support + Hybrid, and a 147% greater capacity than New Members + Hybrid.

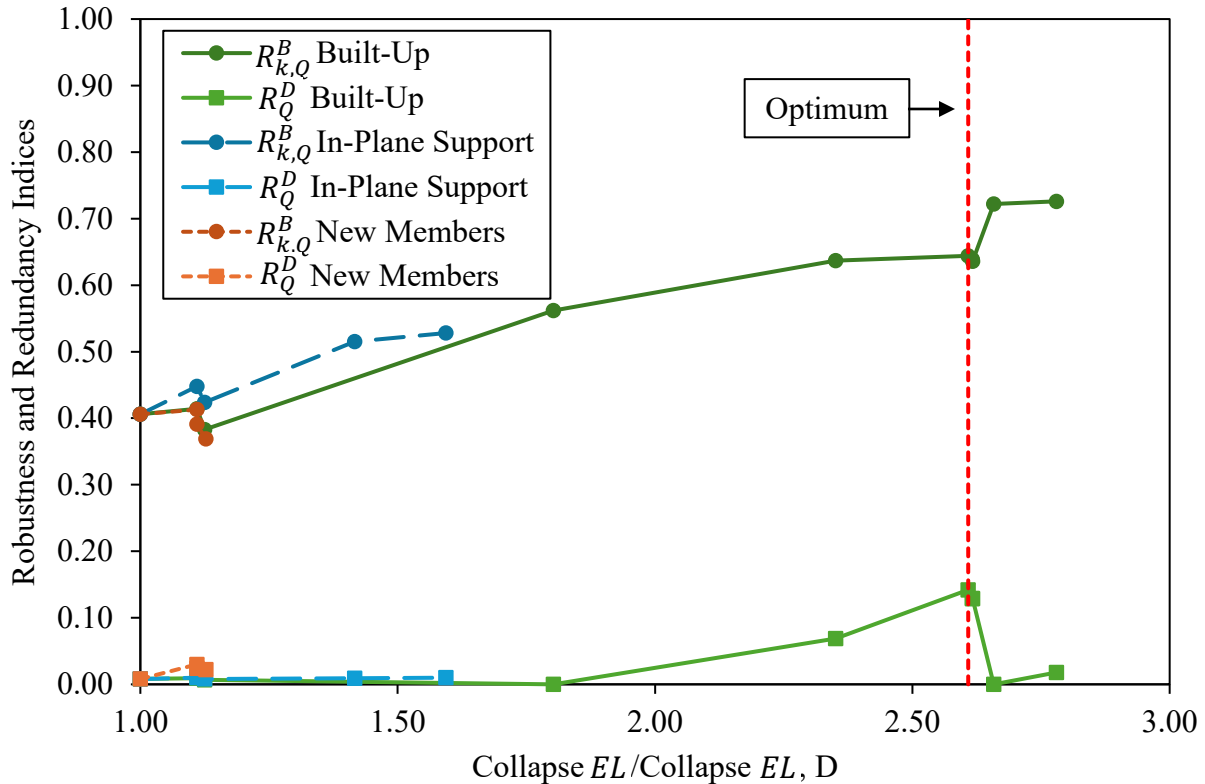


Figure 4.9 Robustness and redundancy versus increase in collapse load achieved from novel optimization framework using all upgrade techniques from Table 4.3.

In general, Figures 4.7 and 4.9 indicate that at least in the early stages of optimization, In-Plane Support, New Members, and Hybrid are not as effective in improving structural robustness and structural redundancy as Built-Up: starting with Optimum from Built-Up, then the maximum values from In-Plane Support, New Members, and Hybrid techniques, the indices for $R_{k,Q}^B$ are 0.644, 0.515, 0.413, 0.528, respectively, and the indices for R_Q^D are 0.142, 0.010, 0.030, 0.022, respectively. One observation is that the alternative techniques are unable to push the first hinge formation to a tension member to initiate strain hardening like Built-Up did to achieve the optimum value. This does not imply that techniques other than the standard one are not useful in improving robustness and redundancy, they were simply not optimal for this case study. For example, it is hypothesized that if the damaged state included member removal, adding new members as an

upgrade could serve as an effective method to increase the structural robustness. Nevertheless, both Figures 4.4 and 4.7 indicate that the robustness and redundancy can be marginally improved using less material than the code-compliant solution if limited budget exists, a conclusion that further validates the novel optimization approach.

4.6 Conclusion

Despite excessive rehabilitation costs and budgetary constraints, it is imperative from a safety perspective that truss bridges exhibit structural robustness and structural redundancy given their vulnerability and history of failure. As such, the first objective of this paper was to develop a novel optimization framework capable of maximizing robustness and redundancy while minimizing the material volume required for repair. The second objective was to use the novel optimization framework on a practical application of an existing steel truss bridge upgrade, followed by a comparison between an optimum upgrade and a repair solution achieved following CSA S6:19 (CSA 2019). A steel truss bridge based off a real-life structure in NB, Canada, subjected to corrosion damage was used as the case study, and the holistic structural robustness and structural redundancy indices formulated by Steeves and Oudah (2024a) were selected to be maximized.

Stemming from the first objective, the novel optimization framework is:

- Transparent and intuitive by strategically targeting the first element failure for every upgrade iteration.
- Applicable for any upgrade technique(s).
- Adaptable for any structural robustness or other related measure(s).

CHAPTER 4: NOVEL OPTIMIZATION FRAMEWORK

Furthermore, results from the practical application upon completing the second objective are as follows:

- The Built-Up upgrade technique revealed an optimum solution with a 10% increase in $R_{k,Q}^B$ and an increased R_Q^D of 0 to 0.142 all for a 9% increase in V as compared with CSA S6:19 Repair.
- Another optimum solution using the Built-Up technique that is constrained to be code-compliant per CSA S6:19 (CSA 2019) achieved a 9% increase in $R_{k,Q}^B$ along with an improvement in R_Q^D of 0 to 0.129 for an additional 18% of V compared with CSA S6:19 Repair.
- Other upgrade techniques were investigated, namely In-Plane Support, New Members, and Hybrid, but Built-Up proved to be the most effective for this practical application.
- The novel optimization algorithm is able to increase the robustness and redundancy of the damaged truss bridge for less material volume than that required for the code-compliant repair achieved per CSA S6:19 (CSA 2019) using Built-Up, In-Plane Support, or New Members.

In summary, these conclusions facilitate a clear technology transfer to industry to help engineers optimally improve the safety of existing truss bridges. To holistically address the declining condition of existing bridges, future research should include maximizing the robustness and redundancy values for the remaining life of the bridge, along with adapting the novel optimization framework to include other bridge types (e.g., girder, arch, cable-stayed, suspension).

CHAPTER 5: CONCLUSIONS AND RECOMMENDATIONS

5.1 Summary

Bridges are critical assets in transportation systems but are vulnerable to hazards and damage which increase the risks of progressive or disproportionate collapse. Steel truss bridges have been identified as more vulnerable to collapse than other bridge types (Li et al. 2022; López et al. 2023) and were therefore selected to focus on for this thesis. Many truss bridges have collapsed throughout history in North America, and are still vulnerable to collapse today, demonstrated by the recent collapse of the Francis Scott Key Bridge in Baltimore in 2024. Therefore, the concept of bridge safety must include structural robustness and structural redundancy, the ability to absorb a local damage and not collapse (Bhattacharya 2021), and the ability to carry additional loads after one of its members' fails (Ghosn et al. 2016), respectively. Despite the importance of these structural properties, measures of robustness and redundancy are rarely used by consulting engineers in Canada, partly because CSA S6:19 (CSA 2019) does not provide such quantitative measures. Generally, structural robustness measures can be used to assess the condition of structures throughout a bridge inventory to help owners strategically prioritize bridges for rehabilitation given their budgetary constraints. Additionally, these measures can be invoked during the rehabilitation process to maximize the robustness of the bridge against the damage under consideration.

Stemming from this background, the objectives for this research were to: 1) formulate new indices for structural robustness and structural redundancy, 2) apply the new indices on a practical application to highlight their value within an asset management framework, and 3) develop a novel optimization framework to maximize structural robustness and other related properties, such as redundancy, while minimizing the volume of material required for upgrade. Chapters 2, 3, and 4

CHAPTER 5: CONCLUSIONS AND RECOMMENDATIONS

address each of these three objectives, where each chapter is a standalone research paper, with outcomes and major findings presented in Section 5.2.

5.2 Outcomes and Major Findings

The outcomes and major findings from each of the three papers making up Chapters 2, 3, and 4 are summarized below:

Chapter 2: *New Holistic Structural Robustness Index for Bridges.*

- This paper developed a new holistic structural robustness index for bridges, $R_{k,Q}^B$, that quantitatively accounts for the performance of all elements in the bridge. Rooted in fundamental concepts of system reliability, the index is bounded between zero and one, and is composed of three terms, one for external loads, one for utilization ratios, and one for system ductility. A formulation for a new structural redundancy index was also presented, R_Q^D , again bounded between zero and one, but in this case is composed of only two terms, one for external loads and the other for utilization ratios.
- The new indices were complemented by a user-friendly framework of analysis to calculate index parameters. The framework involves the development of an FE model, followed by incremental, load-controlled, nonlinear static pushover or pushdown analyses of both intact and damaged states until collapse.
- The framework was demonstrated on a simple 2D truss structure subjected to lateral load, where the structure was modeled in SAP2000 (CSI 2016) with brittle, ductile, and hybrid hinge definitions. Two different damaged states were considered, namely complete element failure, and partial element failure (50% reduction in strength and stiffness). The results of the new indices were compared with those from five existing

measures, showcasing the new structural robustness index's ability to identify critical elements given a specified damage, and highlighting the improved expressiveness of $R_{k,Q}^B$ over other measures.

Chapter 3: *Practical Applications of New Structural Robustness and Structural Redundancy Indices.*

- This paper firstly summarized the results from Chapter 2, where a more in-depth investigation of the square truss subjected to lateral load was provided: using hybrid hinge definitions, the system was evaluated against multiple partial damages of the two braces in the frame, once again illustrating the value and utility of the new indices.
- The new indices were used to assess a steel truss bridge based off a real-life structure in NS, Canada, against three levels of corrosion damage corresponding to 25, 50, and 75 years of atmospheric exposure time. The bridge was pushed to collapse with both a concentrated load at midspan and a uniformly distributed load to form a comparison. The assessment was conducted with the help of a spreadsheet interface operated by MATLAB (The MathWorks, Inc. 2022) scripts, where more details can be found in Appendix D.
- Although the trend was flat, $R_{k,Q}^B$ typically decreased with increasing levels of damage, and as expected R_Q^D was near-zero for all simulations. The uniform loading case produced lesser values than the concentrated, highlighting its utility as a potentially conservative approach when evaluating other existing truss bridges instead of using a more complicated dead and live load distribution.

CHAPTER 5: CONCLUSIONS AND RECOMMENDATIONS

- A new asset management framework was introduced which uses $R_{k,Q}^B$ as an accurate and objective overall bridge condition rating to help owners strategically prioritize bridges for rehabilitation or replacement given budgetary constraints. One procedure was introduced which involved assessing the robustness of all bridges in a given inventory, but a refined procedure was also proposed that assesses the robustness of only the poorly rated bridges to expedite the decision-making process and save engineering costs.

Chapter 4: *Novel Optimization Framework to Maximize the Structural Robustness of Existing Truss Bridges Through Strategic Upgrades.*

- This paper developed a novel optimization framework to maximize the structural robustness and other related properties of existing truss bridges while minimizing the volume of material needed to upgrade the bridge. Functionally, the optimization algorithm strategically upgrades the bridge at each iteration by targeting the first element failure that occurs during the collapse simulation, and the framework is adaptable for any robustness measure(s). The optimum value is the one that maximizes the ROI for all robustness measures under consideration.
- The new framework and CSA S6:19 were used to evaluate and rehabilitate a steel truss bridge based off a real-life structure in NB, Canada, subjected to a 75-year corrosion level. $R_{k,Q}^B$ and R_Q^D were selected as measures to maximize within the new framework. Both member and local connection capacities were taken into account, the bridge was evaluated against dead and live loads from CSA S6:19, and the bridge was pushed to collapse with a uniformly distributed load. Evaluations and robustness assessments were conducted with the help of a spreadsheet interface operated by

CHAPTER 5: CONCLUSIONS AND RECOMMENDATIONS

MATLAB (The MathWorks, Inc. 2022) scripts, with more details provided in Appendix D.

- Using the standard rehabilitation technique of built-up members and connections, the optimum solution (Optimum) provided a 10% increase in $R_{k,Q}^B$, increased R_Q^D from 0 to 0.142, increased the collapse deflection by approximately 273%, and increased the collapse load by 37%, all for a 9% increase in V as compared with the code-compliant repair achieved per CSA S6:19 (CSA 2019).
- Again using the standard rehabilitation technique of built-up members and connections, the optimum solution constrained to be code-compliant (Optimum + CSA S6:19) provided a 9% increase in $R_{k,Q}^B$, increased R_Q^D from 0 to 0.129, increased the collapse deflection by approximately 262%, and increased the collapse load by 38%, all for a 18% increase in V as compared with the code-compliant repair achieved per CSA S6:19 (CSA 2019).
- Two alternative upgrade techniques were considered: adding members to reduce the effective length of compression members (In-Plane Support) and adding new structural members (New Members). After using these strategies, along with a hybrid technique, these alternative measures were not able to surpass $R_{k,Q}^B$ and R_Q^D of the Optimum solution for the same V , proving to not be as effective.
- Nevertheless, it was shown that $R_{k,Q}^B$ and R_Q^D can be marginally improved using less material than the code-compliant solution if limited budget exists, a conclusion that further validates the novel optimization framework.

5.3 Practical Recommendations

Firstly, based on the different studies completed in Chapters 2 and 3, the new structural robustness index, $R_{k,Q}^B$, is the recommended measure to use in engineering practice. The three terms that make up $R_{k,Q}^B$ are multiplied together, as opposed to other options like averaged, meaning that in order to obtain a high index, all three sub-indices must achieve high values. This provides a level of confidence for practicing structural engineers that a value of $R_{k,Q}^B$ close to one is truly indicative of a robust system for the given damage and loading condition under consideration. Moreover, the novel optimization framework from Chapter 4 is simple and intuitive, and achieved an optimum value in five (Optimum) or seven (Optimum + CSA S6:19) iterations (although the algorithm required more to identify these optimums) which certainly has a level of efficiency conducive for use in consulting engineering.

Furthermore, Chapter 4 revealed how a code-compliant repair achieved per CSA S6:19 can have zero redundancy, and by extension a brittle system failure mode, meaning it is a single-load-path structure or a series system (Nowak and Collins 2013); a connection fails first during the pushdown analysis of the rehabilitated truss bridge causing immediate collapse. The approach taken within the novel optimization framework to avoid this situation is to build up connections to the ultimate strength of the member, so that the failure is governed by the member which is typically more ductile. However, clause 10.18.1.1 of CSA S6:19 only requires steel connections to be designed for the maximum of the forces at the connection or 75% of the factored resistance of the member, often causing the connection to have a lesser resistance than the member (CSA 2019). To improve the system performance of code-compliant rehabilitations, it is recommended that structural engineers invoke other code clauses within CSA S6:19 related to connection design. For example:

CHAPTER 5: CONCLUSIONS AND RECOMMENDATIONS

- Clause 4.8.4.4.3.4 related to brace connections in ductile concentrically braced frames in seismic performance category 3 requires their factored resistance to equal or exceed both the probable tensile and compressive resistance of the bracing members (CSA 2019).
- For rehabilitation of structural steel, clause 15.8.1.1 requires that care be taken when repairing and strengthening existing members and connections to ensure failure modes either improve to more ductile ones, or do not change (CSA 2019).

In short, CSA S6:19 has existing clauses already implemented in the code that can potentially be used to help improve system behaviour and achieve solutions closer to the ones produced following the novel optimization framework.

5.4 Future Research

Recommended future research based on the work done in this thesis includes:

- Calibration of target values for $R_{k,Q}^B$ and R_Q^D under specific damages and loading conditions.
- Formulation of new holistic structural resilience index for truss bridges that integrates the concepts of robustness and redundancy, along with a user-friendly optimization tool to enhance the resilience of existing truss bridges while minimizing the cost and carbon footprint associated with upgrading.
- Validation of incremental, load-controlled, nonlinear static pushdown analyses in SAP2000 (CSI 2016) by building bridge models using general-purpose FE to compare results and investigate factors such as geometric and contact nonlinearity, the dynamic effects of applied loading and member failure, 2D versus 3D structural response, and the location and definition of nonlinear hinges used in the SAP2000 (CSI 2016) model.

CHAPTER 5: CONCLUSIONS AND RECOMMENDATIONS

- Adaptation of $R_{k,Q}^B$, R_Q^D , and the new holistic structural resilience index, along with associated frameworks of analyses, to other bridge types beyond truss bridges (e.g., girder, arch, cable-stayed, suspension).

REFERENCES

- AASHTO (American Association of State Highway and Transportation Officials). 2018. *The manual for bridge evaluation*, 3rd Ed. Washington, DC: AASHTO.
- AASHTO (American Association of State Highway and Transportation Officials). 2020. *AASHTO LRFD bridge design specifications*, 9th Ed. Washington, DC: AASHTO.
- Adam, J. M., F. Parisi, J. Sagaseta, and X. Lu. 2018. “Research and practice on progressive collapse and robustness of building structures in the 21st century.” *Engineering Structures*, 173, 122–149.
- Agarwal, J., J. England, and D. Blockley. 2006. “Vulnerability analysis of structures.” *Structural Engineering International*, 16 (2), 124–128.
- Anitori, G., J. R. Casas, and M. Ghosn. 2013. “Redundancy and robustness in the design and evaluation of bridges: European and North American perspectives.” *Journal of Bridge Engineering*, 18 (12), 1241–1251.
- Argyroudis, S. A. 2022. “Resilience metrics for transport networks: A review and practical examples for bridges.” *Proceedings of the Institution of Civil Engineers — Bridge Engineering*, 175 (3), 179–192.
- ASCE (American Society of Civil Engineers). 2017. *Seismic evaluation and retrofit of existing buildings*. ASCE/SEI 41-17. Reston, VA: ASCE.
- ASCE (American Society of Civil Engineers). 2024. “Bridges.” *2021 Infrastructure Report Card*. Accessed July 4, 2024. <https://infrastructurereportcard.org/wp-content/uploads/2020/12/Bridges-2021.pdf>.

REFERENCES

- Baker, J. W., M. Schubert, and M. H. Faber. 2008. “On the assessment of robustness.” *Structural Safety*, 30 (3), 253–267.
- Bhattacharya, B. 2021. “A reliability based measure of structural robustness for coherent systems.” *Structural Safety*, 89, 102050.
- Bontempi, F. 2019. “Elementary concepts of structural robustness of bridges and viaducts.” *Journal of Civil Structural Health Monitoring*, 9, 703–717.
- Brett, C., and Y. Lu. 2013. “Assessment of robustness of structures: Current state of research.” *Frontiers of Structural and Civil Engineering*, 7 (4), 356–368.
- Briggs, W., L. Cochran, and B. Gillett. 2015. *Calculus, Early Transcendentals*, Second Ed. Boston, MA: Pearson Education, Inc.
- Buitrago, M., E. Bertolesi, P. A. Calderón, and J. M. Adam. 2021. “Robustness of steel truss bridges: Laboratory testing of a full-scale 21-metre bridge span.” *Structures*, 29, 691–700.
- Capacci, L., F. Biondini, and D. M. Frangopol. 2022. “Resilience of aging structures and infrastructure systems with emphasis on seismic resilience of bridges and road networks: Review.” *Resilient Cities and Structures*, 1 (2), 23–41.
- Caredda, G., M. C. Porcu, M. Buitrago, E. Bertolesi, and J. M. Adam. 2022. “Analysing local failure scenarios to assess the robustness of steel truss-type bridges.” *Engineering Structures*, 262, 114341.
- Cavaco, E. S., J. R. Casas, L. A. C. Neves, and A. E. Huespe. 2013. “Robustness of corroded reinforced concrete structures — a structural performance approach.” *Structure and Infrastructure Engineering*, 9 (1), 42–58.

REFERENCES

- Charnpis, D. C., and A. Kontogiannis. 2016. “The cost of satisfying design requirements on progressive collapse resistance — Investigation based on structural optimisation.” *Structure and Infrastructure Engineering*, 12 (6), 695–713.
- Chen, Y.-L., L. Huang, Y.-Q. Lu, L. Deng, and H.-Z. Tan. 2016. “Assessment of structural robustness under different events according to vulnerability.” *Journal of Performance of Constructed Facilities*, 30 (5), 04016004.
- Chen, Q., H. Wang, S. El-Tawil, A. K. Agrawal, B. Bhattacharya, and W. Wong. 2023. “Progressive collapse behaviour of a long-span cable-stayed bridge induced by cable loss.” *Journal of Bridge Engineering*, 28 (9), 05023005.
- Choi, J., and D. Chang. 2009. “Prevention of progressive collapse for building structures to member disappearance by accidental actions.” *Journal of Loss Prevention in the Process Industries*, 22 (6), 1016–1019.
- CISC (Canadian Institute of Steel Construction). 2021. *Handbook of steel construction*, 12th Ed. Toronto, ON: CISC.
- CSA (Canadian Standards Association). 2019. *Canadian highway bridge design code*. CSA S6:19. Toronto, ON: CSA Group.
- CSI (Computers & Structures, Inc.). 2016. “SAP2000® version 19.” *CSI Analysis Reference Manual*. Accessed July 14, 2024.
<https://docs.csiamerica.com/manuals/sap2000/CSiRefer.pdf>.

REFERENCES

- El Hajj Diab, M., C. Desprez, A. Orcesi, and J. Bleyer. 2022. “Structural robustness quantification through the characterization of disproportionate collapse compared to the initial local failure.” *Engineering Structures*, 255, 113869.
- Fallon, C. T., S. E. Quiel, and C. J. Naito. 2016. “Uniform pushdown approach for quantifying building-frame robustness and the consequence of disproportionate collapse.” *Journal of Performance of Constructed Facilities*, 30 (6), 04016060.
- Fascetti, A., S. K. Kunnath, and N. Nisticò. 2015. “Robustness evaluation of RC frame buildings to progressive collapse.” *Engineering Structures*, 86, 242–249.
- Fiorillo, G., and M. Ghosn. 2022. “Structural redundancy, robustness, and disproportionate collapse analysis of highway bridge superstructures.” *Journal of Structural Engineering*, 148 (7), 04022075.
- Frangopol, D. M., and J. P. Curley. 1987. “Effects of damage and redundancy on structural reliability.” *Journal of Structural Engineering*, 113 (7), 1533–1549.
- Fu, G., and D. M. Frangopol. 1990. “Balancing weight, system reliability and redundancy in a multiobjective optimization framework.” *Structural Safety*, 7 (2–4), 165–175.
- Galambos, T. V. 1990. “Systems reliability and structural design.” *Structural Safety*, 7 (2–4), 101–108.
- Gerasimidis, S., and B. Ellingwood. 2023. “Twenty years of advances in disproportionate collapse research and best practices since 9/11/2001.” *Journal of Structural Engineering*, 149 (2), 02022002.

REFERENCES

- Ghosn, M., and F. Moses. 1998. *Redundancy in highway bridge superstructures*. NCHRP Report 406. Washington, DC: Transportation Research Board.
- Ghosn, M., L. Dueñas-Osorio, D. M. Frangopol, T. P. McAllister, P. Bocchini, L. Manuel, B. R. Ellingwood, S. Arangio, F. Bontempi, M. Shah, M. Akiyama, F. Biondini, S. Hernandez, and G. Tsiatas. 2016. “Performance indicators for structural systems and infrastructure networks.” *Journal of Structural Engineering*, 142 (9), F4016003.
- Giuliani, L. 2012. “Structural safety in case of extreme actions.” *International Journal of Lifecycle Performance Engineering*, 1 (1), 22–40.
- Hendawi, S., and D. M. Frangopol. 1994. “System reliability and redundancy in structural design and evaluation.” *Structural Safety*, 16 (1–2), 47–71.
- ISO (International Organization for Standardization). 2007. *Petroleum and natural gas industries — Fixed steel offshore structures*. ISO 19902, First Ed. Geneva, Switzerland: ISO.
- ISO (International Organization for Standardization). 2012a. *Corrosion of metals and alloys — Corrosivity of atmospheres — Classification, determination and estimation*. ISO 9223, Second Ed. Geneva, Switzerland: ISO.
- ISO (International Organization for Standardization). 2012b. *Corrosion of metals and alloys — Corrosivity of atmospheres — Guiding values for the corrosivity categories*. ISO 9224, Second Ed. Geneva, Switzerland: ISO.
- Izzuddin, B. A., A. G. Vlassis, A. Y. Elghazouli, and D. A. Nethercot. 2008. “Progressive collapse of multi-storey buildings due to sudden column loss — Part I: Simplified assessment framework.” *Engineering Structures*, 30 (5), 1308–1318.

REFERENCES

- JCSS (Joint Committee on Structural Safety). 2008. *Risk assessment in engineering. Principles, system representation & risk criteria*. JCSS.
- Khandelwal, K., and S. El-Tawil. 2011. “Pushdown resistance as a measure of robustness in progressive collapse analysis.” *Engineering Structures*, 33 (9), 2653–2661.
- Lee, G. C., S. B. Mohan, C. Huang, and B. N. Fard. 2013. *A study of U.S. bridge failures (1980-2012)*. Technical Report MCEER-13-0008. FHWA Contract Number DTFH61-08-C-00012. Buffalo, NY: MCEER.
- Li, H., L. Shen, and S. Deng. 2022. “A generalized framework for the alternate load path redundancy analysis of steel truss bridges subjected to sudden member loss scenarios.” *Buildings*, 12 (10), 1597.
- Lind, N. C. 1995. “A measure of vulnerability and damage tolerance.” *Reliability Engineering & System Safety*, 48 (1), 1–6.
- López, S., N. Makoond, A. Sánchez-Rodríguez, J. M. Adam, and B. Riveiro. 2023. “Learning from failure propagation in steel truss bridges.” *Engineering Failure Analysis*, 152, 107488.
- Maes, M. A., K. E. Fritszons, and S. Glowienka. 2006. “Structural robustness in the light of risk and consequence analysis.” *Structural Engineering International*, 16 (2), 101–107.
- Martinelli, P., M. Colombo, and M. di Prisco. 2024. “Robustness assessment of half-joint RC girder bridges.” *Engineering Structures*, 306, 117712.
- Miao, F., and M. Ghosn. 2016. “Reliability-based progressive collapse analysis of highway bridges.” *Structural Safety*, 63, 33–46.

REFERENCES

- Minaie, E., and F. Moon. 2017. "Practical and simplified approach for quantifying bridge resilience." *Journal of Infrastructure Systems*, 23 (4), 04017016.
- Mondoro, A., D. M. Frangopol, and L. Liu. 2018. "Multi-criteria robust optimization framework for bridge adaptation under climate change." *Structural Safety*, 74, 14–23.
- Nafday, A. M. 2008. "System safety performance metrics for skeletal structures." *Journal of Structural Engineering*, 134 (3), 499–504.
- Nafday, A. M. 2011. "Consequence-based structural design approach for black swan events." *Structural Safety*, 33 (1), 108–114.
- Nowak, A. S., and K. R. Collins. 2013. *Reliability of structures*, Second Ed. Boca Raton, FL: CRC Press, Taylor & Francis Group.
- Olmati, P., K. Gkoumas, F. Brando, and L. Cao. 2013. "Consequence-based robustness assessment of a steel truss bridge." *Steel and Composite Structures*, 14 (4), 379–395.
- Paliou, C., M. Shinozuka, and Y.-N. Chen. 1990. "Reliability and redundancy of offshore structures." *Journal of Engineering Mechanics*, 116 (2), 359–378.
- Parisi, F., and N. Augenti. 2012. "Influence of seismic design criteria on blast resistance of RC framed buildings: A case study." *Engineering Structures*, 44, 78–93.
- Pinto, J. T., D. I. Blockley, and N. J. Woodman. 2002. "The risk of vulnerable failure." *Structural Safety*, 24 (2–4), 107–122.
- Praxedes, C., X.-X. Yuan, and X.-H.-C. He. 2022. "A novel robustness index for progressive collapse analysis of structures considering the full risk spectrum of damage evolution." *Structure and Infrastructure Engineering*, 18 (3), 376–394.

REFERENCES

- Praxedes, C., and X-X. Yuan. 2022. “Robustness-oriented optimal design for reinforced concrete frames considering the large uncertainty of progressive collapse threats.” *Structural Safety*, 94, 102139.
- Smith, J. W. 2003. “Energy approach to assessing corrosion damaged structures.” *Structures and Buildings*, 156 (2), 121–130.
- Sørensen, J. D. 2011. “Framework for robustness assessment of timber structures.” *Engineering Structures*, 33 (11), 3087–3092.
- Sørensen, J. D., E. Rizzuto, H. Narasimhan, and M. H. Faber. 2012. “Robustness: Theoretical framework.” *Structural Engineering International*, 22 (1), 66–72.
- Starossek, U. 2006. “Progressive collapse of bridges — Aspects of analysis and design.” *Invited Lecture, International Symposium on Sea-Crossing Long-Span Bridges*, 1–22. Mokpo, Korea.
- Starossek, U., and M. Haberland. 2011. “Approaches to measures of structural robustness.” *Structure and Infrastructure Engineering*, 7 (7–8), 625–631.
- Steeves, E., and F. Oudah. 2024a. “New holistic structural robustness index for bridges.” *Journal of Bridge Engineering*. In Review.
- Steeves, E., and F. Oudah. 2024b. “Robustness versus redundancy of existing structures: critical review and application.” In *Proceedings, 7th International Conference on Smart Monitoring, Assessment and Rehabilitation of Civil Structures*. Salerno, Italy.
- The MathWorks, Inc. 2022. *MATLAB® version 9.12.0.2039608 (R2022a)*. Natick, MA: The MathWorks, Inc.

REFERENCES

- Vlassis, A. G., B. A. Izzuddin, A. Y. Elghazouli, and D. A. Nethercot. 2008. “Progressive collapse of multi-storey buildings due to sudden column loss – Part II: Application.” *Engineering Structures*, 30 (5), 1424–1438.
- Wang, M., and Z. Zhou. 2012. “Progressive collapse and structural robustness of bridges.” *Applied Mechanics and Materials*, 193–194, 1021–1024.
- Wang, H., Q. Chen, A. K. Agrawal, S. El-Tawil, B. Bhattacharya, and W. Wong. 2022. “Dynamic response and progressive collapse of a long-span suspension bridge induced by suspender loss.” *Journal of Structural Engineering*, 148 (6), 05022001.
- Wardhana, K., and F. C. Hadipriono. 2003. “Analysis of recent bridge failures in the United States.” *Journal of Performance of Constructed Facilities*, 17 (3), 144–150.
- Xiong, W., C. S. Cai, R. Zhang, H. Shi, and C. Xu. 2023. “Review of hydraulic bridge failures: Historical statistic analysis, failure modes, and prediction methods.” *Journal of Bridge Engineering*, 28 (4), 03123001.
- Yan, S., X. Zhao, and Y. Lu. 2017. “Collapse-resisting mechanisms of planar trusses following sudden member loss.” *Journal of Structural Engineering*, 143 (9), 04017114.
- Zhang, G., Y. Liu, J. Liu, S. Lan, and J. Yang. 2022. “Causes and statistical characteristics of bridge failures: A review.” *Journal of Traffic and Transportation Engineering (English Edition)*, 9 (3), 388–406.

REFERENCES

APPENDIX A: SUMMARY OF EXISTING STRUCTURAL ROBUSTNESS MEASURES

This appendix provides a summary of existing structural robustness measures broken down into three tables: Deterministic (Table A.1), Probabilistic (Table A.3), and Risk-based (Table A.4). Table A.2 provides a legend for the categories used to distinguish the different Deterministic measures.

Table A.1 Deterministic measures.

#	Name	Formulation	Bounds	Parameters	Cat.	Ref.
1	Degree of redundancy	$R = F - E$	$(0, +\infty)$	F = number of unknown reactive forces; E = number of independent equilibrium equations.	T	Frangopol and Curley 1987
2	Design load survivability Damaged strength ratio	$R = \frac{L_{damaged}}{L_{design}}$ $DSR = \frac{Q_{damaged}}{Q_{design}}$	$(0, +\infty)$	$L_{damaged}$ = load carrying capacity of the damaged structure; L_{design} = design load. $Q_{damaged}$ = load that causes the collapse of the damaged system; Q_{design} = unfactored design load.	LC	Frangopol and Curley 1987 Fallon et al. 2016 Ghosn et al. 2016
3	Reserve redundant factor Reserve resistance factor Reserve strength ratio Reserve strength ratio Reserve strength ratio Reserve strength ratio	$R = \frac{L_{intact}}{L_{design}}$ Reserve resistance factor $= \frac{L_{env}}{\text{design environmental load}}$ $RSR = \frac{S_{collapse}}{S_{design}}$ $R_{RS} = \frac{F_{collapse}}{F_{100}}$ $RSR = \frac{R_c}{S_c}$ $RSR = \frac{Q_{intact}}{Q_{design}}$	$(0, +\infty)$	L_{intact} = load carrying capacity of the intact structure. L_{env} = environmental load at collapse. $S_{collapse}$ = environmental load at system collapse; S_{design} = original design environmental load. $F_{collapse}$ = unfactored global environmental action which causes collapse of the structure; F_{100} = unfactored 100-year design global environmental action. R_c = characteristic value of the base shear capacity of an offshore platform; S_c = design load corresponding to ultimate collapse. Q_{intact} = load that causes the collapse of the originally intact system; Q_{design} = unfactored design load.	LC	Frangopol and Curley 1987 Paliou et al. 1990 Maes et al. 2006 ISO 2007 Sørensen et al. 2012 Ghosn et al. 2016

#	Name	Formulation	Bounds	Parameters	Cat.	Ref.
4	Residual redundant factor Residual resistant factor Robustness measure RIF (Residual Influence Factor) Residual strength ratio	$R = \frac{L_{damaged}}{L_{intact}}$ Residual resistant factor $= \frac{L_{env} \text{ (damaged)}}{L_{env} \text{ (undamaged)}}$ $R = \min_i \frac{RSR_i}{RSR_0}$ $RIF_i = \frac{RSR_{fail,i}}{RSR_{intact}}$ $RIF = \frac{Q_{damaged}}{Q_{intact}}$	(0,1)	$RSR_i = RSR$ based on member i impaired; $RSR_0 = RSR$ based on no impaired members. $RSR_{fail,i} = RSR$ when member i is failed; $RSR_{intact} = RSR$ for intact structure. $Q_{damaged}$ = load that causes the collapse of the damaged system.	LC	Frangopol and Curley 1987 Paliou et al. 1990 Maes et al. 2006 Sørensen et al. 2012 Ghosn et al. 2016
5	Redundant factor	$R = \frac{L_{intact}}{(L_{intact} - L_{damaged})}$	(1, +∞)	N/A	LC	Frangopol and Curley 1987
6	System reserve ratios Structural redundancy ratio	$R_u = \frac{LF_u}{LF_1} \geq 1.30$ $R_f = \frac{LF_f}{LF_1} \geq 1.10$ $R_d = \frac{LF_d}{LF_1} \geq 0.50$ $SR = \frac{Q_{intact}}{Q_{member}}$	(0, +∞)	LF_u = HS-20 load multiplier for ultimate limit state; LF_1 = HS-20 load multiplier for first member failure limit state; LF_f = HS-20 load multiplier for functionality limit state; LF_d = HS-20 load multiplier for damaged condition limit state.	LC	Ghosn and Moses 1998 Ghosn et al. 2016
7	Separateness	$\gamma = \frac{Q(S) - Q(S')}{Q(S)}$ where $Q = \frac{\sum q_i}{n} = \frac{\sum \det(K_{ii})}{n}$	(0,1)	$Q(S)$ = well-formedness of the intact structure S ; $Q(S')$ = well-formedness of the deteriorated structure S' . q_i = well-formedness of the i^{th} joint in the ring; K_{ii} = sum of the stiffness submatrices of all members contained in the ring that meet at joint i ; n = total number of joints in the ring.	S, T	Pinto et al. 2002

#	Name	Formulation	Bounds	Parameters	Cat.	Ref.
8	Vulnerability index	$\varphi = \frac{\gamma}{D_r}$ <p>where $D_r = \frac{D}{D_{max}}$</p>	(0, +∞)	D_r = relative damage demand; D = damage demand; D_{max} = sum of the damage demand of all members.	S, T	Pinto et al. 2002
9	Energy ratio	$\rho_e = \frac{\sum W_f}{\sum U}$	(0, +∞)	$\sum W_f$ = net work of failure for each element; $\sum U$ = total strain energy in the structure after the failure of each element.	E	Smith 2003
10	Hazard potential	$H_i = \frac{U_i/U_0}{Q_i/Q_0}$	(0, +∞)	U_i = strain energy after the i^{th} event; U_0 = strain energy corresponding to the original state; Q_i = well-formedness after the i^{th} event; Q_0 = well-formedness corresponding to the original state.	E, S, T	Agarwal et al. 2006
11	Structural robustness measure Overload factor Overload factor	$\frac{\text{Capacity}}{\text{Demand}} = \frac{P_f}{P_0}$ <p>Overload Factor (<i>OF</i>)</p> $= \frac{\text{Failure load}}{\text{Nominal gravity loads}}$ $\lambda_{max} = \frac{C_V}{D_V}$	(0, +∞)	P_f = system pseudo-static capacity for sudden column loss scenario; P_0 = applied gravity loading. C_V = vertical resisting force derived from pushdown analysis; D_V = vertical base reaction corresponding to nominal gravity loads.	LC	Izzuddin et al. 2008, Vlassis et al. 2008 Khandelwal and El-Tawil 2011 Parisi and Augenti 2012
12	System safety performance metric for the performance objective of stability	$\delta_S = \frac{n}{\ \mathbf{K}\ \ \mathbf{K}^{-1}\ }$ <p>where $\ \mathbf{K}\ = \left(\sum_{ij}(k_{ij})^2\right)^{1/2}$</p>	(0,1)	\mathbf{K} = stiffness matrix; n = number of rows or columns in \mathbf{K} ; $\ \mathbf{K}\ $ = Euclidean matrix norm of stiffness matrix for skeletal structure.	S	Nafday 2008
13	System safety performance metric for the performance objective of stability	$\Delta_S = \mathbf{K}_N $	(0,1)	$ \mathbf{K}_N $ = determinant of normalized stiffness matrix for the intact, skeletal structure.	S	Nafday 2008

#	Name	Formulation	Bounds	Parameters	Cat.	Ref.
14	Importance measure for the removed member or failure path	$I = \frac{ \mathbf{K}_N }{ \mathbf{K}_N^* }$	$(1, +\infty)$	$ \mathbf{K}_N^* $ = determinant of normalized stiffness matrix for the damaged, skeletal structure.	S	Nafday 2008
15	Sensitivity index Component importance coefficient	$S.I. = \frac{\lambda_0 - \lambda_{damage}}{\lambda_0}$ $\gamma_i = 1 - \frac{R_i}{R_0}$	$(0,1)$ $(-\infty, 1)$	λ_0 = load carrying capacity in the original state; λ_{damage} = load carrying capacity in the state in which a certain member disappeared. γ_i = importance factor of component; R_i = structural bearing capacity after the failure of component i ; R_0 = initial structural bearing capacity.	LC	Choi and Chang 2009 Chen et al. 2016
16	Member consequence factor	$C_f^i = \frac{ \mathbf{K}_N^i }{ \mathbf{K}_N }$	$(0,1)$	$ \mathbf{K}_N^i $ = determinant of normalized stiffness matrix for damaged condition; $ \mathbf{K}_N $ = determinant of normalized stiffness matrix for intact condition.	S	Nafday 2011
17	Stiffness-based robustness measure	$R_s = \min_j \frac{\det \mathbf{K}_j}{\det \mathbf{K}_0}$	$(0,1)$	\mathbf{K}_j = stiffness matrix of the structure after removing a structural element or connection j ; \mathbf{K}_0 = stiffness matrix of the intact structure.	S	Starossek and Haberland 2011
18	Damage-based robustness measure	$R_d = 1 - \frac{p}{p_{lim}}$	$(-\infty, 1)$	p = maximum total damage resulting from the assumable initial damage; p_{lim} = acceptable total damage in addition to the assumable initial damage.	D	Starossek and Haberland 2011
19	Damage-based robustness measure	$R_{d,int} = 1 - 2 \int_0^1 [d(i) - i] di$	$(0,1)$	$d(i)$ = maximum total damage resulting from and including the initial damage of extent i . Both $d(i)$ and i are dimensionless variables.	D	Starossek and Haberland 2011
20	Modified damage-based robustness measure	$R_{d,int,lim} = 1 - \left(\frac{2}{i_{lim} \cdot (2 - i_{lim})} \cdot \int_0^{i_{lim}} [d(i) - i] di \right)$	$(0,1)$	i_{lim} = assumable maximum extent of initial local damage.	D	Starossek and Haberland 2011

#	Name	Formulation	Bounds	Parameters	Cat.	Ref.
21	Energy-based robustness measure	$R_e = 1 - \max_j \frac{E_{r,j}}{E_{f,k}}$	$(-\infty, 1)$	$E_{r,j}$ = energy released during the initial failure of a structural element j and contributing to damaging a subsequently affected structural element k ; $E_{f,k}$ = energy required for the failure of the subsequently affected structural element k .	E	Starossek and Haberland 2011
22	Robustness indicator	$I = \max \left\{ \frac{\lambda_u^d / \lambda_u^0}{d/E} \right\}$	$(1, E)$	λ_u^d = ultimate load multiplier for damaged structure; λ_u^0 = ultimate load multiplier for intact structure; d = damage level; E = number of elements in the structure.	LC, D	Giuliani 2012
23	Robustness index	$\rho = \frac{s_0}{s_d}$	$(0,1)$	s_0 = displacement of the intact system; s_d = displacement of the damaged system.	DP	Anitori et al. 2013
24	Robustness index	$I_{R,D} = \int_{D=0}^{D=1} f(D) dD$	$(0,1)$	$f(D)$ = normalised structural performance; D = normalised damage.	D	Cavaco et al. 2013
25	Consequence index	$C_i = C_{s,i} + C_{u,i} - C_{s,i} \times C_{u,i}$ $C_{s,i} = C_{k,i} + C_{y,i} - C_{k,i} \times C_{y,i}$ $C_{u,i} = C_{u,f,i} + C_{u,d,i} - C_{u,f,i} \times C_{u,d,i}$ where $C_{k,i} = 1 - \frac{k_i}{k_o}$	$(0,1)$	$C_{k,i}$ = stiffness consequence index; $C_{y,i}$ = yield strength consequence index; $C_{u,f,i}$ = ultimate strength consequence index; $C_{u,d,i}$ = ductility consequence index; k_i = elastic stiffness of damaged state i ; k_o = elastic stiffness of the intact state.	LC, S	Brett and Lu 2013
26	Robustness index	$R^{scenario} = 100 - C_f^{scenario}$ where $C_f^{scenario} = \max \left(\frac{(\lambda_i^{un} - \lambda_i^{dam})}{\lambda_i^{un}} 100 \right)_{i=1-N}$	$(0,100)$	λ_i^{un} = i -th eigenvalue of the structural stiffness matrix in the undamaged configuration; λ_i^{dam} = i -th eigenvalue of the structural stiffness matrix in the damaged configuration.	S	Olmati et al. 2013
27	Structural robustness index	$S_{RI} = \frac{n_r}{n_f}$	$(0,1)$	n_r = critical number of removed columns; n_f = total number of columns in the respective floor of the structure.	T	Fascetti et al. 2015

#	Name	Formulation	Bounds	Parameters	Cat.	Ref.
28	Structural robustness index	$S_{RI} = \sum_{i=1}^{n_r} i * L_{n,cr}^i$	$(0, +\infty)$	$L_{n,cr}^i$ = Axial Load Multiplier for the critical column removed in each phase.	LC	Fascetti et al. 2015
29	Structural vulnerability index for single event i	$VI_i = \frac{1}{C_n^1} \sum_{k=1}^n \gamma_{ki} \cdot v_{ki}$	$(0,1)$	C_n^1 = number of all possibilities when 1 out of n components is removed; γ_{ki} = importance coefficient of component k under event i ; v_{ki} = vulnerability coefficient of component k under event i .	LC	Chen et al. 2016
30	Structural robustness index for single event i	$RI_i = 1 - \frac{1}{C_n^1} \sum_{k=1}^n \gamma_{ki} \cdot v_{ki}$	$(0,1)$	N/A	LC	Chen et al. 2016
31	Relative robustness index	$RRI = \frac{\lambda_{damaged} - 1}{\lambda_{undamaged} - 1}$	$(-\infty, 1)$	$\lambda_{damaged}$ = gravity load multiplier for the damaged structure; $\lambda_{undamaged}$ = multiplier for the undamaged structure.	LC	Fallon et al. 2016
32	Robustness measure	$\Delta Q = Q_{intact} - Q_{damaged}$	$(0, +\infty)$	N/A	LC	Ghosn et al. 2016
33	Robustness index	$\rho = \frac{\ \mathbf{s}\ }{\ \mathbf{s}^*\ }$	$(0,1)$	$\ \mathbf{s}\ $ = Euclidean matrix norm of displacement vector of intact structure; $\ \mathbf{s}^*\ $ = Euclidean matrix norm of displacement vector of damaged structure.	DP	Adam et al. 2018

Table A.2 Category legend.

Category Legend	
Load Capacity-based Measure	LC
Stiffness-based Measure	S
Topology-based Measure	T
Energy-based Measure	E
Damage-based Measure	D
Displacement-based Measure	DP

Table A.3 Probabilistic measures.

#	Name	Formulation	Bounds	Parameters	Ref.
1	Probabilistic redundant index	$\beta_R = \frac{\beta_{intact}}{(\beta_{intact} - \beta_{damaged})}$	$(0, +\infty)$	β_{intact} = reliability index of the intact system; $\beta_{damaged}$ = reliability index of the damaged system.	Frangopol and Curley 1987
2	Redundancy index	$RI = \frac{P_{f(dmg)} - P_{f(sys)}}{P_{f(sys)}}$	$(0, +\infty)$	$P_{f(dmg)}$ = probability of damage occurrence to the system; $P_{f(sys)}$ = probability of system failure.	Fu and Frangopol 1990
3	Redundancy measure	$P_r^* = P[\text{system survival} \text{simultaneous failure of one or more members}]$	$(0,1)$	N/A	Paliou et al. 1990
4	Probabilistic redundancy factor	$PRDF = \frac{P(yield) - P(collapse)}{P(collapse)}$	$(0, +\infty)$	$P(yield)$ = probability that any first-member-yielding occurs in the intact structure; $P(collapse)$ = probability of collapse of the intact structure.	Hendawi and Frangopol 1994
5	Reliability-based redundancy factor	$RRDF = \frac{\beta(collapse) - \beta(yield)}{\beta(collapse)}$	$(0,1)$	$\beta(collapse)$ = reliability index of the intact structure with respect to collapse; $\beta(yield)$ = reliability index of the intact structure with respect to any first-member-yielding occurrence.	Hendawi and Frangopol 1994
6	System performance factor	$R = \frac{\beta(intact)}{(\beta(intact) - \beta(damaged))}$	$(0, +\infty)$	$\beta(intact)$ = reliability index of an intact structure with respect to a specific limit state; $\beta(damaged)$ = reliability index of the damaged structure with respect to the same limit state.	Hendawi and Frangopol 1994
7	Vulnerability	$V = \frac{P(R_d, S)}{P(R_0, S)} = \frac{1}{\text{damage tolerance}}$	$(1, +\infty)$	$P(R_d, S)$ = probability of failure of the system in a damaged state R_d , produced by the retrospective loads, for prospective loading S ; $P(R_0, S)$ = probability of failure of the system in an ordinary state R_0 for prospective loading S .	Lind 1995
8	Damage factor	$D_d = \frac{P_d^F}{P_0^F}$	$(1, +\infty)$	P_d^F = probability of failure of the system in a damaged state R_d for prospective loading S ; P_0^F = probability of failure of the system in an ordinary state R_0 for prospective loading S .	Lind 1995

#	Name	Formulation	Bounds	Parameters	Ref.
9	Relative reliability indices	$\Delta\beta_u = \beta_{ult} - \beta_{member} \geq 0.85$ $\Delta\beta_f = \beta_{funct} - \beta_{member} \geq 0.25$ $\Delta\beta_d = \beta_{damaged} - \beta_{member} \geq -2.70$	$(-\infty, +\infty)$	β_{member} = reliability index for first member failure limit state; β_{ult} = reliability index for ultimate limit state; β_{funct} = reliability index for functionality limit state; $\beta_{damaged}$ = reliability index for damaged condition limit state.	Ghosn and Moses 1998
10	Robustness measure	$R = \min_i \frac{P_{s0}}{P_{si}}$	$(0,1)$	P_{s0} = system failure probability of the undamaged system; P_{si} = system failure probability assuming one impaired member i .	Maes et al. 2006
11	Reliability index based robustness index	$I_{rob} = \frac{\beta_{damaged}}{\beta_{intact}}$	$(0,1)$	$\beta_{damaged}$ = system reliability index of the damaged structural system; β_{intact} = system reliability index of the intact structural system.	Sørensen 2011
12	Redundancy index	$R_{red} = \frac{P_{f(intact)}}{P_{f(member)}}$	$(0, +\infty)$	$P_{f(intact)}$ = probability of failure of intact system; $P_{f(member)}$ = probability of member failure.	Anitori et al. 2013
13	Robustness index	$R_{rob} = \frac{P_{f(damaged)}}{P_{f(intact)}}$	$(1, +\infty)$	$P_{f(damaged)}$ = probability of failure of damaged system.	Anitori et al. 2013
14	Structural robustness index for multiple discrete events	$RI = \sum_i \omega_i \cdot \left(1 - \frac{1}{n} \sum_{k=1}^n \gamma_{ki} \cdot \nu_{ki} \right)$	$(0,1)$	ω_i = probability of occurrence of event i ; γ_{ki} = importance coefficient of component k under event i ; ν_{ki} = vulnerability coefficient of component k under event i .	Chen et al. 2016
15	Structural robustness index for continuous events	$RI = \int_{-\infty}^{\infty} \omega(x) \cdot \left(1 - \frac{1}{n} \sum_{k=1}^n \gamma_{kx} \cdot \nu_{kx} \right) dx$	$(0,1)$	$\omega(x)$ = occurrence probability density function.	Chen et al. 2016
16	Structural robustness index	$R_k^B = \exp\left(-\frac{\beta - \beta'_k}{\beta}\right)$	$(0,1)$	β = reliability index of the intact structure; β'_k = reliability index conditioned on the loss of element k .	Bhattacharya 2021

Table A.4 Risk-based measures.

#	Name	Formulation	Bounds	Parameters	Ref.
1	Robustness measure	$R = \frac{1}{H}$	$(0, +\infty)$	H = tail heaviness of the consequences of failure versus minus log-exceedance curve.	Maes et al. 2006
2	Robustness index	$I_{Rob} = \frac{\sum_i R_{Dir_i}}{\sum_i R_{Dir_i} + \sum_j R_{Ind_j}}$	$(0,1)$	R_{Dir_i} = direct risk associated with the i damage scenarios; R_{Ind_j} = indirect risk associated with the j system components. D = damage.	Baker et al. 2008
3	Conditional robustness index	$(I_{Rob} D = y)$ $= \frac{\sum(R_{Dir_i} D = y)}{\sum(R_{Dir_i} D = y) + \sum(R_{Ind_j} D = y)}$	$(0,1)$		Baker et al. 2008
4	Vulnerability index	$I_V = \frac{\sum_i R_{Dir_i}}{\sum_j C_{Dir_{elj}}}$	$(0,1)$	$C_{Dir_{elj}}$ = direct consequences associated with the loss of the j components of the system.	Baker et al. 2008
5	Vulnerability index	$I_V = \frac{R_D}{V_A}$	$(0, +\infty)$	R_D = direct risk; V_A = attribute used to measure the value of the direct risk, e.g. monetary value, lost lives, etc.	JCSS 2008
6	Robustness index	$\rho = 1 - \nu = 1 - \frac{\mu_L}{L_T}$	$(0,1)$	ν = vulnerability index; μ_L = mean loss; L_T = maximum loss.	Praxedes et al. 2022

APPENDIX B: SAMPLE CALCULATION FOR PARTIAL DAMAGE OF SQUARE TRUSS WITH DUCTILE HINGES

This appendix provides a sample calculation for $R_{k,Q}^B$ and the five existing robustness measures outlined in Chapter 2 for the case of $0.5C_2$ when the square truss has ductile hinges.

Intact Performance:

$$EL = [282.69, 318.13, 318.13, 318.13, 318.13, 318.13] \text{ kN}$$

$$UR = [1.00, 1.00, 0.88, 0.71, 0.71, 0.56]$$

$$\delta_{collapse} = 0.003903 \text{ m}; \delta_{ultimate} = 0.008608 \text{ m}$$

Damaged ($0.5C_2$) Performance:

$$EL = [220.48, 276.69, 276.69, 276.69, 276.69, 276.69] \text{ kN}$$

$$UR = [1.00, 1.00, 0.88, 0.71, 0.71, 0.40]$$

$$\delta_{collapse} = 0.003903 \text{ m}; \delta_{ultimate} = 0.005408 \text{ m}$$

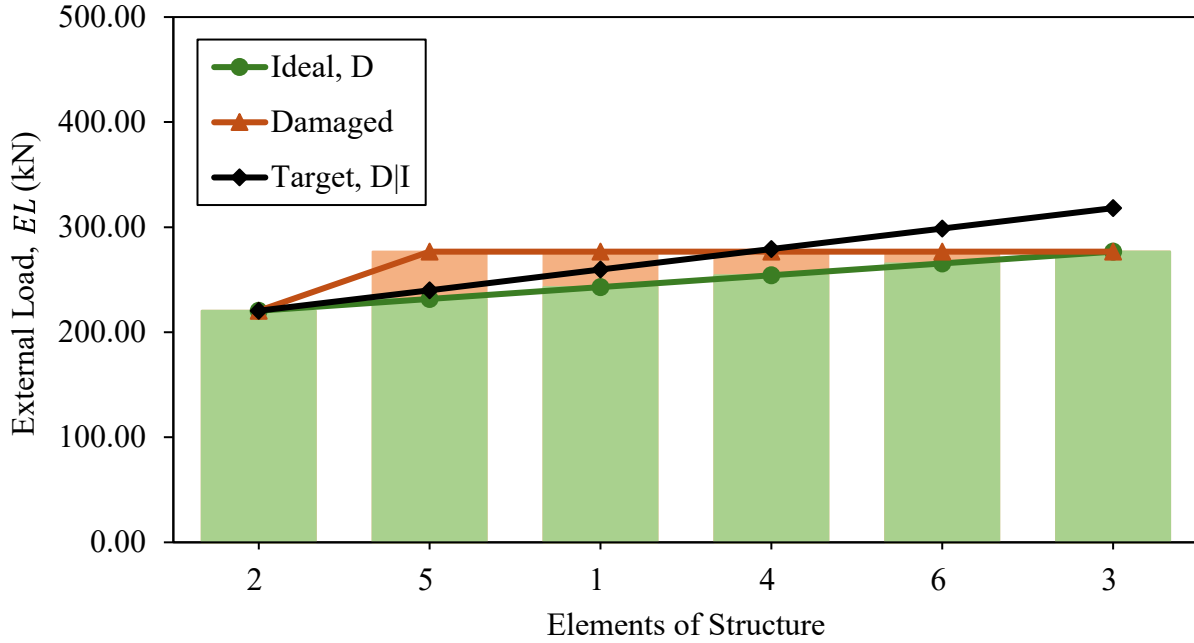


Figure B.1 External loads for structural robustness assessment associated with the square truss with ductile hinges and the $0.5C_2$ damaged state.

$$\text{Eq. (2.6): } R_{k,Q}^B = \left[\frac{\sum_{i=1}^{i=n} EL_i^{Ideal,D} - \sum_{i=1}^{i=n} EL_i^{Deviatoric,D}}{\sum_{i=1}^{i=n} EL_i^{Target,D|I}} \right] \cdot \left[\frac{\sum_{i=1}^{i=n} UR_i^{Ideal,D} - \sum_{i=1}^{i=n} UR_i^{Deviatoric,D}}{\sum_{i=1}^{i=n} UR_i^{Target,D|I}} \right].$$

$$\left[\min \left(\left(\frac{D_D^S}{D_I^S} \right), 1 \right) \right] = \left[\frac{1491.51 \text{ kN} - 112.41 \text{ kN}}{1615.83 \text{ kN}} \right] \cdot \left[\frac{6.00 - 1.30}{6.00} \right] \cdot \left[\min \left(\left(\frac{1.39}{2.21} \right), 1 \right) \right] = [0.85] \cdot [0.78] \cdot$$

$$[0.63] = 0.42$$

$$\text{Eq. (2.1): } R_1 = \frac{L_{damaged}}{L_{intact}} = \frac{276.69 \text{ kN}}{318.13 \text{ kN}} = 0.87$$

$$\text{Eq. (2.2): } R_2 = \frac{L_{intact}}{(L_{intact} - L_{damaged})} = \frac{318.13 \text{ kN}}{(318.13 \text{ kN} - 276.69 \text{ kN})} = 7.68$$

$$\text{Eq. (2.3c): } R_d = \frac{LF_d}{LF_1} = \frac{276.69 \text{ kN}}{282.69 \text{ kN}} = 0.98$$

$$\text{Eq. (2.4): } \gamma_i = 1 - \frac{R_i}{R_0} = 1 - \frac{276.69 \text{ kN}}{318.13 \text{ kN}} = 0.13$$

$$\text{Eq. (2.5): } \Delta Q = Q_{intact} - Q_{damaged} = 318.13 \text{ kN} - 276.69 \text{ kN} = 41.44 \text{ kN}$$

APPENDIX C: HINGE DEFINITIONS FROM ASCE 41-17

Figure C.1 illustrates generalized hinge definitions from ASCE 41-17 (ASCE 2017) used when modeling the truss bridges in Chapters 3 and 4. Prescriptive guidelines for the values of F_T , F_C , and F_B , as well as a , b , and c for the tension and compression force-displacement curves, are provided within Table 9-8 of ASCE 41-17 (ASCE 2017) for different section types and slenderness ratios.

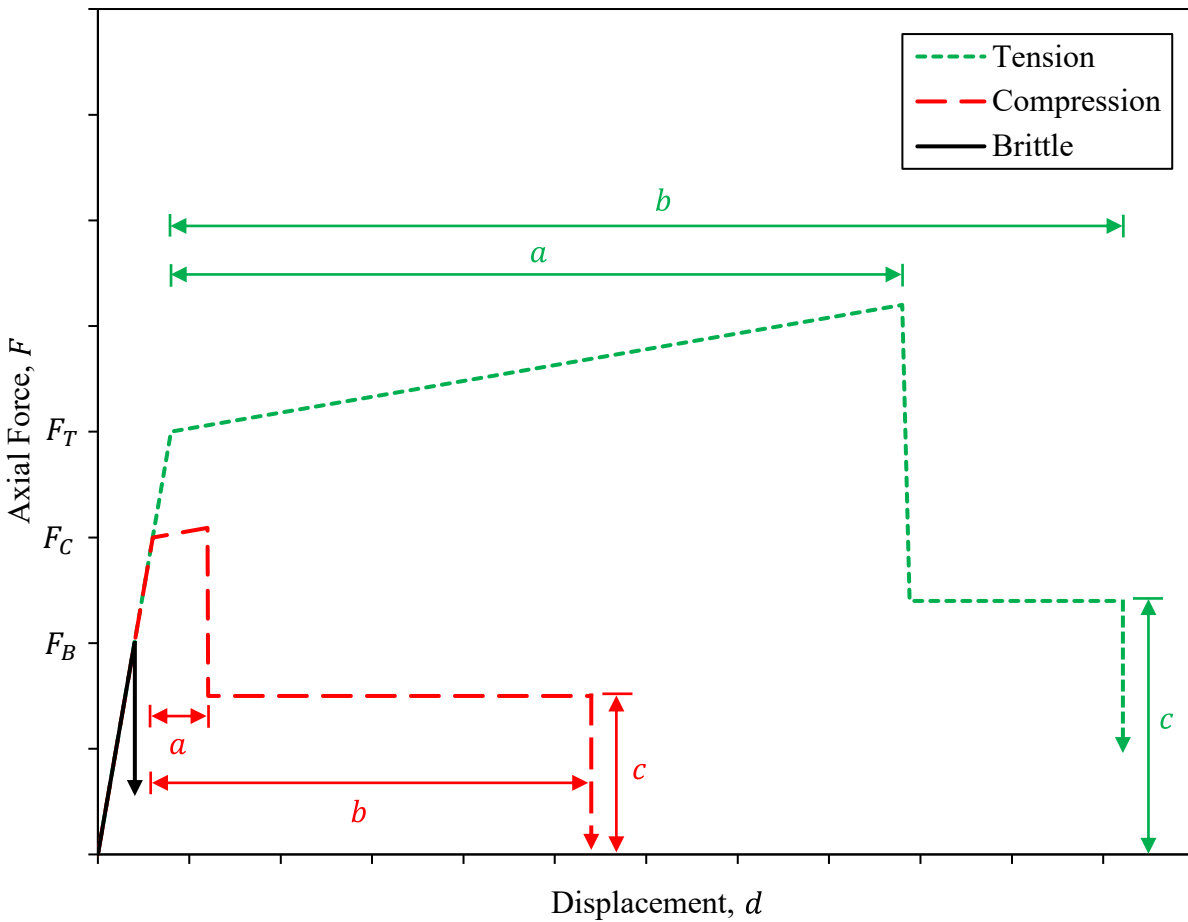


Figure C.1 Generalized force-displacement curves for tension, compression, and brittle hinge definitions from ASCE 41-17 (ASCE 2017).

APPENDIX D: SPREADSHEET INTERFACE WITH MATLAB SCRIPTS

This appendix refers to supplementary material that can be found on DalSpace. A total of three (3) supplementary zip files are provided. Each supplementary file is a folder with seven (7) files, one (1) Excel spreadsheet labeled *Spreadsheet_Interface*, and six (6) MATLAB scripts. The *Spreadsheet_Interface* is operated by a *Master_Code* that computes the member resistances and modeling inputs, and a *Master_Code_Part_2* that performs the robustness assessment. Within the *Spreadsheet_Interface*, white cells imply user input, light yellow imply input from the FE model, light red imply input from MATLAB, and light green imply an upgrade. Descriptions of the three supplementary files are provided below along with the chapter they are referenced in:

Chapter 3:

Chapter_3_Three_Damages_Robustness_Assessment: robustness assessment of steel truss bridge in NS, Canada, subjected to three levels of corrosion damage.

Chapter 4:

Chapter_4_CSA_S6_19_Evaluation_and_Robustness_Assessment: CSA S6:19 evaluation and robustness assessment of the damaged steel truss bridge from NB, Canada.

Chapter_4_Upgrade_1_Robustness_Assessment: robustness assessment of first upgrade achieved using the novel optimization framework.

APPENDIX E: CONNECTION CAPACITY CALCULATIONS

This appendix refers to supplementary material in the form of an Excel spreadsheet labeled *Chapter_4_Connection_Capacity_Calculations* that can be found on DalSpace. The spreadsheet has a summary tab at the beginning, followed by calculations in the subsequent tabs for each of the member connection resistances of the steel truss bridge discussed in Chapter 4 and shown in Figure 4.3, with the understanding that the truss is symmetrical about its vertical centerline. Calculations were performed for the intact and damaged states. The cells highlighted in yellow in the summary tab indicate which connection capacity governs for every member, where factored and nominal compressive and tensile capacities were calculated separately for each connection: factored pertain to code requirements, and nominal pertain to hinge definitions. Not all connection details are provided given that the owner has requested the drawing package remain confidential for this research. The results of the summary tab can be found in the *Spreadsheet_Interface* in the Chapter 4 supplementary material outlined in Appendix D.